ROTATION OF COUPLED COLD MOLECULES IN THE PRESENCE OF A MANY-BODY ENVIRONMENT

by

Xiang Li

December, 2020

A thesis presented to the
Graduate School
of the
Institute of Science and Technology Austria, Klosterneuburg, Austria
in partial fulfillment of the requirements
for the degree of
Doctor of Philosophy

Institute of Science and Technology

The thesis of Xiang Li, titled *rotation of coupled cold molecules in the presence of a many-body environment*, is approved by:

Supervisor: Prof. Dr. Mikhail Lemeshko, IST Austria, Klosterneuburg, Austria

Signature: _____

Committee Member: Prof. Dr. Robert Seiringer, IST Austria, Klosterneuburg, Austria

Signature: _____

Committee Member: Priv.-Doz. Dr. Hendrik Weimer, Institute for Theoretical Physics, Leibniz University Hannover, Germany

Signature: _____

Defense Chair: Asst. Prof. Dr. Julian Ludwig Fischer, IST Austria, Klosterneuburg, Austria

Signature: _____

signed page is on file

IST Austria Thesis, ISSN: 2663-337X

I hereby declare that this thesis is my own work and that it does not contain other people's work without this being so stated; this thesis does not contain my previous work without this being stated, and the bibliography contains all the literature that I used in writing the dissertation.

I declare that this is a true copy of my thesis, including any final revisions, as approved by my thesis committee, and that this thesis has not been submitted for a higher degree to any other university or institution.

I certify that any republication of materials presented in this thesis has been approved by the relevant publishers and co-authors.

Signature: _____

Xiang Li
December, 2020
signed page is on file

Abstract

The oft-quoted dictum by Arthur Schawlow: “A diatomic molecule has one atom too many” has been disavowed. Inspired by the possibility to experimentally manipulate and enhance chemical reactivity in helium nanodroplets, we investigate the rotation of coupled cold molecules in the presence of a many-body environment.

In this thesis, we introduce new variational approaches to quantum impurities and apply them to the Fröhlich polaron - a quasiparticle formed out of an electron (or other point-like impurity) in a polar medium, and to the angulon - a quasiparticle formed out of a rotating molecule in a bosonic bath.

With this theoretical toolbox, we reveal the self-localization transition for the angulon quasiparticle. We show that, unlike for polarons, self-localization of angulons occurs at finite impurity-bath coupling already at the mean-field level. The transition is accompanied by the spherical-symmetry breaking of the angulon ground state and a discontinuity in the first derivative of the ground-state energy. Moreover, the type of symmetry breaking is dictated by the symmetry of the microscopic impurity-bath interaction, which leads to a number of distinct self-localized states.

For the system containing multiple impurities, by analogy with the bipolaron, we introduce the biangulon quasiparticle describing two rotating molecules that align with respect to each other due to the effective attractive interaction mediated by the excitations of the bath. We study this system from the strong-coupling regime to the weak molecule-bath interaction regime. We show that the molecules tend to have a strong alignment in the ground state, the biangulon shows shifted angulon instabilities and an additional spectral instability, where resonant angular momentum transfer between the molecules and the bath takes place. Finally, we introduce a diagonalization scheme that allows us to describe the transition from two separated angulons to a biangulon as a function of the distance between the two molecules.

Acknowledgments

I am grateful to all of those with whom I have had the pleasure to work during this and other related projects. I am also indebted to Dr. Enderalp Yakaboylu, Dr. Giacomo Bighin, and Dr. Andreas Deuchert for their encouragement, insightful comments, and helpful discussions.

Each of the members of my Dissertation Committee has provided me extensive personal and professional guidance and taught me a great deal about both scientific research and life in general. I would especially like to thank Prof. Mikhail Lemeshko. As my teacher and mentor, he has taught me more than I could ever give him credit for here. He has shown me, by his example, what a good scientist (and person) should be.

Last but not the least, I would like to thank my family for their support.

This work would not have been possible without the financial support from the Austrian Science Fund (FWF) under Project No. P29902-N27 and from the European Research Council (ERC) Starting Grant No. 801770 (ANGULON).

About the Author

Xiang Li completed a BSc in College of Physics at Northwest University China and an MSc in Optics at the Northwest University China, before joining IST Austria in September 2015. His main research interests include revealing optical, mechanical, thermodynamic, and topological properties of impurities in the presence of a many-body environment, and revealing physical and chemical properties of molecules at ultracold temperatures. During his PhD studies, Xiang has worked on the research project “Quantum rotations in the presence of a many-body environment” in the Lemeshko group at IST Austria from September 2015.

List of Publications

1. **Xiang Li**, E. Yakaboylu, G. Bighin, R. Schmidt, M. Lemeshko, and A. Deuchert,
   Intermolecular forces and correlations mediated by a phonon bath,
   J. Chem. Phys. 152, 164302 (2020);

2. **Xiang Li**, G. Bighin, E. Yakaboylu, and M. Lemeshko,
   Variational approaches to quantum impurities: from the Fröhlich polaron to the angulon
   Molecular Physics 117, 1981 (2019)

3. **Xiang Li**, R. Seiringer, and M. Lemeshko,
   Angular self-localization of impurities rotating in a bosonic bath
   Physics Review A 95, 033608 (2017)

Table of Contents

List of Figures

1 Introduction

1.1 From single to multiple impurities: polaron and bipolaron

Impurity problems, describing the behavior of individual quantum particles coupled to a complex many-body environment, amount to an active and important research field in condensed matter, with far-reaching applications into chemistry and ultracold quantum gases. Several examples show that the properties of a quantum many-body system can be drastically modified by the presence of impurities. A spectacular example, for instance, is the orthogonality catastrophe, where the unperturbed ground state of a fermionic system has zero overlap, in the thermodynamic limit, with the ground state of the same system in the presence of a single impurity. This phenomenon – a testimony of the great importance of a single impurity even among a macroscopic number of other particles – has been observed in X-ray absorption experiments [Anderson, 1967], as well as in electron transport in quantum dots [Geim *et al.*, 1994]. Another celebrated example is the Kondo effect, in which scattering of conduction electrons from a localized spin inhibits electron transport at low temperatures [Kondo, 1964].

Historically, the first impurity problem was originally introduced by Landau and Pekar [Landau, 1933b; Landau and Pekar, 1948], Fröhlich [Fröhlich, 1954], and Holstein [Holstein, 1959a; Holstein, 1959b], as they considered the interactions of an electron with a polarizable crystal. A charge-induced polarization cloud was shown to follow the electron as it moves through the medium, thereby modifying the electron's properties. In order to describe the latter a quasiparticle was introduced – the *polaron*, which represents an electron dressed by the cloud of lattice excitations. A distinction can be made

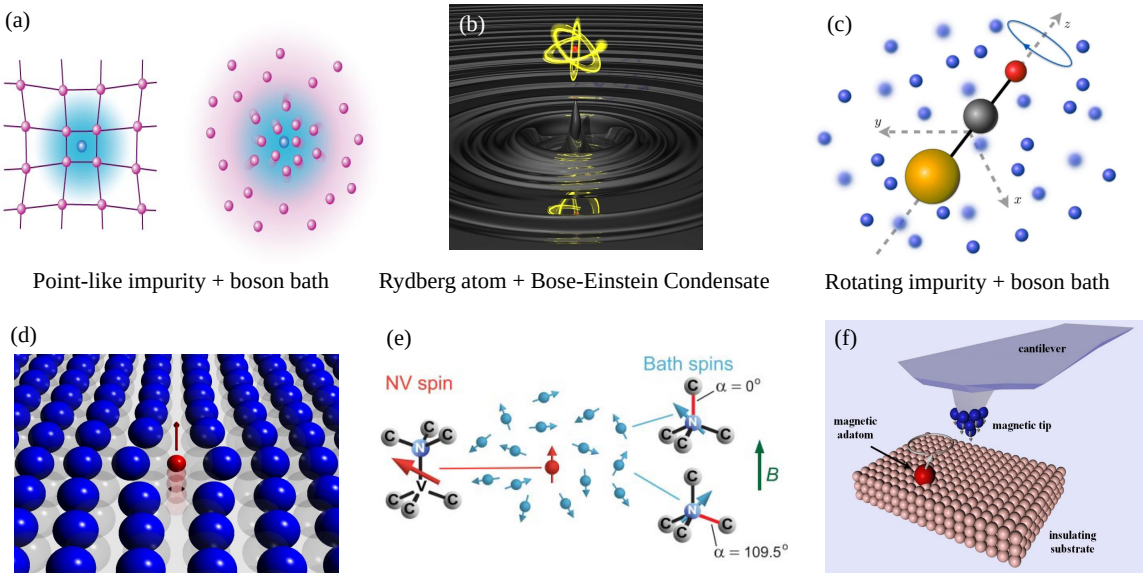

Figure 1.1: The "family" of impurity problems*, as introduced in the main text. (a) Fröhlich polaron (or boson polaron), adapted from Physics **9**, 86 (2016), (b) Rydberg impurity, adapted from `http://www.rle.mit.edu/cua/highlights/viewpoint-swimming-in-the-fermi-sea/`, (c) angulon, adapted from Physics **10**, 20 (2017), (d) spin-boson model, adapted from `http://www.rle.mit.edu/cua/highlights/wp-content/uploads/2009/06/swimming1.png`, (e) NV center, adapted from Scientific Reports **(**2) 382 (2012), and (d) magnetic impurity, adapted from `http://www.nanoscience.de/furore/projects.html`.

between polarons in the continuum approximation, where the long-range electron-lattice interaction prevails (Fröhlich, or large polaron) [Devreese, 2007], and polarons for which the short-range interaction is essential (Holstein or small polaron) [Holstein, 1959a; Holstein, 1959b; Devreese and Alexandrov, 2009]. In what follows, we will mainly consider the former case. Recent revival of interest in the problem of Fröhlich polaron [Devreese, 2007; Devreese and Alexandrov, 2009; Tempere *et al.*, 2009a; Bruderer *et al.*, 2007; Rath and Schmidt, 2013; Li and Sarma, 2014; Ardila and Giorgini, 2015] comes from the rapid progress in the field of ultracold atoms: this new experimental platform not only allows to create a large variety of polaronic systems with different impurity masses and tunable interactions, but also provides a versatile toolbox for studying equilibrium and dynamical properties of mobile impurities interacting with a many-body environment [Spethmann *et al.*, 2012; Koschorreck *et al.*, 2012; Chin *et al.*, 2010].

The concept of polarons is essential to understand several solid state systems including ionic crystals, polar semiconductors [Crawford and Slifkin, 2013] and has been proposed a possible mechanism of high-temperature superconductivity [Devreese, 2007; Salje *et al.*, 2005]. More recently, the idea of polaronic dressing has been extended to doped antiferromagnetic Mott insulators [Dagotto, 1994] and magnetic semiconductors [Kaminski and Sarma, 2002]. By now polarons emerged as a key theoretical tool to describe electron transport in condensed matter physics and chemistry [Appel, 1968; Emin, 2013; Kuper and Whitfield, 1962; Devreese, 2015], as well as to understand the behaviour of atomic impurities in ultracold quantum gases [Chikkatur *et al.*, 2000; Schirotzek *et al.*, 2009; Palzer *et al.*, 2009; Kohstall *et al.*, 2012; Koschorreck *et al.*, 2012; Spethmann *et al.*, 2012; Fukuhara *et al.*, 2013a; Scelle *et al.*, 2013; Cetina *et al.*, 2015; Massignan *et al.*, 2014; Jørgensen *et al.*, 2016; Hu *et al.*, 2016a; Cetina *et al.*, 2016], and also been fruitfully employed to describe electrons on the surface of liquid helium [Devreese, 2007; Jackson and Platzman, 1981]..

Among various topics about the polaron, the self-localization has received interest since 1933. Landau predicted that electrons moving in solids can undergo a self-localization transition [Landau, 1933a]. The latter takes place when the electron-induced

distortion of the crystal lattice is strong enough to affect the motion of the electron itself, confining its wavefunction in space. While the phenomenon of self-localization attracted attention of several generations of physicists, its existence in various polaron models is still under an active debate. Several theories predicted the existence of a self-localization transition in the Fröhlich polaron [Gross, 1959a; Matz and Burkey, 1971b; Mańka, 1978; Lépine *et al.*, 1979; Luttinger and Lu, 1980b] as well as in related models such as a polaronic exciton [Sumi, 1977] and an optical polaron in an external magnetic [Peeters and Devreese, 1982c] or Coulomb potential [Tokuda *et al.*, 1981]. Later, however, the effect had been proven to be a consequence of the approximations employed rather than an intrinsic property of the polaron Hamiltonian [Lieb, 1977; Peeters and Devreese, 1982a; Gerlach and Löwen, 1991a; Mishchenko *et al.*, 2000a]. Self-localization has been also predicted for a particle coupled to acoustic phonons and collective excitations in a Bose-Einstein condensate (BEC) [Toyozawa, 1961; Sumi and Toyozawa, 1973; Peeters and Devreese, 1985; Wang, 1998; Cucchietti and Timmermans, 2006a; Kalas and Blume, 2006; Sacha and Timmermans, 2006a; Bruderer *et al.*, 2008; Tempere *et al.*, 2009a; Roberts and Rica, 2009; Rica and Roberts, 2009; Casteels *et al.*, 2012; Fantoni, 2012; Boudjemâa, 2014; Shadkhoo and Bruinsma, 2015; Vlietinck *et al.*, 2015]. Still, recent numerical results reveal a smooth crossover of the BEC-polaron energy between the weakly- and strongly-coupled regimes, suggesting an absence of the self-localization transition [Grusdt *et al.*, 2015; Grusdt and Demler, 2016; Grusdt, 2016; Grusdt and Fleischhauer, 2016; Shchadilova *et al.*, 2016a].

Single-impurity problems constitute an elementary ‘building block’ of strongly-correlated systems and a convenient starting point to understand their properties. Therefore, a natural question is: what happens if multiple impurities are simultaneously present in the system? Due to the impurity-impurity interactions, the physics of the system is expected to be much richer than a simple ‘linear combination’ of individual impurities. In the context of solid state physics, where electrons (or holes) interact with each other, simultaneously through the Coulomb force and via the phonon-mediated interaction, a two-polaron bound state can arise, commonly known as the bipolaron [Devreese and Alexandrov, 2009; Devreese, 2007; Kashirina and Lakhno, 2010]. Many theoretical models exist for the Fröhlich bipolaron, and they can be classified into two kinds: one-

center and two-center models [Kashirina and Lakhno, 2010]. Both of them reveal that the correlations between the impurities can significantly reduce the bipolaron energy and play an important role in the formation of the bound state.

Bipolarons have attracted considerable attention because of their possible role as an unconventional pairing mechanism for high-temperature superconductivity [Kashirina and Lakhno, 2010; Alexandrov, 2003]. Due to the possibility to engineer interparticle interactions, ultracold Bose gases recently became a new testing ground for the bipolaron (and multi-polaron) theory. At weak polaronic coupling, the theoretical formalism provides a precise description of the ground state properties and of the response to Bragg spectroscopy of ultracold weakly interacting binary mixtures [Tempere and Devreese, 2001], to be compared with experiments. In the intermediate coupling regime, it has been shown that the spatial structure of a bipolaron is that of an axially symmetric quasi-molecular dimer [Mukhomorov, 2001]. Finally, in the strong coupling region, the condensate-mediated interaction can lead to not only a bipolaron bound state, but also the clustering of the impurities [Santamore and Timmermans, 2011]. Novel quantum phases were predicted in multi-impurities system, e.g. impurity crystal which exhibits supersolid behavior [Roberts and Rica, 2009] and bubble state of repulsive neutral-atom impurities [Blinova *et al.*, 2013]. The theory of multi-impurities is also relevant in the description of optical lattice systems [Bruderer *et al.*, 2007], and spin-wave models [Fukuhara *et al.*, 2013b].

Even though the polaron constitutes the most paradigmatic – and historically the first – impurity problem, the 'family' of impurity problems is large, comprising many members of theoretical and experimental relevance. A few examples are illustrated in Fig. 1.1. A local spin $1/2$ impurity coupled to both a bath of harmonic oscillators and a transverse field can be described by the spin-boson model, well known from the theory of dissipative systems [Leggett *et al.*, 1987]. In the nitrogen-vacancy (NV) center system, on the other hand, an effective spin $S = 1$ – formed out of a substitutional N impurity – interacts with surrounding bath of electron spins ($S = 1/2$) [De Lange *et al.*, 2012]. Furthermore, a single highly-excited Rydberg atom in a Bose-Einstein condensate can carry angular momentum that can be perturbed by the surrounding bosons [Dudin and

Kuzmich, 2012], whereas magnetic impurities interacting with delocalized fermions lead to the Kondo effect mentioned above.

An impurity problem becomes significantly more involved if the impurity possesses internal degrees of freedom, such as orbital angular momentum. This situation can be experimentally realized in molecules rotating in superfluid Helium nanodroplets [Toennies and Vilesov, 2004a] or ultracold gases [Midya *et al.*, 2016a], highly-excited Rydberg states in Bose-Einstein condensates [Balewski *et al.*, 2013], or in solids, where the angular momentum is transferred from electrons to the crystal lattice [Stamm *et al.*, 2007].

1.2 Cold polar molecules

The structural complexity of molecules results in a richer, denser spectrum, as compared to atoms. The rotational and vibrational modes couple to each other, as well as with the electronic spin and orbital degrees of freedom [Lefebvre-Brion and Field, 2004], giving rise to an intricate phenomenology. Moreover, the 'molecular' degrees of freedom occupy the low-energy part of the energy spectrum, and therefore can be easily altered by the interactions with the surrounding medium, rendering molecules an ideal candidate to study novel aspects of many-body physics.

During the last decades, great advances in experimental techniques have allowed for the cooling of atoms and molecules to ultracold temperature, and for their subsequent precise control. A Bose-Einstein condensate [Dürr *et al.*, 2004], as well as a degenerate Fermi gas [Regal *et al.*, 2003; Cubizolles *et al.*, 2003] can be obtained combining a number of experimental techniques, among which we mention Feshbach resonances [Chin *et al.*, 2010], photoassociation [Krems *et al.*, 2009], molecular beam deceleration, and laser cooling [Carr *et al.*, 2009]. The transfer from excited or only weakly bound molecular states to the lowest rotational and vibrational state without major losses can be realized using a coherent population transfer tech-

nique, known as stimulated Raman adiabatic passage (STIRAP) [Ni *et al.*, 2008].This progress played a key role in numerous applications of cold molecules [Carr *et al.*, 2009; Krems *et al.*, 2009], from controllable cold chemical reactions, to measurements of fundamental physical constants, to quantum simulation and quantum information processing.

Experiments involving molecules entail completely new features, as compared with the analogous experiments on atoms: apart from possessing vibrational and rotational degrees of freedom, molecules may carry electric and magnetic dipole moments. Polar molecules are characterized by large electric dipole moments associated with rotational excitations, giving rise to large dipole-dipole interactions between molecules, which can be manipulated with external electric and microwave fields [Krems *et al.*, 2009; Lemeshko *et al.*, 2013]. These strong, long-range and anisotropic interactions raise extremely interesting prospects for cold ensembles of polar molecules as strongly correlated systems. While two parallel dipoles repel each other, dipoles aligned along the collision axis will attract each other, possibly leading to instabilities in a many-body system, and influencing the collision properties of cold polar molecules [Carr *et al.*, 2009; Krems *et al.*, 2009]. In addition to this, the long-range dipole-dipole interactions offers the possibility of realizing off-site interactions in the Hubbard Hamiltonian. This gives rise to novel previously unobserved quantum phenomena, such as checkerboard solids and two-dimensional supersolids [Sengupta *et al.*, 2005]. Moreover, various self-assembled quantum structures [Pupillo *et al.*, 2008; Hazzard *et al.*, 2014] arising due to the competition between short-range contact and long-range dipole-dipole interactions were discovered. Finally, adding a spin degree of freedom to polar molecules trapped in an optical lattice allows to construct a complete toolbox for the simulation of any permutation-symmetric lattice spin model [Micheli *et al.*, 2006].

1.3 Molecules in superfluid helium

In the 1990s, it was demonstrated that atoms and molecules can be trapped in helium if the latter forms small superfluid droplets [Toennies and Vilesov, 2004a; Szalewicz, 2008]. Over the following years, this approach was established as one of the most convenient ways to study molecular properties. Helium nanodroplets – sometimes called nanocryostats – cool molecules down to about 0.4 Kelvin and isolate them from external perturbations [Stienkemeier and Lehmann, 2006]. This allows to record spectra free of collision and Doppler broadening, as well as to trap and study otherwise reactive species. Currently, spectroscopy of molecules in helium droplets represents a large and active field of its own [Toennies and Vilesov, 2004a; Lemeshko and Schmidt, 2017].

How can this situation be understood from a theoretical point of view? A phenomenological approach would describe the rotational spectrum of molecules in superfluid helium droplets by considering them as free rotors with an effective, higher rotational inertia, to account for the Helium-impurity interaction. Of course such an approach lacks a microscopical understanding of the mechanism leading to the rotational inertia renormalization. An alternative approach consists in employing Monte Carlo techniques, to numerically study a molecule interacting with a finite cluster of helium. Even though many groups performed sophisticated numerical calculations for several different molecules trapped inside small and large He_n clusters, which has substantially advanced our understanding of molecule-superfluid interactions [Szalewicz, 2008], these approaches have some drawbacks. For instance, due to the computational complexity, Monte Carlo simulations are not well-suited to study real-time dynamics. Very recently – in 2015 – a fully analytical theory describing the redistribution of orbital angular momentum in quantum many-body systems has been introduced by Schmidt and Lemeshko [Schmidt and Lemeshko, 2015; Lemeshko and Schmidt, 2017], formalizing and rationalizing the concept of a rotor interacting with a many-body environment by means of the angulon quasiparticle.

1.4 The angulon quasiparticle

In 2015, it was shown that the problem of angular momentum redistribution between an impurity and a bosonic environment can be efficiently described in terms of a new quasiparticle, the angulon. The angulon can be understood as a quantum rotor dressed by a quantum field of many-body excitations. As schematically illustrated in Fig 3.1, the angulon is a collective object, characterized by the total angular momentum of the system, of which it is an eigenstate. Ultracold molecules in optical lattices amount to one of the most promising platforms for studying many-particle physics in a fully controlled environment [Moses *et al.*, 2017]. This includes both quantum simulation of condensed-matter models, see e.g. [Gorshkov *et al.*, 2011; Yan *et al.*, 2013], as well as the study of novel, previously unexplored phases of matter, e.g. [Cooper and Shlyapnikov, 2009; Syzranov *et al.*, 2014].

In the quasiparticle language, the renormalization of molecular moments of inertia is a phenomenon similar to renormalization of the effective mass for electrons moving in solids [Devreese and Alexandrov, 2009]. The angulon theory allows to describe strong renormalization for heavy molecules by constructing a quantum many-body wavefunction similar to the co-rotating ”non-superfluid shell“: if the molecule is rotating slow enough, some helium atoms ”stick” to it and co-rotate with it [Koch *et al.*, 2018; Grebenev *et al.*, 2000; Callegari *et al.*, 1999]. On the other hand, weak renormalization observed for light molecules has been described in terms of the ‘rotational Lamb shift’ – differential renormalization of molecular states due to virtual phonon excitations carrying angular momentum.

The angulon theory was able to describe, in good agreement with experiment, renormalization of rotational constants [Lemeshko and Schmidt, 2017; Shchadilova *et al.*, 2016b; Cherepanov and Lemeshko, 2017] and laser-induced dynamics [Shepperson *et al.*, 2017b; Shepperson *et al.*, 2017a] of molecules in superfluid helium nanodroplets. The angulon theory offers a way to study the impurity properties with rotational degrees of freedoms. The studies have shown novel phenomena the rotating impurity presents in external field [Redchenko and Lemeshko, 2016b; Yakaboylu and Lemeshko, 2017; Rzadkowski and Lemeshko, 2018; Cherepanov *et al.*, 2019].

Since the coupling in angular space follow the $SO(3)$ algebra, and as a standard quasiparticle concept, the angulon quasiparticle requires a series of new theoretical techniques. In what follows, I will first briefly introduce the basic Fröhlich polaron theory (chapter 2) and derive the angulon Hamiltonian (chapter 3). In chapter 4, several variational approaches I developed during my study will be presented. Following it, we shall discuss the self-localization in angular space and the concept of the biangulon quasiparticle in chapter 5 and 6, respectively.

2 The basic Fröhlich polaron theory

2.1 Bogoliubov approximation up to quadratic terms

Quantum gases are used as an excellent test-bed for many-body theory, and are particularly useful to investigate strong-coupling regimes or strongly correlated regimes that have remained out of reach in the solid state [Bloch *et al.*, 2008]. The Hamiltonian of an impurity in a Bose-Einstein condensate can be mapped onto the polaron Hamiltonian when the Bogoliubov approximation is valid [Cucchietti and Timmermans, 2006b; Sacha and Timmermans, 2006a; Tempere *et al.*, 2009a]. The polaronic effects comes about through the coupling of the impurity with the Bogoliubov excitations.

The Hamiltonian of a single atomic impurity in the presence of a Bose gas is given by

$$H = \frac{p_I^2}{2m} + \sum_k \epsilon_k a_k^+ a_k + \frac{1}{2}\sum_{k,k',q}\left[U_{BB}(q) a_{k'-q}^+ a_{k+q}^+ a_k a_{k'}\right] + \sum_{k',q}\left[U_{IB}(q)\rho_q(q) a_{k'-q}^+ a_{k'}\right]. \quad (2.1)$$

The first term represents the kinetic energy of the “impurity” atom with mass m. The operator $\hat{a}_{\mathbf{k}}^\dagger$, $\hat{a}_{\mathbf{k}}$ create and annihilate a boson with mass m_B, wave number $\mathbf{k}$, and energy $\epsilon_{\mathbf{k}} = (\hbar k)^2/(2m_B) - \mu$ where μ is the chemical potential. These bosons interact, and $U_{BB}(q)$ is the Fourier transform of the boson-boson interaction potential. The interaction between the bosonic atoms and the impurity atom is described by a potential $U_{IB}(q)$ coupling the boson density to the impurity density $\hat{\rho}_I(q)$, which can be expressed as a function of the impurity position operator $\hat{r}$. The crucial point of the theory now is to use the Bogoliubov approximation, i.e. substitute $a_k = a_0\delta_{k,0} + \sum_{k\neq 0} a_k$ into (2.1), and

neglect the cubic and quartic terms in a_k,

$$\begin{aligned} H &= \frac{p_I^2}{2m} + \epsilon_0 a_0^+ a_0 + \sum_{k\neq 0} \epsilon_k a_k^+ a_k \\ &+ \frac{1}{2}\sum_{k\neq 0} U_{BB}(k)\left(a_0^+ a_0^+ a_0 a_0 + 4a_0^+ a_k^+ a_0 a_k + a_0^+ a_0^+ a_k a_{-k} + a_k^+ a_{-k}^+ a_0 a_0\right) \\ &+ \sum_{k\neq 0} U_{IB}(k)\rho_I(k)\left(a_0^+ a_0 + a_k^+ a_0 + a_0^+ a_k\right) \\ &+ \sum_{k,q\neq 0} U_{IB}(k-q)\rho_I(k-q) a_q^+ a_k. \end{aligned} \tag{2.2}$$

In the last term, we have replaced the $k'-q$ as q and k' as k. It is worth to mention that the potential $U_{IB}(k-q)$ and the density $\rho_I(k-q)$ are the functions of the difference between k and q. Under Bogoliubov approximation, a_0^+ and a_0 can be replaced with $\sqrt{N}$, but for high accuracy, the quadratic term need to be kept: $a_0^+ a_0^+ a_0 a_0 = N^2 - 2N\sum_{k\neq 0} a_k^+ a_k$. Now we have

$$\begin{aligned} H &= \frac{p_I^2}{2m} + \epsilon_0 N + \sum_{k\neq 0} \epsilon_k a_k^+ a_k + \frac{1}{2}\sum_{k\neq 0}\left[U_{BB}(k)(N^2 - 2N a_k^+ a_k)\right] \\ &+ \frac{1}{2}\sum_{k\neq 0} U_{BB}(k)\left(4N a_k^+ a_k + N a_k a_{-k} + N a_k^+ a_{-k}^+\right) + U_{IB}(0)\rho_I(0)N \\ &+ \sum_{k\neq 0} U_{IB}(k)\rho_I(k)\left(\sqrt{N}a_k^+ + \sqrt{N}a_k\right) + \sum_{k,q\neq 0} U_{IB}(k-q)\rho_I(k-q) a_q^+ a_k \\ &= E_0 + \sum_{k\neq 0} E_1 A_1 + \sum_{k\neq 0} E_2 A_2 + \sum_{k\neq 0} E_3\sqrt{N} A_3 + \sum_{k,q\neq 0} E_3 A_4, \end{aligned} \tag{2.3}$$

where

$$E_0 = \left(\frac{p_I^2}{2m} + \epsilon_0 N + \frac{1}{2}U_{BB}(0)N^2 + U_{IB}(0)\rho_I N(0)\right), \tag{2.4a}$$

$$E_1 = \epsilon_k + U_{BB}(k)N, \tag{2.4b}$$

$$E_2 = \frac{1}{2}U_{BB}(k)N, \tag{2.4c}$$

$$E_3 = U_{IB}(k-q)\rho_I(k-q), \tag{2.4d}$$

$$A_1 = a_k^+ a_k, \tag{2.4e}$$

$$A_2 = a_k a_{-k} + a_k^+ a_{-k}^+, \tag{2.4f}$$

$$A_3 = a_k^+ + a_k, \tag{2.4g}$$

$$A_4 = a_q^+ a_k. \tag{2.4h}$$

To diagonalize the Hamiltonian, we apply a Bogoliubov rotation which means substituting

$$a_k = u_k b_k + v_{-k}^* b_{-k}^+, \quad a_{-k} = u_{-k} b_{-k} + v_k^* b_k^+ \tag{2.5}$$

and their complex conjugates into Hamiltonian (3). We calculate the transformation assuming the symmetry between k and $-k$, we can separate the results of transformation as diagonal terms and off-diagonal terms with the help of $[b_i, b_j^+] = \delta_{ij}$, $[b_i, b_j] = [b_i^+, b_j^+] = 0$:

$$A_{1d} = |v_{-k}|^2 + \left(|u_k|^2 + |v_{-k}|^2\right) b_k^+ b_k, \tag{2.6a}$$

$$A_{1o} = u_k v_{-k} b_k b_{-k} + u_k^* v_{-k}^* b_k^+ b_{-k}^+, \tag{2.6b}$$

$$A_{2d} = u_k^* v_{-k} + u_k v_{-k}^* + \left(2u_k^* v_{-k} + 2u_k v_{-k}^*\right) b_k^+ b_k, \tag{2.6c}$$

$$A_{2o} = (u_k^2 + v_{-k}^2) b_k b_{-k} + (u_k^{*2} + v_{-k}^{*2}) b_k^+ b_{-k}^+, \tag{2.6d}$$

$$A_3 = (u_k + v_{-k}) b_k + (u_k^* + v_{-k}^*) b_k^+, \tag{2.6e}$$

$$A_4 = (u_q^* u_k + v_{-q} v_{-k}^*) b_q^+ b_k + u_q^* v_{-k}^* b_q^+ b_k^+ + u_k v_{-q} b_q b_k. \tag{2.6f}$$

Now the Hamiltonian can be rewritten as

$$\begin{aligned} H \;=\; & \left[E_0 + \sum_{k\neq 0} E_1 |v_{-k}|^2 + \sum_{k\neq 0} E_2 (u_k^* v_{-k} + u_k v_{-k}^*)\right] \\ & + \sum_{k\neq 0} \left[E_1(|u_k|^2 + |v_{-k}|^2) + E_2(2u_k^* v_{-k} + 2u_k v_{-k}^*)\right] b_k^+ b_k \\ & + \sum_{k\neq 0} E_3 \sqrt{N} \left[(u_k + v_{-k}) b_k + (u_k^* + v_{-k}^*) b_k^+\right] \\ & + \sum_{k,q\neq 0} E_3 \left[(u_q^* u_k + v_{-q} v_{-k}^*) b_q^+ b_k + + u_q^* v_{-k}^* b_q^+ b_k^+ + u_k v_{-q} b_q b_k\right] \\ & + \sum_{k\neq 0} \left\{\left[E_1 u_k v_{-k} + E_2(u_k^2 + v_{-k}^2)\right] b_k b_{-k} + \left[E_1 u_k^* v_{-k}^* + E_2(u_k^{*2} + v_{-k}^{*2})\right] b_k^+ b_{-k}^+\right\}. \end{aligned} \tag{2.7}$$

The commutation relations for b_k are satisfied if

$$|u_k|^2 - |v_{-k}|^2 = 1, \tag{2.8}$$

i.e. if one can write

$$u_k = \cosh \alpha_k, \quad v_{-k} = \sinh \alpha_k. \tag{2.9}$$

The parameter α_k will be chosen in order to make the coefficients of the off-diagonal terms $b_k b_{-k}$ and $b_k^+ b_{-k}^+$ in the Hamiltonian (2.7) vanish. This condition takes the equations

$$\begin{aligned}(\epsilon_k + U_{BB}N)u_k v_{-k} + \frac{1}{2}U_{BB}N(u_k^2 + v_{-k}^2) = 0,\\ (\epsilon_k + U_{BB}N)u_k^* v_{-k}^* + \frac{1}{2}U_{BB}N(u_k^{*2} + v_{-k}^{*2}) = 0,\end{aligned} \tag{2.10}$$

Using the properties $\cosh 2\alpha = \cosh^2\alpha + \sinh^2\alpha$ and $\sinh 2\alpha = 2\cosh\alpha\sinh\alpha$, we find the equations (2.10) can be solved by choosing

$$\coth 2\alpha_k = \frac{\cosh 2\alpha_k}{\sinh 2\alpha_k} = -\frac{\epsilon_k + U_{BB}N}{U_{BB}N} = C, \tag{2.11}$$

To solve out u_k and v_{-k}, we square both sides of

$$\frac{u_k^2 + v_{-k}^2}{2u_k v_{-k}} = C, \tag{2.12}$$

and by taking $v_{-k}^2 = u_k^2 - 1$, we have

$$\begin{aligned}\frac{(2u_k^2 - 1)^2}{4u_k^2(u_k^2 - 1)} &= C^2\\ \frac{4u_k^4 - 4u_k^2 + 1}{4u_k^4 - 4u_k^2} &= C^2\\ (4 - 4C^2)u_k^4 - (4 - 4C^2)u_k^2 + 1 &= 0,\end{aligned} \tag{2.13}$$

which is same to

$$ax^2 - ax + 1 = 0, \tag{2.14}$$

where $a = 4 - 4C^2$ and $x = u_k^2$. Its solution is

$$\begin{aligned}u_k^2 &= \frac{a + \sqrt{a^2 - 4a}}{2a}\\ &= \frac{(4 - 4C^2) + 4C\sqrt{C^2 - 1}}{2(4 - 4C^2)}\\ &= \frac{-C}{2\sqrt{C^2 - 1}} + \frac{1}{2}\\ &= \frac{\epsilon_k + U_{BB}N}{U_{BB}N}\frac{1}{2\sqrt{\frac{(\epsilon_k + U_{BB}N)^2}{(U_{BB}N)^2} - 1}} + \frac{1}{2}\\ &= \frac{\epsilon_k + U_{BB}N}{2\sqrt{\epsilon_k^2 + 2\epsilon_k U_{BB}N}} + \frac{1}{2}.\end{aligned} \tag{2.15}$$

Then we have

$$u_k = \left(\frac{\epsilon_k + U_{BB}N}{2E_k} + \frac{1}{2}\right)^{\frac{1}{2}}, \tag{2.16a}$$

$$v_{-k} = -\left(\frac{\epsilon_k + U_{BB}N}{2E_k} - \frac{1}{2}\right)^{\frac{1}{2}}, \tag{2.16b}$$

where

$$E_k = \sqrt{\epsilon_k[\epsilon_k + 2U_{BB}(k)N]}. \tag{2.17}$$

So we have $u_k^* = u_{-k}^* = u_k = u_{-k}$ and $v_{-k}^* = v_k^* = v_{-k} = v_k$. Now, substitute solutions (2.16b) into the first line of representation (2.7) and get

$$\begin{aligned}
& E_0 + \sum_{k\neq 0}\left[(\epsilon_k + U_{BB}N)\left(\frac{\epsilon_k + U_{BB}N}{2\sqrt{\epsilon_k^2 + 2\epsilon_k U_{BB}N}} - \frac{1}{2}\right)\right. \\
& \left. -U_{BB}N\sqrt{\left(\frac{\epsilon_k + U_{BB}N}{2\sqrt{\epsilon_k^2 + 2\epsilon_k U_{BB}N}} + \frac{1}{2}\right)\left(\frac{\epsilon_k + U_{BB}N}{2\sqrt{\epsilon_k^2 + 2\epsilon_k U_{BB}N}} - \frac{1}{2}\right)}\right] \\
= \; & E_0 + \sum_{k\neq 0}\left[\frac{(\epsilon_k + U_{BB}N)^2}{2\sqrt{\epsilon_k^2 + 2\epsilon_k U_{BB}N}} - \frac{\epsilon_k + U_{BB}N}{2} - U_{BB}N\sqrt{\frac{(\epsilon_k + U_{BB}N)^2}{4(\epsilon_k^2 + 2\epsilon_k U_{BB}N)} - \frac{1}{4}}\right] \\
= \; & E_0 + \sum_{k\neq 0}\left[\frac{(\epsilon_k + U_{BB}N)^2 - (\epsilon_k + U_{BB}N)\sqrt{\epsilon_k^2 + 2\epsilon_k U_{BB}N}}{2\sqrt{\epsilon_k^2 + 2\epsilon_k U_{BB}N}}\right. \\
& \left. -U_{BB}N\frac{\sqrt{\epsilon_k^2 + 2\epsilon_k U_{BB}N + U_{BB}^2N^2 - \epsilon_k^2 - 2\epsilon_k U_{BB}N}}{2\sqrt{\epsilon_k^2 + 2\epsilon_k U_{BB}N}}\right] \\
= \; & E_0 + \sum_{k\neq 0}\left[\frac{\epsilon_k^2 + 2\epsilon_k U_{BB}N + U_{BB}^2N^2 - (\epsilon_k + U_{BB}N)\sqrt{\epsilon_k^2 + 2\epsilon_k U_{BB}N} - U_{BB}^2N^2}{2\sqrt{\epsilon_k^2 + 2\epsilon_k U_{BB}N}}\right] \\
= \; & \frac{p_I^2}{2m} + \epsilon_0 N + \frac{1}{2}U_{BB}(0)N^2 + U_{IB}(0)\rho_I(0)N + \frac{1}{2}\sum_{k\neq 0}[E_k - \epsilon_k - U_{BB}(k)N] \\
= \; & E_0',
\end{aligned} \tag{2.18}$$

After neglect the energy off set, i.e., $\epsilon_0 N + \frac{1}{2}U_{BB}(0)N^2 + U_{IB}(0)\rho_I(0)N$, we have

$$E_0' = \frac{p_I^2}{2m} + \frac{1}{2}\sum_{k\neq 0}[E_k - \epsilon_k - U_{BB}(k)N] \tag{2.19}$$

Then, substitute the solutions into the second line of Hamiltonian (2.7) and get

$$\begin{aligned}
& \sum_{k\neq 0}\left[\left(\frac{(\epsilon_k + U_{BB}N)^2}{\sqrt{\epsilon_k^2 + 2\epsilon_k U_{BB}N}} - 2U_{BB}N\sqrt{\frac{(\epsilon_k + U_{BB}N)^2}{4(\epsilon_k^2 + 2\epsilon_k U_{BB}N)} - \frac{1}{4}}\right)b_k^+ b_k\right] \\
= \; & \sum_{k\neq 0}\left[\left(\frac{(\epsilon_k + U_{BB}N)^2}{\sqrt{\epsilon_k^2 + 2\epsilon_k U_{BB}N}} - \frac{U_{BB}^2N}{\sqrt{\epsilon_k^2 + 2\epsilon_k U_{BB}N}}\right)b_k^+ b_k\right] \\
= \; & \sum_{k\neq 0}\left[\frac{\epsilon_k^2 + 2\epsilon_k U_{BB}N}{\sqrt{\epsilon_k^2 + 2\epsilon_k U_{BB}N}}b_k^+ b_k\right] \\
= \; & \sum_{k\neq 0} E_k b_k^+ b_k.
\end{aligned} \tag{2.20}$$

Then the third line

$$\begin{aligned}
&\sum_{k\neq 0}\left[\left(U\left(\sqrt{\frac{\epsilon_k+U_{BB}N}{2\sqrt{\epsilon_k^2+2\epsilon_k U_{BB}N}}+\frac{1}{2}}-\sqrt{\frac{\epsilon_k+U_{BB}N}{2\sqrt{\epsilon_k^2+2\epsilon_k U_{BB}N}}-\frac{1}{2}}\right)\right)(b_k^+ + b_k)\right]\\
=&\sum_{k\neq 0}\left[\left(U\sqrt{\left(\sqrt{\frac{\epsilon_k+U_{BB}N}{2\sqrt{\epsilon_k^2+2\epsilon_k U_{BB}N}}+\frac{1}{2}}-\sqrt{\frac{\epsilon_k+U_{BB}N}{2\sqrt{\epsilon_k^2+2\epsilon_k U_{BB}N}}-\frac{1}{2}}\right)^2}\right)(b_k^+ + b_k)\right]\\
=&\sum_{k\neq 0}\left[\left(U\sqrt{\frac{\epsilon_k+U_{BB}N}{\sqrt{\epsilon_k^2+2\epsilon_k U_{BB}N}}-2\sqrt{\frac{(\epsilon_k+U_{BB}N)^2-(\epsilon_k^2+2\epsilon_k U_{BB}N)}{4(\epsilon_k^2+2\epsilon_k U_{BB}N)}}}\right)(b_k^+ + b_k)\right]\\
=&\sum_{k\neq 0}\left[\left(U\sqrt{\frac{\epsilon_k+U_{BB}N}{\sqrt{\epsilon_k^2+2\epsilon_k U_{BB}N}}-\frac{U_{BB}N}{\sqrt{\epsilon_k^2+2\epsilon_k U_{BB}N}}}\right)(b_k^+ + b_k)\right]\\
=&\sum_{k\neq 0}\left[\left(U_{IB}\rho_I\sqrt{\frac{\epsilon_k N}{E_k}}\right)(b_k^+ + b_k)\right].
\end{aligned} \tag{2.21}$$

The fourth line of (2.7) becomes

$$\sum_{k,q\neq 0} U_{IB}(k-q)\rho_I(k-q)\left[(u_q u_k + v_q v_k)b_q^+ b_k + u_q v_k b_q^+ b_k^+ + u_k v_q b_q b_k\right] \tag{2.22}$$

Specially, if $U_{IB}(k-q)\rho_I(k-q)$ both are even or odd functions, i.e. $U_{IB}(\Delta k)\rho_I(\Delta k) = U_{IB}(-\Delta k)\rho_I(-\Delta k)$, then we have

$$\begin{aligned}
&\sum_{k,q\neq 0} U_{IB}(k-q)\rho_I(k-q)\left[(u_q u_k + v_q v_k)b_q^+ b_k + u_q v_k b_q^+ b_k^+ + u_k v_q b_q b_k\right]\\
=&\sum_{k,q\neq 0} U_{IB}(k-q)\rho_I(k-q)\Big[(u_q u_k + v_q v_k)b_q^+ b_k\\
&+\frac{1}{2}(u_q v_k + u_k v_q)b_q^+ b_k^+ + \frac{1}{2}(u_q v_k + u_k v_q)b_q b_k\Big]\\
=&\sum_{k,q\neq 0}\left[V_{qk}^{(1)} b_q^+ b_k + V_{qk}^{(2)}\left(b_q^+ b_k^+ + b_q b_k\right)\right].
\end{aligned} \tag{2.23}$$

where

$$V_{qk}^{(1)} = U_{IB}(k-q)\rho_I(k-q)(u_q u_k + v_q v_k), \tag{2.24a}$$

$$V_{qk}^{(2)} = \frac{1}{2}U_{IB}(k-q)\rho_I(k-q)(u_q v_k + u_k v_q). \tag{2.24b}$$

Then we have a simplified representation of the Hamiltonian:

$$\begin{aligned}
H =& E_0' + \sum_{k\neq 0} E_k b_k^+ b_k + \sum_{k\neq 0}\left[\left(U_{IB}\rho_I\sqrt{\frac{\epsilon_k N}{E_k}}\right)(b_k^+ + b_k)\right]\\
&+ \sum_{k,q\neq 0}\left[V_{q,k}^{(1)} b_q^+ b_k + V_{q,k}^{(2)}(b_q^+ b_k^+ + b_q b_k)\right],
\end{aligned} \tag{2.25}$$

2.2 The Fröhlich Hamiltonian

The concept of polaron is first proposed by L. D. Landau [Landau, 1933b]. Nowadays it is a well-known concept in solid-state physics, where it represents the quasiparticle that consists of an electron in a polar or ionic lattice, dressed with the self-induced polarization cloud, which is described by the lattice vibrations or phonons [Devreese, 2007]. In the context of ultracold atomic gases the electron is replaced by an impurity atom, and the role of the phonons is played by the Bogoliubov excitations of the condensate.

If the spatial extension of a polaron is large compared to the lattice parameter of the solid, the latter can be treated as a polarizable continuum. This is the case of a Fröhlich (large) polaron. The polarization, carried by the longitudinal optical phonons is represented by a set of quantum oscillators with frequency ω_{LO}, the long-wavelength phonon frequency, and the interaction between the charge and the polarization field is linear in the field. When the self-induced polarization caused by an electron or hole becomes of the order of the lattice parameter, a Holstein (small) polaron can arise. As distinct from large polarons, small polarons are governed by short-range interactions. In the following, we will focus on the large polaron theory.

The Fröhlich Hamiltonian is

$$H = \frac{\mathbf{p}^2}{2m_b} + \sum_k \hbar\omega_{\mathsf{LO}}\hat{a}_k^\dagger\hat{a}_k + \sum_k (V_k\hat{a}_{\mathbf{k}}e^{i\mathbf{k}\cdot\mathbf{r}} + V_k^*\hat{a}_{\mathbf{k}}^\dagger e^{-i\mathbf{k}\cdot\mathbf{r}}) \tag{2.26}$$

where $\mathbf{r}$ is the position corrdinate operator of the electron with band mass m_b, $\mathbf{p}$ is its canonically conjugate momentum operator; $\hat{a}_{\mathbf{k}}^\dagger$ and $\hat{a}_{\mathbf{k}}$ are the creation and annihilation operators for longitudinal optical phonons of wave vector $\mathbf{k}$ and energy $\hbar\omega_{\mathsf{LO}}$. The V_k are Fourier components of the electron-phonon interaction

$$V_k = -i\frac{\hbar\omega_{\mathsf{LO}}}{k}(\frac{4\pi\alpha}{V})^{\frac{1}{2}}(\frac{\hbar}{2m_b\omega_{\mathsf{LO}}})^{\frac{1}{4}} \tag{2.27}$$

The strength of the electron-phonon interaction is expressed by a dimensionless coupling constant α, which is defined as:

$$\alpha = \frac{e^2}{\hbar}\sqrt{\frac{m_b}{2\hbar\omega_{\mathsf{LO}}}}(\frac{1}{\epsilon_\infty} - \frac{1}{\epsilon_0}) \tag{2.28}$$

Here, ϵ_∞ and ϵ_0 are the electronic and the static dielectric constant of the polar crystal, respectively. In deriving the form of V_k, expressions (2.27) and (2.28), it was assumed

that (i) the spatial extension of the polaron is large compared to the lattice parameter of the solid ("continuum" approximation), (ii) spin and relativistic effects can be neglected, (iii) the band-electron has parabolic dispersion, (iv) in line with the first approximation it is also assumed that the LO-phonons of interest for the interaction, are the long-wavelength phonons with constant frequency ω_{LO}.

2.3 The Lee-Low-Pines transformation approach

Lee, Low and Pines introduce a canonical transformation when they studied the motion of slow electrons in a polar crystal [Lee *et al.*, 1953]. Using this approach, the Hamiltonian can be transformed from the laboratory frame to a moving frame of the impurity. With this approach, one can obtain a variational upper bound for the ground-state energy.

The wave equation corresponding to the Fröhlich Hamiltonian (2.26) is

$$H\phi = E\phi \tag{2.29}$$

The total momentum of the system is a constant of motion because it commutes with the Hamiltonian (2.26)

$$\mathbf{P}_{op} = \sum_{k} \hbar\mathbf{k}\hat{a}^{\dagger}_{\mathbf{k}}\hat{a}_{\mathbf{k}} + \mathbf{p} \tag{2.30}$$

where $\mathbf{p} = -i\hbar\nabla$ is the momentum of the electron. Indeed, we have

$$\begin{aligned}
[\mathbf{p}, H] &= \sum_{k} \hbar\mathbf{k}(V_k\hat{a}_{\mathbf{k}}e^{i\mathbf{k}\cdot\mathbf{r}} + V_k^*\hat{a}^{\dagger}_{\mathbf{k}}e^{-i\mathbf{k}\cdot\mathbf{r}}); \\
\left[\sum_{k} \hbar\mathbf{k}\hat{a}^{\dagger}_{\mathbf{k}}\hat{a}_{\mathbf{k}}, H\right] &= -\sum_{k} \hbar\mathbf{k}(V_k\hat{a}_{\mathbf{k}}e^{i\mathbf{k}\cdot\mathbf{r}} + V_k^*\hat{a}^{\dagger}_{\mathbf{k}}e^{-i\mathbf{k}\cdot\mathbf{r}}) \\
[\mathbf{P}_{op}, H] &= \left[\sum_{k} \hbar\mathbf{k}\hat{a}^{\dagger}_{\mathbf{k}}\hat{a}_{\mathbf{k}} + \mathbf{p}, H\right] = 0
\end{aligned} \tag{2.31}$$

Therefore, the operators H and $\mathbf{P}_{op}$ have a common set of basis functions: $H\phi = E\phi$ and $\mathbf{P}_{op}\phi = \mathbf{P}\phi$. It is possible to transform to a representation in which $\mathbf{P}_{op}$ becomes a constant number $\mathbf{P}$, and in which the Hamiltonian no longer contains the electron coordinates. The canonical transformation required is $\phi = S_1\psi$, where

$$S_1 = \exp\left[-\frac{i}{\hbar}(\sum_{k} \hbar\mathbf{k}\hat{a}^{\dagger}_{\mathbf{k}}\hat{a}_{\mathbf{k}}) \cdot \mathbf{r}\right] \tag{2.32}$$

With this transformation, one arrives at

$$H' = S_1^{-1} H S_1 = \frac{\left(\mathbf{P} - \sum_k \hbar\mathbf{k}\hat{a}_{\mathbf{k}}^\dagger \hat{a}_{\mathbf{k}}\right)}{2m_b} + \sum_k \hbar\omega_{\mathsf{LO}} \hat{a}_{\mathbf{k}}^\dagger \hat{a}_{\mathbf{k}} + \sum_k (V_k \hat{a}_{\mathbf{k}} + V_k^* \hat{a}_{\mathbf{k}}^\dagger), \tag{2.33}$$

where $\mathbf{p}$ is set to its eigenvalue P. The aim is to calculate for a given momentum $\mathbf{P}$ the lowest eigenvalue $E(P)$ of the Hamiltonian (2.33). The canonical transformation (2.32) formally eliminates the electron operators from the Hamiltonian. LLP use further a variational method of calculation. The trial wave function is chosen as $\psi = S_2\psi_0$, where ψ is the eigenstate of the unperturbed Hamiltonian with no phonons present (vacuum state). Specifically, ψ_0 is defined by $\hat{a}_{\mathbf{k}}\psi_0 = 0$, and the second canonical transformation:

$$S_2 = \exp\left[\sum_k (a_k^\dagger f_k - a_k f_k^*)\right], \tag{2.34}$$

where f_k are treated as variational functions and will be chosen to minimize the energy. The physical significance of Eq. (2.34) is that it "dresses" the electron with the virtual phonon field, which describes the polarization. Viewed as a unitary transformation, S_2 is a displacement operator on $\hat{a}_k$ and $\hat{a}_k^\dagger$. With virtue of transformation (2.34), we obtain:

$$\begin{aligned} S_2^{-1} H' S_2 &= \frac{\left[\left(\mathbf{P} - \sum_k \hbar\mathbf{k}\hat{a}_k^\dagger \hat{a}_k\right) - \sum_k \hbar\mathbf{k}|f_k|^2 - \sum_k \hbar\mathbf{k}\left(\hat{a}_k^\dagger f_k + a_k f_k^*\right)\right]^2}{2m_b} \\ &+ \sum_k \hbar\omega_{\mathsf{LO}}\left(hata_k^\dagger \hat{a}_k + |f_k|^2 + \hat{a}_k^\dagger f_k + \hat{a}_k f_k^*\right) \\ &+ \sum_k \left[V_k(a_k + f_k) + V_k^*(a_k^\dagger + f_k^*)\right] \\ &= H_0 + H_1 \end{aligned} \tag{2.35}$$

where

$$\begin{aligned} H_0 &= \frac{\left[\mathbf{P} - \sum_k \hbar\mathbf{k}\hat{a}_k^\dagger \hat{a}_k\right]^2 + \left[\sum_k \hbar\mathbf{k}|f_k|^2\right]^2}{2m_b} + \sum_k [V_k f_k + V_k^* f_k^*] \\ &+ \sum_k |f_k|^2 \left[\hbar\omega_{\mathsf{LO}} - \frac{\hbar\mathbf{k}\cdot\mathbf{P}}{m_b} + \frac{\hbar^2 k^2}{2m_b}\right] + \frac{\hbar^2}{m_b}\sum_k \mathbf{k}\hat{a}_k^\dagger \hat{a}_k \sum_{k'} \mathbf{k}'|f_{k'}|^2 \\ &+ \left\{\sum_k \hat{a_k}\left[V_k + f_k^*\left(\hbar\omega_{LO} - \frac{\hbar\mathbf{k}\cdot\mathbf{P}}{m_b} + \frac{\hbar^2 k^2}{2m_b} + \frac{\hbar^2\mathbf{k}}{m_b}\sum_{k'} \mathbf{k}'|f_{k'}|^2\right)\right] + H.c.\right\} \\ &+ \sum_k \hbar\omega_{\mathsf{LO}} \hat{a}_k^\dagger \hat{a}_k \end{aligned} \tag{2.36}$$

$$\begin{aligned} H_1 &= \sum_{k,k'} \frac{\hbar^2\mathbf{k}\cdot\mathbf{k}'}{2m_b}\left(\hat{a}_k \hat{a}_{k'} f_k^* f_{k'}^* + 2\hat{a}_k^\dagger \hat{a}_{k'} f_k f_{k'}^* + \hat{a}_k^\dagger \hat{a}_{k'}^\dagger f_k f_{k'}\right) \\ &+ \sum_{k,k'} \frac{\hbar^2\mathbf{k}\cdot\mathbf{k}'}{2m_b}\left(\hat{a}_k^\dagger \hat{a}_k \hat{a}_{k'} f_{k'}^*\right) \end{aligned} \tag{2.37}$$

With the help of $\hat{a}_{\mathbf{k}}\psi_0 = 0$, we can minimize the energy corresponding to (2.36) by imposing

$$\frac{\delta E}{\delta f_k} = 0, \frac{\delta E}{\delta f_k^\dagger} = 0 \tag{2.38}$$

The H_0 is diagonal in a representation in which $\hat{a}_k^\dagger \hat{a}_k$ is diagonal. Therefore, the variational calculation by LLP is equivalent to the use of (2.36) as the total Hamiltonian provided f_k^* sovled by minimization equations. An estimate of the accuracy of the LLP variational procedure was obtained by an estimate of the effect of H_1 using a perturbation theory.

As a summary, Bogoliubov transformation and LLP transformation were introduced in this chapter. These two methods are widely used to diagonalize Hamiltonians, which yields the stationary solutions of the corresponding Schrödinger equation. In what follows, we are going to apply these concepts to the ”angulon problem” - a rotating impurity coupled to a many-body environment.

3 The angulon Hamiltonian

3.1 The concept of angulon quasiparticle

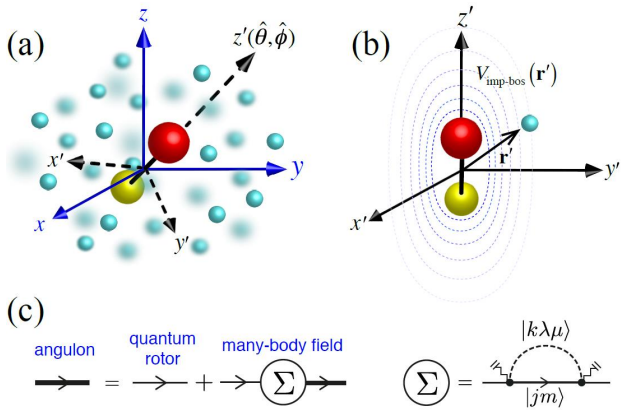

Figure 3.1: Schematic illustration of the angulon: a quantum rotor dressed by a quantum field (adapted from [Schmidt and Lemeshko, 2015]). (a) The interaction of a quantum rotor with a quantum many-body system explicitly depends on the rotor angular coordinates, $(\hat{\theta}, \hat{\phi})$, in the laboratory frame. (b) The anisotropic rotor-boson interaction is defined in the rotor coordinate frame $\mathbf{r}$. (c) Feynman diagrams for the angulon quasiparticle.

The angulon can be understood as a quantum rotor dressed by a quantum field of many-body excitations. As schematically illustrated in Fig 3.1, the angulon is a collective object, characterized by the total angular momentum of the system, of which it is an eigenstate. In 2017, it has been shown that the angulon quasiparticles are indeed formed out of molecules rotating in superfluid ^{4}He [Lemeshko, 2017]. One of the key predictions of the angulon theory are the so called 'angulon instabilities' [Lemeshko and Schmidt, 2017; Schmidt and Lemeshko, 2015; Schmidt and Lemeshko, 2016] occurring at some critical value of the molecule-superfluid coupling, where the angulon

quasiparticle becomes unstable and one or a few quanta of angular momentum are transferred from the impurity to the superfluid. Further research [Lemeshko, 2017; Cherepanov and Lemeshko, 2017; Shepperson *et al.*, 2017b] has verified that the predictions of the angulon theory are in very good agreement with experiment for a broad range of molecular impurities, and can be used to explain the anomalous broadening of the spectroscopic lines observed for molecules in superfluid helium nanodroplets [Shepperson *et al.*, 2017a]. Very recently, the concept of rotating quasiparticle was also tackled through a different approach based on the path-integral formalism [Bighin and Lemeshko, 2017].

The angulon is quite different from other impurities: as opposed to translations, quantum rotations in three dimensions are described by a non-Abelian $SO(3)$ algebra and possess a discrete energy spectrum. This leads to a series of novel, highly nontrivial phenomena [Yakaboylu and Lemeshko, 2017; Redchenko and Lemeshko, 2016b; Shepperson *et al.*, 2017b; Yakaboylu *et al.*, 2017; Midya *et al.*, 2016a; Li *et al.*, 2017]: for instance, a strong screening can take place in the presence of a neutral polarizable environment [Yakaboylu and Lemeshko, 2017], and molecular impurities with field induced pendular motion can form spherical harmonic librators, whose pendular motion is altered by the field of phonon excitations. [Redchenko and Lemeshko, 2016b]. The first-principle Hamiltonian which describes the systems in terms of bosonic atoms interacting with a single molecule can be written as

$$\hat{H} = \hat{H}_{mol} + \hat{H}_{bos} + \hat{H}_{mol-bos} \tag{3.1}$$

where the three terms are, respectively, the Hamiltonians of the isolated molecule, the unperturbed bath of bosons, and the interaction between molecule and bosonic bath. In what follows we describe each term in detail.

3.2 Molecular Hamiltonian

Because of their much larger mass, the nuclei in a molecule move much slower than electrons. This implies that the electrons can nearly immediately adjust their positions to the new nuclear configuration when the nuclei move. Although the electronic wave functions $\psi(r, R)$ depend parametrically on the internuclear distance R they are barely

affected by the velocity of the moving nuclei. The kinetic energy of the nuclear motion $E_{kin} = \frac{1}{2}Mv^2$ is small compared to that of the electrons. We therefore write the total Hamiltonian of a diatomic molecule as the sum $H_{mol} = H_0 + T_k$ of the Hamiltonian H_0 of the rigid molecule and T_k of the kinetic energy of the nuclei. Since the latter is small compared to the total energy of a rigid molecule we can regard T_k as a small perturbation of H_{mol}. In this case the total wave function

$$\psi(r_i, \mathbf{R}_k) = \chi(\mathbf{R}_k) \cdot \Phi(r_i, \mathbf{R}_k) \tag{3.2}$$

can be written as the product of the molecular wave function $\chi(\mathbf{R}_k)$ (which depends on the positions $\mathbf{R}_k$ of the nuclei), and the electronic wave function $\Phi(r_i, \mathbf{R}_k)$ of the rigid molecule at arbityary but fixed nuclear positions $\mathbf{R}_k$, where the electron coordinates r_i are the variables. The total energy is the sum of the energy the rigid molecule in the nth electronic state and the kinetic energy ($E_{vib} + E_{rot}$) of the nuclei. The molecular electronic energy depends only on the internuclear distance, and not on the angles, therefore it is spherically symmetric. Moreover, interaction s with the environment are rarely strong enough to disturb the electronic spectrum of the molecule. Therefore, within the Born-Oppenheimer approximation Eq.(3.2), we set the electron wavefunction $\Phi(r_i, \mathbf{R}_k)$ in its ground state, and focus exclusively on the rotational degrees of freedom. The wave function $\chi(\mathbf{R}) = \chi(R, \theta, \varphi)$ depends on all three variables, including the angles θ and φ. We therefore try the product ansatz

$$\chi(R, \theta, \varphi) = S(R) \cdot Y(\theta, \varphi) \tag{3.3}$$

The radial function $S(R)$ depends on the radial form of the potential, while the spherical surface harmonics $Y(\theta, \varphi)$ are solutions for all spherically symmetric potentials, independent of their radial form. A diatomic molecule with the atomic masses M_A and M_B can rotate around any axis through the center of mass perpendicular to the internuclear axis with the angular velocity ω. Its rotational energy is then

$$E_{rot} = \frac{1}{2}I\omega^2 = J^2/(2I) \tag{3.4}$$

Here $I = M_A R_A^2 + M_B R_B^2 = MR^2$ and $M = M_A M_B/(M_A + M_B)$ is the moment of inertia of the molecule with respect to the rotational axis and $|J| = I\omega$ is its rotational angular momentum. For a rotation around the internuclear axis the contribution of the nuclei to the moment of inertia is vanishingly small, because they lie on this axis. The contribution

of the electron shell is also small because of the small electron mass. Therefore, the rotational energy for a rotation around this axis is very large and cannot be excited at thermal energies. Since the square of the angular momentum $|J|^2 = J(J+1)\hbar^2$ can take only discrete values that are determined by the rotational quantum number J , the rotational energies of a molecule in its equilibrium position with an internuclear distance R_e are represented by a series of discrete values

$$E_{rot} = \frac{J(J+1)\hbar^2}{2MR_e^2} \tag{3.5}$$

In the spectroscopic literature, the rotational term values $F(J) = E(J)/(hc)$ are used instead of the energies, then we have

$$F_{rot}(J) = \frac{J(J+1)\hbar^2}{2hcMR_e^2} = B_e J(J+1) \tag{3.6}$$

with the rotational constatn

$$B_e = \frac{\hbar}{4\pi cMR_e^2} \tag{3.7}$$

which is determined by the reduced mass M and the equilibrium nuclear distance R_e. For historical reasons one writes B_e in units of cm^{-1} instead of m_{-1}.

3.3 Boson Hamiltonian

Consider a system of interacting bosons without a molecule being present. Its Hamiltonian can be written in momentum representation as:

$$\hat{H}_{bos} = \sum_{\mathbf{k}} \epsilon(\mathbf{k}) \hat{a}^\dagger_{\mathbf{k}} \hat{a}_{\mathbf{k}} + \frac{1}{2} \sum_{\mathbf{k},\mathbf{k}',\mathbf{q}} V_{bb}(q) \hat{a}^\dagger_{\mathbf{k}'-\mathbf{q}} \hat{a}^\dagger_{\mathbf{k}'+\mathbf{q}} \hat{a}_{\mathbf{k}'} \hat{a}_{\mathbf{k}} \tag{3.8}$$

The first term of Eq. (3.8) describes the kinetic energy of bosons, $\epsilon(k) = k^2/(2m)$, with m the bosonic mass. The second term gives the boson-boson interactions, whose strength in momentum space is given by $V_{bb}(q)$. Note that in our convention the operators $\hat{a}_{\mathbf{k}}$ and $\hat{a}_{\mathbf{k}}$ are not dimensionless, but carry a dimension of [Length]$^{-3}$. Furthermore, since the Fourier transform involves three-dimensional integration in real space, the momentum-dependent interaction potential $V_{bb}(q)$ carries a unit of [Energy]$\times$[Length]^3. In the region of weakly-interacting Bose gas, with the Bogoliubov approximation, $\hat{a}_{\mathbf{k}} = (2\pi)^3 \hat{\phi}_0 \delta_{\mathbf{k},0} + \hat{\phi}_{\mathbf{k}\neq 0}$, we can obtain

$$\hat{H}_{bos} = \sum_{\mathbf{k}} [\epsilon(\mathbf{k}) + V_{bb}(\mathbf{k})n] \hat{\phi}^\dagger_{\mathbf{k}} \hat{\phi}_{\mathbf{k}} + \frac{n}{2} \sum_{\mathbf{k}} V_{bb}(\mathbf{k}) \left[\hat{\phi}^\dagger_{\mathbf{k}} \hat{\phi}^\dagger_{-\mathbf{k}} + \hat{\phi}_{\mathbf{k}} \hat{\phi}_{-\mathbf{k}} \right] \tag{3.9}$$

As discussed in chapter 2, by applying Bogoliubov transformation of the field operators [Pitaevskii and Stringari, 2016]

$$\hat{\phi}_{\mathbf{k}} = u_{\mathbf{k}}\hat{b}_{\mathbf{k}} + v^*_{-\mathbf{k}}\hat{b}^\dagger_{-\mathbf{k}} \tag{3.10}$$

$$\hat{\phi}^\dagger_{\mathbf{k}} = u^*_{\mathbf{k}}\hat{b}^\dagger_{\mathbf{k}} + v^*_{-\mathbf{k}}\hat{b}_{-\mathbf{k}} \tag{3.11}$$

we can rewrite the (3.9) as (up to a constant shift)

$$\hat{H}_{bos} = \sum_{\mathbf{k}} \omega(k)\hat{b}^\dagger_{\mathbf{k}}\hat{b}_{\mathbf{k}} \tag{3.12}$$

where $\omega(\mathbf{k}) \equiv \omega(k)$ is given by

$$\omega(k) = \sqrt{\epsilon(k)[\epsilon(k) + 2V_{bb}(k)n]} \tag{3.13}$$

Thus, the Bogoliubov transformation allows to describe the bosonic systems in terms of non-interacting Bogoliubov quasiparticles with a dispersion relation $\omega(k)$. Since we are interested in rotating impurities and the angular momentum properties of the condensate, it is much more convenient to work in the angular momentum representation for the single-particle basis instead of the Cartesian one. Hence we perform a single-particle basis change which yields the following transformation of the creation operators:

$$\hat{b}^\dagger_{k\lambda\mu} = \frac{k}{(2\pi)^{3/2}} \int d\Phi_k d\Theta_k \sin\Theta_k \hat{b}^\dagger_{\mathbf{k}} i^{-\lambda} Y_{\lambda\mu}(\Theta_k, \Phi_k) \tag{3.14}$$

$$\hat{b}^\dagger_{\mathbf{k}} = \frac{(2\pi)^{3/2}}{k} \sum_{\lambda\mu} \hat{b}^\dagger_{k\lambda\mu} i^{\lambda} Y^*_{\lambda\mu}(\Theta_k, \Phi_k) \tag{3.15}$$

Here, the quantum numbers λ and μ label the angular momentum of the bosonic excitation and its projection onto the laboratory-frame Z-axis, respectively.

3.4 Molecule-boson interaction

The interaction between an impurity and the bosonic gas is given in the most general form by

$$\hat{H}_{mol-bos} = \sum_{\mathbf{k},\mathbf{q}} \hat{V}_{mol-bos}(\mathbf{q}, \hat{\phi}, \hat{\theta}, \hat{\gamma})\hat{\rho}(\mathbf{q})\hat{a}^\dagger_{\mathbf{k}+\mathbf{q}}\hat{a}_{\mathbf{k}} \tag{3.16}$$

where $\hat{\rho}(\mathbf{q}) = e^{-i\mathbf{q}\cdot\mathbf{r}}$ is the Fourier-transformed density of an impurity which is situated at position $\mathbf{r}$, the corresponding density in real space is given by a Dirac δ-function. The fact that anisotropic molecular geometry gives rise to anisotropic molecule-boson

interactions is represented in Eq. (3.16) by the operator $\hat{V}_{mol-bos}(\mathbf{q}, \hat{\phi}, \hat{\theta}, \hat{\gamma})$ which explicitly depends on the orientation of the molecule in space, as given by the Euler angle operators $(\hat{\phi}, \hat{\theta}, \hat{\gamma})$. Now, we define two coordinate frames: the laboratory frame, (X, Y, Z), in which the bosonic atoms are at rest when the molecule is absent, and the molecular one, (x, y, z), used to define the microscopic molecule-boson interaction potential. The interaction potential between a molecule and an atom is a function of the spherical coordinates in the molecular frame, (θ_r, ϕ_r). Such a potential can be expanded over the spherical harmonics as:

$$V_{mol-bos}(r) = \sum_{\lambda} V_{\lambda}(r) Y_{\lambda 0}(\theta_r, \phi_r) \tag{3.17}$$

In order to transform Eq. (3.17) to the laboratory frame, where the bosonic part of the Hamiltonian is defined, we use Wigner rotation matrices [Varshalovich *et al.*, 1988b]:

$$Y_{\lambda 0}(\theta_r, \phi_r) = \sum_{\mu} \hat{D}^{\lambda}_{\mu 0}(\hat{\phi}, \hat{\theta}, \hat{\gamma}) Y_{\lambda \mu}(\Theta_R, \Phi_R) \tag{3.18}$$

For a linear molecule, the third angle, $\hat{\gamma}$, can be set to zero. In this case, we obtain

$$\hat{V}_{mol-bos}(\mathbf{r}, \hat{\theta}, \hat{\phi}) = \sum_{\lambda\mu} \sqrt{\frac{4\pi}{2\lambda+1}} V_{\lambda}(r) Y_{\lambda\mu}(\Theta_R, \Phi_R) \hat{Y}^{*}_{\lambda\mu}(\hat{\theta}, \hat{\phi}) \tag{3.19}$$

Here $\mathbf{r} \equiv (r, \Theta_R, \Phi_R)$ gives the boson's position in the laboratory-frame coordinates, whose axis' orientation is measured by the operators $(\hat{\theta}, \hat{\phi})$. The corresponding Fourier transform is

$$\hat{V}_{mol-bos}(\mathbf{k}, \hat{\theta}, \hat{\phi}) = \sum_{\lambda\mu} (2\pi)^{3/2} i^{-\lambda} \hat{V}_{\lambda}(k) Y_{\lambda\mu}(\Theta_k, \Phi_k) \hat{Y}^{*}_{\lambda\mu}(\hat{\theta}, \hat{\phi}) \tag{3.20}$$

Then we apply the Bogoliubov approximation and transformation to Eq. (3.20) and obtain:

$$\hat{H}_{mol-bos} = n\hat{V}_{mol-bos}(\mathbf{k}=0, \hat{\theta}, \hat{\phi}) + \sqrt{n} \sum_{\mathbf{k}} \hat{V}_{mol-bos}(\mathbf{k}, \hat{\theta}, \hat{\phi}) \sqrt{\frac{\epsilon(k)}{\omega(k)}} (\hat{b}^{\dagger}_{\mathbf{k}} + \hat{b}_{-\mathbf{k}}) \tag{3.21}$$

In the end, by substituting into Eq. (3.21) the spherical representation of the boson operators, Eq. (3.14), and after integrating over angles, we finally have

$$\hat{H}_{mol-bos} = \sum_{k\lambda\mu} U_{\lambda}(k) \left[\hat{Y}^{*}_{\lambda\mu}(\hat{\theta}, \hat{\phi}) \hat{b}^{\dagger}_{k\lambda\mu} + \hat{Y}_{\lambda\mu}(\hat{\theta}, \hat{\phi}) \hat{b}_{k\lambda\mu} \right] \tag{3.22}$$

where

$$U_{\lambda}(k) = \left[\frac{8nk^2\epsilon(k)}{\omega(k)(2\lambda+1)} \right]^{1/2} \int dr r^2 V_{\lambda}(r) j_{\lambda}(kr) \tag{3.23}$$

For the case of a linear-rotor molecule, we obtain the total Hamiltonian as

$$\hat{H} = B\hat{\mathbf{J}}^2 + \sum_{k\lambda\mu} \omega(k)\hat{b}^\dagger_{k\lambda\mu}\hat{b}_{k\lambda\mu} + \sum_{k\lambda\mu} U_\lambda(k)\left[\hat{Y}^*_{\lambda\mu}(\hat{\theta},\hat{\phi})\hat{b}^\dagger_{k\lambda\mu} + H.c.\right] \tag{3.24}$$

It is important to note that although we have initially derived the specific form of $\omega(k)$ and $U_\lambda(k)$ in for the case of an ultracold molecule coupled to a weakly-interacting BEC, this Hamiltonian can be used to study the transfer of angular momentum between a localized impurity and a bath of harmonic oscillators in the context of other experiments.

4 Variational approaches to quantum impurities

Over the years, the polaron became one of the standard, textbook models of condensed-matter physics, which has been studied using (and thereby spurred the development of) many theoretical approaches. Among those are perturbative techniques [Hubač and Wilson, 2010], canonical transformations [Lee *et al.*, 1953], the Landau-Pekar strong-coupling approach [Casteels *et al.*, 2011b], Feynman's variational path integral method [Feynman, 1955b; Tempere *et al.*, 2009a], as well as numerical techniques based on Monte Carlo [Becker *et al.*, 1983; Peeters and Devreese, 1982c] and renormalization group [Grusdt and Demler, 2015a].

Notably, the polaron concept has proven useful far beyond the original physics problem (electrons in crystals), and was successfully applied to systems as diverse as electrons on the surface of liquid helium [Devreese, 2007; Jackson and Platzman, 1981], doped antiferromagnetic Mott insulators [Dagotto, 1994], magnetic semiconductors [Kaminski and Sarma, 2002], and ultracold gases [Tempere *et al.*, 2009a]. In the quasiparticle picture, the polaron accounts for the effect of the many-body environment on the quantum impurity by means of the renormalisation of the particle parameters – such as its energy and mass. In such a way, the effect of $\sim 10^{23}$ particles of the bath can be understood in terms of a handful of renormalised parameters – a drastic simplification, which in many cases allows to obtain extremely accurate results.

All quantum impurities described by the Fröhlich polaron model are structureless (such as electrons) or can be considered structureless (such as atoms whose electronic structure is not perturbed by their surroundings). A compelling question is whether molecules and – in general – more complex quantum systems can be described as quantum impurities using the quasiparticle approach. Recently, a new quasiparticle, the angulon, has been introduced to describe a molecule interacting with a bosonic many-

body field, such as a superfluid [Schmidt and Lemeshko, 2015; Lemeshko and Schmidt, 2017; Lemeshko, 2017]. While angulons can be thought of as “rotational analogues” of polarons, there are several important differences. First, as opposed to translational motion, rotations in three-dimensional space are described by a non-Abelian $\mathrm{SO}(3)$ algebra, which leads to intricate theoretical machinery of angular momentum addition. Furthermore, anisotropic molecular geometry results in anisotropic impurity-boson coupling, which renders many-body interactions explicitly dependent on the molecular orientation. The unique properties of such a system motivated the introduction of new analytical [Lemeshko and Schmidt, 2017; Bighin and Lemeshko, 2017; Yakaboylu *et al.*, 2018] and numerical techniques [Bighin *et al.*, 2018a], which can be applied to the Fröhlich polaron as well.

In this chapter, we introduce new variational methods for the Fröhlich polaron and for the angulon. In particular, we introduce two variational approaches based on a single-phonon expansion either over the ground-state or after a canonical transformation, leading to two different non-perturbative descriptions of the Fröhlich polaron, as well as a diagonalization technique based on the well-known Pekar ansatz [Pekar, 1946b]. We dub this new technique as ‘Pekar diagonalization’. The results we obtain are benchmarked against Feynman’s all-coupling theory [Feynman, 1955a] and against the Pekar ansatz [Pekar, 1946b].

4.1 Fröhlich Hamiltonian

The Fröhlich Hamiltonian, describing an impurity immersed in a bosonic bath, is given by:

$$\hat{H}_F = \frac{\hat{\mathbf{P}}^2}{2m} + \sum_{\mathbf{k}} \omega(k) \hat{b}^\dagger_{\mathbf{k}} \hat{b}_{\mathbf{k}} + \sum_{\mathbf{k}} V(k) \left(e^{-i\mathbf{k}\cdot\hat{\mathbf{x}}} \hat{b}^\dagger_{\mathbf{k}} + e^{i\mathbf{k}\cdot\hat{\mathbf{x}}} \hat{b}_{\mathbf{k}} \right) . \tag{4.1}$$

Here the first term represents the kinetic energy of an impurity with mass m. The second term, with $\sum_{\mathbf{k}} \equiv \int d^3k/(2\pi)^3$, corresponds to the kinetic energy of the bosons, as parametrised by the dispersion relation $\omega(k)$. The bosonic creation and annihilation operators, $\hat{b}^\dagger_{\mathbf{k}}$ and $\hat{b}_{\mathbf{k}}$, obey the commutation relation $[\hat{b}_{\mathbf{k}}, \hat{b}^\dagger_{\mathbf{k}'}] = (2\pi)^3 \delta(\mathbf{k} - \mathbf{k}')$. Finally, the last term is the impurity-bath interaction, where $V(k)$ determines the coupling strength, and $\hat{\mathbf{x}}$ is the position operator of the impurity with respect to the laboratory frame.

In what follows, we use Fröhlich's original parameters, i.e. a constant dispersion relation for gapped optical phonons, $\omega(k) = \omega_0$, and the coupling strength,

$$V(k) = \sqrt{\frac{2^{3/2}\pi\alpha}{k^2}}\,, \tag{4.2}$$

α being the electron-phonon coupling constant in units of $m = \omega_0 = \hbar \equiv 1$. The Hamiltonian of Equation (4.1) possesses translational symmetry, which follows from the fact that the total linear momentum of the system,

$$\hat{\mathbf{\Pi}} = \hat{\mathbf{P}} + \sum_{\mathbf{k}} \mathbf{k}\hat{b}^\dagger_{\mathbf{k}}\hat{b}_{\mathbf{k}}\,, \tag{4.3}$$

commutes with the Hamiltonian (4.1). Conservation of the total linear momentum allows us to label the polaron quasiparticle with the momentum quantum number.

4.2 Single phonon expansion

Inspired by the so-called 'Chevy ansatz', originally introduced for an imbalanced Fermi-gas [Chevy, 2006a; Ngampruetikorn *et al.*, 2012; Lan and Lobo, 2014], we expand the state vector up a single phonon excitation. Taking into account the conservation of the total linear momentum, we write down the following variational ansatz:

$$|\psi_{\mathbf{p}}\rangle = \sqrt{Z_{\mathbf{p}}}\,|\mathbf{p}\rangle\,|0\rangle + \sum_{\mathbf{k}} \beta_{\mathbf{p}}(\mathbf{k})\,|\mathbf{p}-\mathbf{k}\rangle\,\hat{b}^\dagger_{\mathbf{k}}\,|0\rangle\ , \tag{4.4}$$

where $\sqrt{Z_{\mathbf{p}}}$ and $\beta_{\mathbf{p}}(\mathbf{k})$ are variational parameters with the normalization condition $\sqrt{Z_{\mathbf{p}'}}^*\sqrt{Z_{\mathbf{p}}} + \sum_{\mathbf{k}} \beta_{\mathbf{p}'}(\mathbf{k})^*\beta_{\mathbf{p}}(\mathbf{k}) = \delta(\mathbf{p}'-\mathbf{p})$. Minimization of the functional $\langle\psi_{\mathbf{p}'}|\,\hat{H}_F - E\,|\psi_{\mathbf{p}}\rangle$ with respect to the parameters $\sqrt{Z_{\mathbf{p}}}^*$ and $\beta_{\mathbf{p}}(\mathbf{k})^*$ yields the following coupled equations

$$\frac{\partial F}{\partial \sqrt{Z_{\mathbf{p}}}^*} = |Z_{\mathbf{p}}|\left(\frac{\mathbf{p}^2}{2m} - E\right) + \sum_{\mathbf{k}} \beta_{\mathbf{p}}(\mathbf{k})V(k) = 0, \tag{4.5}$$

$$\frac{\partial F}{\partial \beta_{\mathbf{p}}(\mathbf{k})^*} = \beta_{\mathbf{p}}(\mathbf{k})\left(\frac{(\mathbf{p}-\mathbf{k})^2}{2m} + \omega(k) - E\right) + \sqrt{Z_{\mathbf{p}}}V(k) = 0. \tag{4.6}$$

If we substitute $\beta_{\mathbf{p}}(\mathbf{k})$ from Equation (4.6) into Equation (4.5), we obtain the Dyson equation

$$E = \frac{\mathbf{p}^2}{2m} - \Sigma_{\mathbf{p}}(E)\,, \tag{4.7}$$

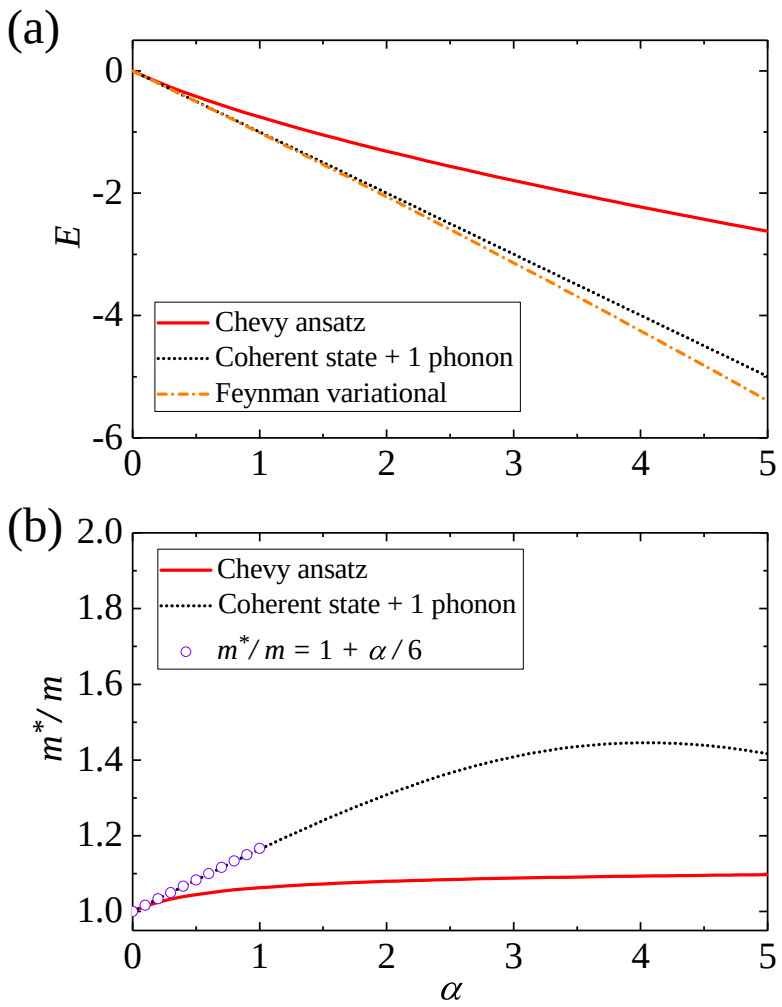

Figure 4.1: (a) The polaron energy as a function of the Fröhlich coupling constant, α, for the Chevy ansatz, Eq.(4.4) (red solid line), coherent state on top of single phonon excitation, Eqs.(4.12) and (4.16) (black dotted line), and the Feynman variational method [Feynman, 1955a] (orange dash-dotted line). (b) Renormalization of the polaron mass as a function of the Fröhlich coupling constant, α, for the Chevy ansatz (red solid line), coherent state on top of single phonon excitation (black dot line), and the weak coupling theory [Devreese, 2015] (purple circles). See the text.

which can be solved to obtain the variational energy E. The self-energy is given by

$$\Sigma_{\mathbf{p}}(E) = \sum_{\mathbf{k}} \frac{V(k)^2}{(\mathbf{p}-\mathbf{k})^2/(2m) + \omega(k) - E}\,, \tag{4.8}$$

which can be solved self-consistently. Combining the variational energy E, the normalization condition, Equation (4.5) and Equation (4.6), one can obtain the values of variational coefficients $\sqrt{Z_{\mathbf{p}}}$ and $\beta_{\mathbf{p}}(\mathbf{k})$.

In the iterative solution to Equation (4.7), the leading-order term is given by $E^{(1)} = \mathbf{p}^2/(2M)$, and the second-order term reads $E^{(2)} = \mathbf{p}^2/(2M) - \Sigma_{\mathbf{p}}(E^{(1)})$, which matches the result of second order perturbation theory. Therefore, the variational energy (4.7) is non-perturbative as it corresponds to resummation over all diagrams describing single-phonon excitations, see Refs. [Lemeshko and Schmidt, 2017; Bighin and Lemeshko, 2017] for further details.

Figure 4.1 (a) shows the Fröhlich polaron energy as calculated from Equation (4.7). In 1955, Feynman developed a superior all-coupling polaron theory using his path-integral formalism, and obtained the self-energy and the effective mass of polarons [Feynman, 1955a]. A comparison with Feynman's all-coupling theory shows that, the Chevy-like ansatz in the case of the Fröhlich polaron, its effectiveness in determining the ground state energy is limited to the weak-coupling region. In addition to this, Figure 4.1 (b), present results for the renormalized polaron mass m^*, defined by

$$\frac{1}{m^*} = \left.\frac{\partial^2 E}{\partial \mathbf{p}^2}\right|_{\mathbf{p}=0} . \tag{4.9}$$

Here, except for very small values of the coupling α, our Chevy-like ansatz deviates from the classical perturbation-theory result $m^*/m = 1 + \alpha/6$ [Feynman, 1955a], tending to a constant value for sufficiently large α. The scope of applicability of the present treatment, however, in the light of the results for the energy presented in Figure 4.1 (a), should not be extended to that region.

In this section, we have shown that the variational ansatz of Equation (4.4) yields a good prediction of ground energy in weak coupling region through a simple, fully analytical calculation. Moreover, working with a variational ansatz makes the underlying physics clear: the variational coefficient $\sqrt{Z_{\mathbf{p}}}$ is the quasiparticle weight, i.e. a measure of the overlap between the dressed impurity and a bare particle, whereas the variational coefficient $\beta_{\mathbf{p}}(\mathbf{k})$ contains information about the occupation of phonon states.

4.3 Coherent state on top of single phonon excitation

Recently a new variational ansatz has been introduced in order to tackle the angulon problem [Schmidt and Lemeshko, 2016] in the limit of a slowly-rotating impurity. This method is based on single phonon excitation expansion after a coherent state transformation that brings the Hamiltonian to a diagonal form in the limit of a slowly rotating impurity. Aiming to use this method for the Fröhlich polaron, we start by applying the Lee-Low-Pines transformation [Lee *et al.*, 1953],

$$\hat{T} = \exp\left(-i\hat{\mathbf{x}} \cdot \sum_{\mathbf{k}} \mathbf{k}\hat{b}_{\mathbf{k}}^{\dagger}\hat{b}_{\mathbf{k}}\right) , \tag{4.10}$$

after which the Fröhlich Hamiltonian then can be written as

$$\hat{H}_F^{'} = \hat{T}^{-1}\hat{H}_F\hat{T} = \frac{1}{2m}\left(\hat{\mathbf{P}} - \sum_{\mathbf{k}} \mathbf{k}\hat{b}_{\mathbf{k}}^{\dagger}\hat{b}_{\mathbf{k}}\right)^2 + \sum_{\mathbf{k}} \omega(k)\hat{b}_{\mathbf{k}}^{\dagger}\hat{b}_{\mathbf{k}} + \sum_{\mathbf{k}} V(k)\left(\hat{b}_{\mathbf{k}}^{\dagger} + \hat{b}_{\mathbf{k}}\right) , \tag{4.11}$$

commuting with $\hat{\mathbf{P}}$, i.e., $[\hat{H}_F^{'}, \hat{\mathbf{P}}] = 0$. Then, the corresponding state vector can be written as a product state,

$$|\Phi_{\mathbf{p}}\rangle = |\varphi\rangle \otimes |\mathbf{p}\rangle \ . \tag{4.12}$$

A similar approach having been introduced in [Shchadilova *et al.*, 2016b]. Here the state vector $|\mathbf{p}\rangle$ with $\mathbf{p}$ being the eigenvalue of the total momentum operator $\hat{P}$, while the bosonic state $|\varphi\rangle$ refers to the bosonic part of the following Hamiltonian

$$\hat{H}_F^{'} = \frac{\mathbf{p}^2}{2m} + \sum_{\mathbf{k}} \tilde{\omega}(\mathbf{k})\hat{b}_{\mathbf{k}}^{\dagger}\hat{b}_{\mathbf{k}} + \sum_{\mathbf{k}} V(k)\left(\hat{b}_{\mathbf{k}}^{\dagger} + \hat{b}_{\mathbf{k}}\right) + \frac{1}{2m}\hat{\Gamma} , \tag{4.13}$$

where $\tilde{\omega}(\mathbf{k}) = \omega(k) - \mathbf{k}\cdot\mathbf{p}/m + k^2/(2m)$, and $\hat{\Gamma} = \sum_{\mathbf{k},\mathbf{k}'} \mathbf{k}\cdot\mathbf{k}'\hat{b}_{\mathbf{k}}^{\dagger}\hat{b}_{\mathbf{k}'}^{\dagger}\hat{b}_{\mathbf{k}}\hat{b}_{\mathbf{k}'}$. In the limit of $m \to \infty$, the Hamiltonian (4.13) can be diagonalized using the following coherent state transformation

$$\hat{U} = \exp\left(-\sum_{\mathbf{k}} \frac{V(k)}{\tilde{\omega}(\mathbf{k})}(\hat{b}_{\mathbf{k}}^{\dagger} - \hat{b}_{\mathbf{k}})\right) . \tag{4.14}$$

After applying this transformation to Equation (4.13) we obtain

$$\hat{H}_F{}'' = \hat{U}^{-1}\hat{H}_F^{'}\hat{U} = \frac{\mathbf{p}^2}{2m} + \sum_{\mathbf{k}} \tilde{\omega}(\mathbf{k})\hat{b}_{\mathbf{k}}^{\dagger}\hat{b}_{\mathbf{k}} - \sum_{\mathbf{k}} \frac{V(k)^2}{\tilde{\omega}(\mathbf{k})} + \frac{1}{2m}\hat{U}^{-1}\hat{\Gamma}\hat{U} . \tag{4.15}$$

Next we introduce the following variational ansatz for the bosonic state:

$$|\varphi\rangle = g\,|0\rangle + \sum_{\mathbf{k}} \alpha(\mathbf{k})\hat{b}_{\mathbf{k}}^{\dagger}\,|0\rangle \ . \tag{4.16}$$

Then, minimization of the functional $F = \langle\varphi|\, \hat{H}_F{}'' - E\,|\varphi\rangle$ with respect to the parameters g^* and $\alpha(\mathbf{k})^*$ gives the following system of equations

$$\frac{\partial F}{\partial g^*} = -g\tilde{E} - \frac{1}{m}\sum_{\mathbf{k},\mathbf{k}'}\alpha(\mathbf{k})\left(\frac{V(k')}{\tilde{\omega}(\mathbf{k}')}\right)^2\frac{V(k)}{\tilde{\omega}(\mathbf{k})}\mathbf{k}\cdot\mathbf{k}' = 0 \tag{4.17}$$

$$\begin{aligned}\frac{\partial F}{\partial \alpha(\mathbf{k})^*} = &-\frac{g}{m}\sum_{\mathbf{k}'}\left(\frac{V(k')}{\tilde{\omega}(\mathbf{k}')}\right)^2\frac{V(k)}{\tilde{\omega}(\mathbf{k})}\mathbf{k}\cdot\mathbf{k}' + \alpha(\mathbf{k})\left[-\tilde{E} + \tilde{\omega}(\mathbf{k}) + \frac{1}{m}\sum_{\mathbf{k}'}\mathbf{k}\cdot\mathbf{k}'\left(\frac{V(k')}{\tilde{\omega}(\mathbf{k}')}\right)^2\right] \\ &+ \frac{1}{m}\sum_{\mathbf{k}'}\alpha(\mathbf{k}')\mathbf{k}\cdot\mathbf{k}'\frac{V(k')}{\tilde{\omega}(\mathbf{k}')}\frac{V(k)}{\tilde{\omega}(\mathbf{k})} = 0\,,\end{aligned} \tag{4.18}$$

where

$$\tilde{E} = E - \frac{\mathbf{p}^2}{2m} + \sum_{\mathbf{k}}\frac{V(k)^2}{\tilde{\omega}(\mathbf{k})} - \frac{1}{2m}\sum_{\mathbf{k},\mathbf{k}'}\mathbf{k}\cdot\mathbf{k}'\left(\frac{V(k)}{\tilde{\omega}(\mathbf{k})}\right)^2\left(\frac{V(k')}{\tilde{\omega}(\mathbf{k}')}\right)^2. \tag{4.19}$$

We further use the rotational symmetry of the problem, and, without loss of generality, assume that $\mathbf{p} \parallel \hat{z}$. Then, solving $\alpha(\mathbf{k})$ from Equation (4.18) as function of g and plugging into Equation (4.17) gives us Dyson equation

$$E = \frac{\mathbf{p}^2}{2m} - \Sigma_{\mathbf{p}}(E)\,, \tag{4.20}$$

from which one can solve for the variational energy E. The self-energy here has the following form

$$\Sigma_{\mathbf{p}}(E) = \sum_{\mathbf{k}}\frac{V(k)^2}{\tilde{\omega}(\mathbf{k})} - \frac{1}{2m}I_z^2 + A_z I_z\,. \tag{4.21}$$

Moreover, we have defined

$$I_z = \sum_{\mathbf{k}} k_z\left(V(k)/\tilde{\omega}(\mathbf{k})\right)^2 \tag{4.22}$$

and

$$A_z = \frac{I_z}{m}\sum_{\mathbf{k}}\frac{k_z^2}{m}\frac{(V(k)/\tilde{\omega}(\mathbf{k}))^2}{-\tilde{E} + \tilde{\omega}(\mathbf{k}) + k_z I_z/m}\left(1 + \sum_{\mathbf{k}}\frac{k_z^2}{m}\frac{(V(k)/\tilde{\omega}(\mathbf{k}))}{-\tilde{E} + \tilde{\omega}(\mathbf{k}) + k_z I_z/m}\right)^{-1}. \tag{4.23}$$

Of course, in the limit of $m \to \infty$, we obtain the deformation energy of the bath, $E = -\sum_{\mathbf{k}} V(k)^2/\omega(k)$.

In Figure 4.1 (a), we study the resulting polaron energy as a function of the Fröhlich coupling constant, α. The treatment developed in the present Section provides an energy estimate remarkably better than the Chevy-like ansatz introduced in the previous Section, and in particular the energy is considerably close to Feynman's all-coupling theory [Feynman, 1955a] over a broad range of values of α. In addition to this, Figure 4.1

(b) shows the renormalization of the polaron mass as a function of α, the result of the approach developed in the present Section being considerably larger than that obtained in previous Section, coinciding with the the perturbation-theory result $m^*/m = 1 + \alpha/6$ up to $\alpha \sim 1$.

4.4 Pekar Diagonalization

4.4.1 Polaron

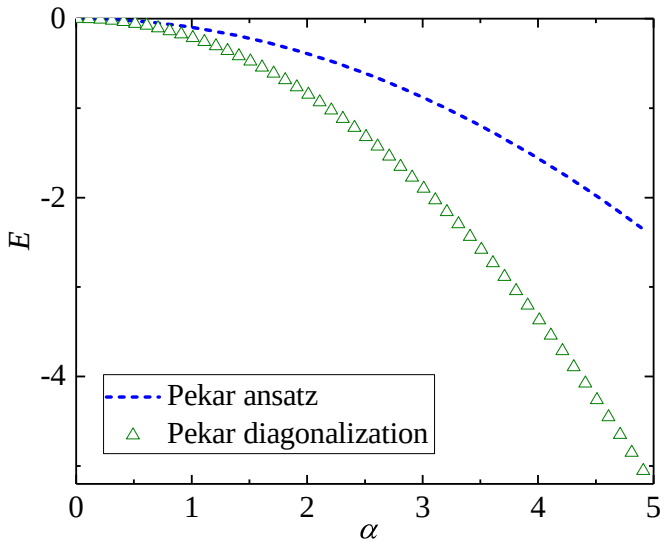

Figure 4.2: The polaron energy as a function of the Fröhlich coupling constant, α, for the Pekar ansatz, Eq.(4.24) (blue dash line), and the Pekar diagonalization technique, Eqs.(4.29) and (4.33) (green triangles). See the text.

The strong-coupling theory of the Fröhlich Hamiltonian can be studied within the Pekar ansatz [Pekar, 1946b; Devreese, 2015]:

$$|\Psi_P\rangle = |\varphi\rangle \otimes |\xi_B\rangle \ , \tag{4.24}$$

where $|\varphi\rangle$ and $|\xi_B\rangle$ correspond to the impurity wavefunction and the bosonic state, respectively. The Pekar treatment that we are now going to briefly review essentially corresponds to the Born-Oppenheimer approximation. It is assumed that the phonons and the impurity have two completely different timescales, or, more precisely, that the

phonons can adjust instantaneously as the slowly moving impurity changes its position. In order to carry out this plan one takes the expectation value, $\langle\varphi|\,\hat{H}_F\,|\varphi\rangle$, the resulting effective bosonic Hamiltonian can be diagonalized using the following coherent-state transformation:

$$\hat{U} = \exp\left[-\sum_{\mathbf{k}} \frac{V(\mathbf{k})}{\omega(k)}\left(\langle e^{-i\mathbf{k}\cdot\hat{\mathbf{x}}}\rangle \hat{b}^{\dagger}_{\mathbf{k}} - \text{H.c.}\right)\right], \tag{4.25}$$

where $\langle\hat{A}\rangle \equiv \langle\varphi|\,\hat{A}\,|\varphi\rangle$. The bosonic state minimizing the Pekar energy is given by $|\xi_B\rangle = \hat{U}\,|0\rangle$, and the respective ground-state energy is:

$$\varepsilon_0 = \frac{1}{2m}\langle\hat{\mathbf{P}}^2\rangle - \sum_{\mathbf{k}} \frac{|V(\mathbf{k})\langle e^{-i\mathbf{k}\cdot\hat{\mathbf{x}}}\rangle|^2}{\omega(k)}\,. \tag{4.26}$$

In general, the impurity wavefunction is assumed to be a localized function in the real space. Here we model it by the following radial Gaussian function [Devreese, 2015]

$$\varphi(\mathbf{x}) = \left(\frac{\beta}{\pi}\right)^{3/4} e^{-\beta r^2/2}\,. \tag{4.27}$$

Minimization of the Pekar energy (4.26) with respect to the variational parameter β yields [Devreese, 2015]

$$\varepsilon_0 = -\frac{\alpha^2}{3\pi}\,. \tag{4.28}$$

In what follows we present an extension of the Pekar approach that we dub ‘Pekar diagonalization’. For this purpose, we introduce the following state vectors

$$|\Psi_n\rangle = |\varphi_n\rangle \exp\left(-\hat{X}_{nn}\right)|0\rangle\,, \tag{4.29}$$

where

$$\hat{X}_{nn} = \sum_{\mathbf{k}} \frac{V(\mathbf{k})}{\omega(k)}\left(\langle e^{-i\mathbf{k}\cdot\hat{\mathbf{x}}}\rangle_{nn}\hat{b}^{\dagger}_{\mathbf{k}} - \text{H.c.}\right), \tag{4.30}$$

with $\langle\hat{A}\rangle_{nm} \equiv \langle\varphi_n|\,\hat{A}\,|\varphi_m\rangle$ and φ_n is the impurity wavefunction. Then, the corresponding matrix element can be written as

$$H_{F\,nm} \equiv \langle\Psi_n|\,\hat{H}_F\,|\Psi_m\rangle = \frac{e^{-\Gamma_{nm}}}{2m}\langle\hat{\mathbf{P}}^2\rangle_{nm} + e^{-\Gamma_{nm}}\sum_{\mathbf{k}}\frac{V(\mathbf{k})^2}{\omega(k)}\times \tag{4.31}$$

$$\left(N_{nm}\langle e^{i\mathbf{k}\cdot\hat{\mathbf{x}}}\rangle_{nn}\langle e^{-i\mathbf{k}\cdot\hat{\mathbf{x}}}\rangle_{mm} - \langle e^{-i\mathbf{k}\cdot\hat{\mathbf{x}}}\rangle_{nm}\langle e^{i\mathbf{k}\cdot\hat{\mathbf{x}}}\rangle_{nn} - \langle e^{i\mathbf{k}\cdot\hat{\mathbf{x}}}\rangle_{nm}\langle e^{-i\mathbf{k}\cdot\hat{\mathbf{x}}}\rangle_{mm}\right),$$

where we define $N_{nm} \equiv \langle\varphi_n|\varphi_m\rangle$, and

$$\Gamma_{nm} = \frac{1}{2}\sum_{\mathbf{k}}\left(\frac{V(\mathbf{k})}{\omega(k)}\right)^2\left(\langle e^{-i\mathbf{k}\cdot\hat{\mathbf{x}}}\rangle_{nn}\langle e^{i\mathbf{k}\cdot\hat{\mathbf{x}}}\rangle_{mm} - \langle e^{i\mathbf{k}\cdot\hat{\mathbf{x}}}\rangle_{nn}\langle e^{-i\mathbf{k}\cdot\hat{\mathbf{x}}}\rangle_{mm}\right) \tag{4.32}$$

Naturally, the diagonal terms correspond to Equation (4.26). We note that a similar diagonal technique has been applied in ultracold fermionic and bosonic mixtures [Cao *et al.*, 2017; Mistakidis *et al.*, 2018].

In order to use the diagonalization technique (4.31), we use the following ansatz for the impurity wave function [Hagen *et al.*, 1970]

$$\varphi_n(\mathbf{x}) = N_n e^{-\beta r}(1 + a_1 r + \cdots a_n r^n)\,, \tag{4.33}$$

corresponding to s-wave states. Here β and a_n are the variational parameters with n labeling excited states. After finding the optimum values of the variation parameters for each excited state, we can diagonalize Equation (4.31). In Figure 4.2, we show the corresponding energy, where we use only 2 basis vectors. It can be seen that the Pekar diagonalization technique remarkably improves the Pekar ansatz Eq.(4.24) in the strong-coupling region, and more accurate results can be given with larger matrix or with a better trial state $\varphi_n(x)$. Our aim here is to show the improvement of Pekar diagonalization as compared to the Pekar treatment, the comparison with other methods will be discussed in the next subsection.

4.4.2 Angulon

As a next step, we show that the Pekar diagonalization we have just introduced can be applied to the angulon, i.e. a quasiparticle describing a quantum molecular impurity with rotational degrees of freedom. In order to do so, let us introduce the angulon Hamiltonian [Schmidt and Lemeshko, 2015; Lemeshko and Schmidt, 2017]:

$$\hat{H_A} \;=\; B\hat{\mathbf{J}}^2 + \sum_{k\lambda\mu} \omega(k)\hat{b}^\dagger_{k\lambda\mu}\hat{b}_{k\lambda\mu} + \sum_{k\lambda\mu} U_\lambda(k)\left[Y^*_{\lambda\mu}(\hat{\Omega})\hat{b}^\dagger_{k\lambda\mu} + \text{H.c.}\right] \tag{4.34}$$

describing a molecular impurity – schematised as a rigid rotor exchanging angular momentum with a bosonic many-body environment. Let us briefly discuss the structure of Equation (4.34). In the first term, expressing the rotational kinetic energy of the molecular impurity, B and $\hat{\mathbf{J}}$ are the rotational constant and the angular momentum operator, respectively. The second term of Equation (4.34) represents the kinetic energy of the non-interacting bosons with dispersion relation $\omega(k)$; the bosonic creation and annihilation operators, $\hat{b}^\dagger_{\mathbf{k}}$ and $\hat{b}_{\mathbf{k}}$, are expressed in the angular momentum basis: $\hat{b}^\dagger_{k\lambda\mu} = k(2\pi)^{-3/2}\int d\Omega_k \hat{b}^\dagger_k i^\lambda Y^*_{\lambda\mu}(\Omega_k)$, while λ and μ define the boson angular mementum

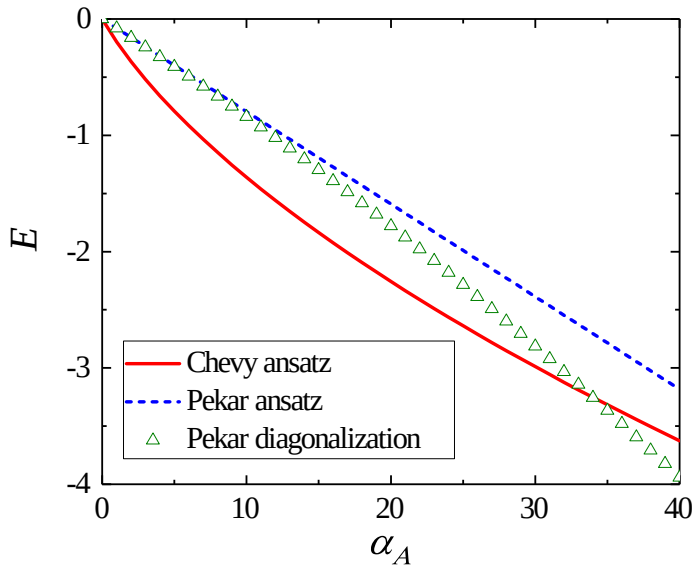

Figure 4.3: The angulon ground state energy as a function of the angulon coupling constant, α_{A}, for the Chevy ansatz [Schmidt and Lemeshko, 2015; Lemeshko and Schmidt, 2017] (red solid line), the Pekar ansatz [Li *et al.*, 2017] (blue dashed line), and the Pekar diagonalization method of Equation (4.35) (green triangles). The basis consists of the vectors with $j = 0, 1, 2$. See the text.

and its projection onto the laboratory-frame z axis, see Ref. [Lemeshko and Schmidt, 2017] for more details. Finally, the third term of Equation (4.34) describes the impurity-bath interaction, where the coupling potential, $U_\lambda(k)$, parametrises the interaction of impurity with bosons carrying angular momentum λ and linear momentum k.

To apply the Pekar diagonalization technique to the angulon, we consider the following basis vector

$$|\Psi_{jm}\rangle = |jm\rangle \exp\left[-\hat{X}_{jm}\right]|0\rangle, \tag{4.35}$$

where the free rotor eigenstates, $|jm\rangle$, are labeled by the angular momentum, j, and its projection, m, on the laboratory z axis. Furthermore, in writing Equation (4.35) we introduced $\hat{X}_{jm}$ defined as follows

$$\hat{X}_{jm} = \sum_{k\lambda\mu} \frac{U_\lambda(k)}{\omega(k)} \left[\langle jm|Y^*_{\lambda\mu}(\hat{\Omega})|jm\rangle\ \hat{b}^\dagger_{k\lambda\mu} - \text{H.c.}\right]. \tag{4.36}$$

Following the scheme outlined in Section 4.4, we obtain for the angulon

$$\begin{aligned}\langle j'm'|H_A|jm\rangle &= Be^{-\Gamma_{j'm',jm}}\langle j'm'|\hat{\mathbf{J}}^2|jm\rangle + e^{-\Gamma_{j'm',jm}}\sum_{k\lambda\mu}\frac{U_\lambda^2(k)}{\omega(k)}\times \\ &\Big[\langle j'm'|Y_{\lambda\mu}(\hat{\Omega})|j'm'\rangle\langle jm|Y^*_{\lambda\mu}(\hat{\Omega})|jm\rangle\delta_{j'j}\delta_{m'm} \\ &-\langle j'm'|Y^*_{\lambda\mu}(\hat{\Omega})|jm\rangle\langle j'm'|Y_{\lambda\mu}(\hat{\Omega})|j'm'\rangle \\ &-\langle j'm'|Y_{\lambda\mu}(\hat{\Omega})|jm\rangle\langle jm|Y^*_{\lambda\mu}(\hat{\Omega})|jm\rangle\Big] \end{aligned} \tag{4.37}$$

where

$$\begin{aligned}\Gamma_{j'm',jm} &= \frac{1}{2}\sum_{k\lambda\mu}\left(\frac{U_\lambda(k)}{\omega(k)}\right)^2\Big(\langle j'm'|Y^*_{\lambda\mu}(\hat{\Omega})|j'm'\rangle\langle jm|Y_{\lambda\mu}(\hat{\Omega})|jm\rangle \\ &-\langle j'm'|Y_{\lambda\mu}(\hat{\Omega})|j'm'\rangle\langle jm|Y^*_{\lambda\mu}(\hat{\Omega})|jm\rangle\Big) \end{aligned} \tag{4.38}$$

becomes zero due to the symmetry of Clebsch-Gordan coefficients [Varshalovich *et al.*, 1988a]. It is worth noting that this is due to the basis vector we chose, see Equation (4.35), and would not necessarily be zero for other choices of basis vectors.

As a simplifying assumption, here we ignore the detailed structure of the anisotropic interaction potential, introducing the following dimensionless impurity-bath interaction parameters:

$$\alpha_\lambda = \sum_k \frac{U_\lambda^2(k)}{\omega_k B}. \tag{4.39}$$

and assuming $U_\lambda(k) \equiv U(k)$, and therefore $\alpha_\lambda \equiv \alpha_{\mathsf{A}}$.

In Figure 4.3 we compare the results of the Pekar diagonalization technique with the 'standard' Pekar approach [Pekar, 1946b; Li *et al.*, 2017] and with the Chevy ansatz for the angulon [Schmidt and Lemeshko, 2015; Lemeshko and Schmidt, 2017]. One can see that, over the whole range of couplings we consider, the Pekar diagonalization technique leads to a lower variational ground state-energy than the standard Pekar approach, which only considers the diagonal term of Hamiltonian, i.e taking only $j' = j$ and $m' = m$ in Equation (4.37). Figure 4.3 also shows that, beyond a critical coupling strength the technique gives a lower ground state energy with respect to Chevy ansatz [Schmidt and Lemeshko, 2015; Cherepanov and Lemeshko, 2017]. An all coupling theory for the angulon system will be considered in further studies.

The Pekar diagonalization technique, as compared with the 'standard' Pekar approach, is particularly powerful in the angulon case as a consequence of the non-Abelian

$\mathrm{SO}(3)$ algebra describing the coupling of angular momenta. More precisely: a phonon coupling two impurity states with angular momentum j and j' will have an angular momentum λ in the range $\{\ |j'-j|, |j'-j|+1, ..., j'+j-1, j'+j\ \}$, thereby leading to a number of nonzero off-diagonal terms in Equation (4.37). The technique we have introduced allows one to obtain more accurate estimates since it accounts for these off-diagonal entries, as opposed to the 'standard' Pekar treatment. This is particularly evident when higher angular momenta are considered; in Figure 4.3, $j = 0, 1, 2$ and $\lambda = 0, 1, 2, 3, 4$ due to the selection rules imposed by the Clebsch-Gordan coefficients.

In this chapter 4, we develop analytic approaches to quantum impurity problems, namely two variational ansaetze and a new diagonalization approach that we called 'Pekar diagonalization'. The results of the variational techniques were compared with well-established benchmarks such as the Pekar ansatz – as far as the strong-coupling regime is concerned – and Feynman's all-coupling variational theory. As expected, an approach inspired by the Chevy ansatz works accurately for smaller values of the coupling whereas approaches based on the Pekar ansatz are reliable in the strong-coupling region. On the other hand, the approximation involving a single-phonon excitation on top of a coherent state transformation provides an estimate remarkably close to Feynman's all-coupling theory in a wide parameter region. A promising future direction consists in using such an ansatz for other polaron problems beyond the Fröhlich model, as well as for other quantum impurity problems.

We have also exemplified the Pekar diagonalization technique by studying the ground energy of both the polaron and the angulon quasiparticles. The results have shown that the diagonalization technique we developed here represents an improvement compared to the 'standard' Pekar ansatz over a wide range of coupling strengths, especially in the strong-coupling region. Pekar diagonalization represents a promising approach to quantum impurities, especially for systems – such as the angulon – where the 'standard' Pekar approach can not provide reliable results.

5 Angular self-localization of impurities rotating in a bosonic bath

The possibility of self localization in electron-lattice system was first pointed out by Landau as early as in 1933 [Landau, 1933a]. It was believed that if the interaction of an electron with lattice vibration strong enough, the electron is supposed to dig its own hole and be trapped there. This self localization transition characters itself by finding a critical coupling strength where discontinuity in the first and/or second derivative of the polaron ground state energy observed. Though the self localization transition is not a phase transition in the strict sense due to the absence of a collective effect, its similarities with the theory of phase transitions still attracted the attention of numerous physicists.

The first candidate for the self localization transition is the free optical polaron described by the Fröhlich Hamiltonian [Fröhlich, 1954; Devreese, 2007]. The system is governed by the long range interaction between polaron and long wavelength longitudinal optical (LO) phonons. The self localization transition in such a system was directly obtained by Lepine-Matz theory [Matz and Burkey, 1971a; Lépine and Matz, 1979], Gaussian model [Gross, 1959b; Luttinger and Lu, 1980a], and Mańka approximation [Manka, 1978]. However, it was subsequently proved to be a property of the approximations themselves rather than an intrinsic property of polaron [Peeters and Devreese, 1982b; Mishchenko *et al.*, 2000b]. The transition was also claimed to exist in the related systems, for instance, optical polaron in external magnetic field [Peeters and Devreese, 1982d], in external Coulomb like potential [Tokuda *et al.*, 1981] and the Wannier exciton system [Sumi, 1977]. Optical polarons in an external attractive short-range potential [Spohn, 1986; Löwen, 1988b; Löwen, 1988a] and in dissipative environment [Guinea *et al.*, 1985] are also believed to exhibit a self localization transition. However, the mathematical proof given by B. Gerlach and H. Löwen argued that there is no self

localization transition exist in optical polaron with the presence of external Coulomb like potential [Gerlach and Löwen, 1991b].

The acoustic polaron corresponds to the interaction of a charge carrier with acoustic phonons, the acoustic phonons have a linear dispersion coupled to the electron through a short-range potential (deformation potential), which is believed to play a crucial role in forming the self localization state [Peeters and Devreese, 1985; Toyozawa, 1961; Sumi and Toyozawa, 1973]. In 2009, Devreese et al. studied the impurity atom in a Bose-Einstein condensate (BEC) with Feynman path-integral treatment [Tempere *et al.*, 2009b], casted the system Hamiltonian in the form of Fröhlich's polaron Hamiltonian, and found the similarities between the impurity in BEC and the acoustic polaron. The self localization transition in BEC-impurity system is obtained with the Pekar ansatz [Cucchietti and Timmermans, 2006a; Kalas and Blume, 2006]. Such a transition in acoustic polaron and BEC impurity was numerically analyzed with the Monte Carlo approach [Wang, 1998; Kornilovitch, 2007; Fantoni, 2012; Vlietinck *et al.*, 2015; Akram and Pelster, 2016]. Various effects on localized impurity were studied in last decade: the localization of a Fermion in a Bosonic bath [Lühmann *et al.*, 2008; Nakano and Yabu, 2016], localization in reduced dimensions [Casteels *et al.*, 2012], at a finite temperature [Boudjemâa, 2014], in the case of multiple bands [Yin *et al.*, 2015], and localization of impurity with a repulsive/attractive interaction potential [Bruderer *et al.*, 2008], to name a few It is also worth to mention that, an understanding of self-localized impurities as a parametric soliton behavior was proposed by K. Sacha and E. Timmermans [Sacha and Timmermans, 2006b], and was applied to study the behavior of impurity in BEC coupled to a transversely laser-pumped multi-mode cavity [Shadkhoo and Bruinsma, 2015] and in BEC with finite temperature [Boudjemâa, 2014]. But new theoretical approaches suggested by F. Grusdt et al. show that the effective mass and energy of polaron have a smooth crossover between weak- and intermediate-coupling strength, no non-analyticity in the accessible parameter range observed [Grusdt *et al.*, 2015; Grusdt and Demler, 2015b; Grusdt, 2016; Grusdt and Fleischhauer, 2016; Shchadilova *et al.*, 2016a]. These results type a question mark on the existence of self localization transition in the BEC-impurity system.

In this chapter, we introduce a novel platform to study the self-localization/delocalization transition – that consisting of an impurity with nonzero orbital angular momentum interacting with a bosonic bath. Such a setting can be represented e.g. by an ultracold alkaline or alkaline-earth dimer immersed into a BEC [Krems *et al.*, 2009; Jin and Ye, 2012], a chemically relevant polyatomic molecule trapped inside a superfluid helium nanodroplet [Toennies and Vilesov, 2004a], as well as by an electronic excitation in a BEC [Balewski *et al.*, 2013] or a solid [Kazimierczuk *et al.*, 2014; Mahan, 1990; Weiss, 2012]. As it has been recently demonstrated, in such settings the impurity-bath interaction leads to formation of quasiparticles of a new kind, the angulons – quantum rotors dressed by a many-particle field [Schmidt and Lemeshko, 2015; Lemeshko and Schmidt, 2017]. While the angulons can be thought of as rotational analogues of polarons, the non-Abelian algebra and discrete energy spectrum associated with quantum rotations makes the angulon physics remarkably different from that of any other impurity problem [Schmidt and Lemeshko, 2015; Schmidt and Lemeshko, 2016; Lemeshko and Schmidt, 2017; Midya *et al.*, 2016a; Redchenko and Lemeshko, 2016a].

In what follows, we develop a strong-coupling angulon theory and reveal the angular self-localization transition, corresponding to the breaking of the impurity spherical symmetry. The transition takes place at a finite impurity-bath coupling strength and is accompanied by a discontinuity in the first derivative of the angulon ground-state energy. Furthermore, we demonstrate that the type of the symmetry breaking depends on the symmetry of the microscopic impurity-atom potential, which results in a number of distinct self-localized states. It is important to note that angulon self-localization takes place in the continuous space of the impurity angles, and is therefore fundamentally different from localization in the Caldeira-Leggett and related models [Leggett *et al.*, 1987; Weiss, 2012].

5.1 The Hamiltonian

We start from the angulon Hamiltonian as derived in Ref. [Schmidt and Lemeshko, 2015]:

$$H = B\hat{\mathbf{J}}^{\mathbf{2}} + \sum_{\mathbf{k}\lambda\mu} \omega_{\mathbf{k}} \hat{\mathbf{b}}^{+}_{\mathbf{k}\lambda\mu} \hat{\mathbf{b}}_{\mathbf{k}\lambda\mu} + \sum_{\mathbf{k}\lambda\mu} \mathbf{U}_{\lambda}(\mathbf{k}) \left[\mathbf{Y}^{*}_{\lambda\mu}(\hat{\theta},\hat{\phi}) \hat{\mathbf{b}}^{+}_{\mathbf{k}\lambda\mu} + \mathbf{Y}_{\lambda\mu}(\hat{\theta},\hat{\phi}) \hat{\mathbf{b}}_{\mathbf{k}\lambda\mu} \right] \qquad (5.1)$$

where $\sum_k \equiv \int dk$ and $\hbar \equiv 1$. For simplicity, we consider a linear-rotor impurity whose kinetic energy is given by the first term of Eq. (5.1), where B is the rotational constant and $\hat{\mathbf{J}}$ is the angular momentum operator. The rotor eigenstates, $|j,m\rangle$, are labeled by the angular momentum, j, and its projection, m, onto the laboratory z-axis. While a rigid linear rotor provides a perfect model for rotation of a diatomic molecule, the first term of Eq. (5.1) is straightforward to extend to more complex polyatomic species or electronic states with nonzero angular momentum [Bernath, 2005; Lefebvre-Brion and Field, 2004; Rudzikas, 1997]. The second term of Eq. (5.1) gives the kinetic energy of the bosons with a dispersion relation ω_k. For convenience, the bosonic creation and annihilation operators, $\hat{b}^+_{\mathbf{k}}$ and $\hat{b}_{\mathbf{k}}$, are expressed in the angular momentum basis, $\hat{b}^+_{k\lambda\mu} = k(2\pi)^{-3/2}\int d\Omega_k \hat{b}^+_{\mathbf{k}} i^\lambda Y^*_{\lambda\mu}(\Omega_k)$. Here, $k = |\mathbf{k}|$, while λ and μ define the boson angular momentum and its projection onto the laboratory-frame z-axis, see Refs. [Schmidt and Lemeshko, 2015; Schmidt and Lemeshko, 2016; Lemeshko and Schmidt, 2017] for details. The third term of Eq. (5.1) describes the impurity-bath interaction which explicitly depends on the impurity orientation in the laboratory frame, as given by the spherical harmonic operators, $Y_{\lambda\mu}(\hat{\theta},\hat{\phi})$ [Varshalovich *et al.*, 1988a]. The coupling constants, $U_\lambda(k)$, parametrize the interaction of the impurity with phonons carrying angular momentum λ and linear momentum k. In Ref. [Schmidt and Lemeshko, 2015] we provided analytic expressions for ω_k and $U_\lambda(k)$ for the case of an ultracold molecule rotating inside a weakly-interacting BEC. For more involved cases, such as molecules in superfluid helium or electronic excitations in solids, the corresponding coupling constants can be used as phenomenological parameters. However, as we demonstrate below, the qualitative properties of the self-localization transition do not depend on the momentum dependence of the impurity-bath interaction and are determined solely by its symmetry. Therefore, in what follows we will consider the Hamiltonian (5.1) from a completely general perspective, without focusing on a particular physical system.

5.2 Product ansatz

In the regime of strong impurity-bath interactions, the angulon ground state can be described using the product (mean-field) ansatz [Landau, 1933a; Pekar, 1946a]:

$$|\psi\rangle = |\mathrm{imp}\rangle \otimes |\mathrm{bos}\rangle \tag{5.2}$$

where $|\mathsf{imp}\rangle$ and $|\mathsf{bos}\rangle$ describe the impurity and the bosonic bath, respectively. By evaluating the expectation value of the Hamiltonian (5.1) relatively to the state (5.2), we obtain that the ground state of the bosonic bath is given by:

$$|\mathsf{bos}\rangle = \exp\left[\sum_{k\lambda\mu}\left(\beta^{\mathsf{imp}}_{k\lambda\mu}\,\hat{b}_{k\lambda\mu} - \beta^{\mathsf{imp}*}_{k\lambda\mu}\,\hat{b}^{+}_{k\lambda\mu}\right)\right]|0\rangle \tag{5.3}$$

where $\beta^{\mathsf{imp}}_{k\lambda\mu} = U_\lambda(k)\langle\mathsf{imp}|Y_{\lambda\mu}(\hat{\theta},\hat{\phi})|\mathsf{imp}\rangle/\omega_k$ parametrically depends on the state of the impurity and $|0\rangle$ is the bosonic vacuum.

The corresponding ground-state angulon energy is given by (in units of B):

$$\frac{E}{B} = \langle\mathsf{imp}|\hat{J}^2|\mathsf{imp}\rangle - \sum_{\lambda\mu}\alpha_\lambda|\langle\mathsf{imp}|Y_{\lambda\mu}(\hat{\theta},\hat{\phi})|\mathsf{imp}\rangle|^2, \tag{5.4}$$

where the dimensionless impurity-bath interaction parameter $\alpha_\lambda = \sum_k U^2_\lambda(k)/(\omega_k B)$. From the form of Eq. (5.4), one can already see that the ground state energy depends on the momentum distribution of the impurity-bath coupling only through the parameters α_λ.

In what follows, we solve Eq. (5.4) variationally assuming the most general form of the impurity state:

$$|\mathsf{imp}\rangle = \sum_{j=0}^{j_{\mathsf{max}}}\sum_{m=-j}^{j} c_{jm}|jm\rangle, \tag{5.5}$$

where c_{jm} are the variational parameters obeying a normalization condition, $\sum_{jm}|c_{jm}|^2 \equiv 1$, and j_{max} provides the angular momentum cutoff. In order to simplify the variational calculations, we assume the rotational symmetry with respect to z-axis and therefore restrict the variational space to $m = 0$ subspace, and use the notation $c_j \equiv c_{j0}$. However, the behavior of the ground-state energies does not change qualitatively if all m-levels are taken into account.

5.3 Self-localization

Let us start from considering the most transparent model with the coupling constants independent of angular momentum, $\alpha_{\forall\lambda} = \alpha$. Fig. 5.1(a) shows the dependence of the ground state energy on the magnitude of the constant potential, α, for different values of the cutoff j_{max}. We see that the energy possesses a nonanalyticity around a critical value $\alpha_c \sim 6$. The inset of Fig. 5.1(a) zooms into the vicinity of the non-analyticity point:

one can see that for larger $j_{\max}$, the nonanaliticity reaches the value of $\alpha_c \approx 5.85$. In the limit of $j_{\max} \to \infty$, the minimizer for $\alpha < \alpha_c$ corresponds to a spherically-symmetric ground state ($c_j = \delta_{j0}$), while for $\alpha > \alpha_c$ the ground state corresponds to a δ-function in the angular space (all $c_j = j_{\max}^{-1/2}$). This result coincides with the one obtained by solving a corresponding nonlinear Schrödinger equation on a two-dimensional plane, where $\alpha \approx 1.86225\pi$ was found to be a critical coupling constant [Weinstein, 1983]. Since the qualitative behavior of the ground-state energies does not depend on the cutoff, in what follows we focus on the case of $j_{\max} = 6$.

For most systems available in experiment, the impurity-bath interaction is dominated by a few first λ-terms and is usually decaying such that α_λ is negligibly small for $\lambda \gtrsim 5$ [Stone, 2013a; Midya *et al.*, 2016a]. In order to cover experimentally relevant cases and illustrate the fact that the transition is universal, we consider several different types of the impurity-bath interactions. Fig. 5.1(b) shows the behavior of ground-state energies for the cases of $\alpha_1 = \alpha$, $\alpha_{\neq 1} = 0$ (yellow crosses); $\alpha_2 = \alpha$, $\alpha_{\neq 2} = 0$ (green dotted line); $\alpha_{\text{odd}} = \alpha$, $\alpha_{\text{even}} = 0$; $\alpha_{\text{even}} = \alpha$, $\alpha_{\text{odd}} = 0$; as well as $\alpha_\lambda = \alpha/(1+\lambda)$ (empty triangles). For comparison, the case of $\alpha_{\forall\lambda} = \alpha$ is shown by the blue solid line. One can see that while the position of the transition point shifts depending on the form of the interaction, the transition still takes place independently of the latter.

In order to get insight into the angular symmetry of the localized impurity, we plot the orientation cosines, $\langle \cos\theta \rangle \equiv \langle \text{imp}| \cos\hat{\theta} |\text{imp}\rangle$, and the alignment cosines, $\langle \cos^2\theta \rangle \equiv \langle \text{imp}| \cos\hat{\theta}^2 |\text{imp}\rangle$, in Figs. 5.1(c) and (d), respectively. One can see that to the left of the transition point, $\langle \cos\theta \rangle = 0$ and $\langle \cos^2\theta \rangle = 1/3$, which reflects the spherical symmetry of the ground angulon state, i.e. $c_{jm} = \delta_{j,0}$ in Eq. (5.5). The transition, on the other hand, is accompanied by an abrupt change in the alignment and/or orientation cosine, which implies the breaking of the impurity spherical symmetry, i.e. angular localization of the angulon. It is important to emphasize that such a symmetry breaking takes place at a finite value of α_c, which is clearly distinct from the case of polarons. There, the same level of approximation – the Landau-Pekar ansatz [Devreese, 2015] – results in a localized impurity with a nonzero ground-state momentum already at infinitely weak coupling.

While the transition occurs independently of the exact form of the α_λ distribution, different symmetries of the impurity-bath interaction result in different symmetries of

the localized states. In particular, the interaction dominated by even λ-terms results in aligned states of definite parity, which are characterized by $\langle \cos\theta \rangle = 0$ and $\langle \cos^2\theta \rangle > 1/3$, which implies $c_{\text{even}} \neq 0$ and $c_{\text{odd}} = 0$ in Eq. (5.5). On the other hand, the α_{odd} terms break the parity symmetry, leading to the oriented localized states with both even and odd c_j's populated.

Unlike in polarons, the angulon Hamiltonian can feature competing interactions of different symmetry, which results in a richer localization behavior. In order to illustrate the latter, in Fig. 5.2(a) we show the 'localization diagram' describing the symmetry of the impurity depending on the magnitudes of α_1 and α_2 (with other coupling constants set to zero). The top subpanel illustrates the distribution of the c_j coefficients and the wavefunctions for corresponding states. The blue region corresponds to a delocalized, spherically-symmetric ground state with $c_j = \delta_{j0}$, the red one corresponds to an aligned impurity state with only even c_j's populated, while the yellow one – to an oriented state with the population spread over both even and odd c_j's.

Fig. 5.2(b) illustrates the dependence of the ground-state energy on α_2 for $\alpha_1 = 0$ and $\alpha_1 = 1$, while Figs. 5.2(c) and (d) show the corresponding orientation cosine, $\langle \cos\theta \rangle$, and alignment cosine, $\langle \cos^2\theta \rangle$. For the case of $\alpha_1 = 0$, there occurs a localization transition in the vicinity of $\text{Ln}[\alpha_2] = 3$, which corresponds to a transition from a spherically symmetric to an aligned impurity. As shown in Figs. 5.2(d), such an isotropic-to-aligned transition is characterized by a sudden change in the alignment cosine, $\langle \cos^2\theta \rangle$.

At a finite value of $\alpha_1 = 1$, however, the behavior of the system changes. Around $\text{Ln}[\alpha_2] = 3$ there occurs an isotropic-to-oriented transition, accompanied by a sudden change in $\langle \cos\theta \rangle$, see Figs. 5.2(c). However, once the parity-preserving coupling approaches the value of $\text{Ln}[\alpha_2] = 5$, a smooth crossover to the aligned phase occurs. This crossover, marked in Figs. 5.2(a) by a dashed line, is not accompanied by a change in the derivative of the ground-state energy and therefore does not represent a sharp transition between the states of different symmetry.

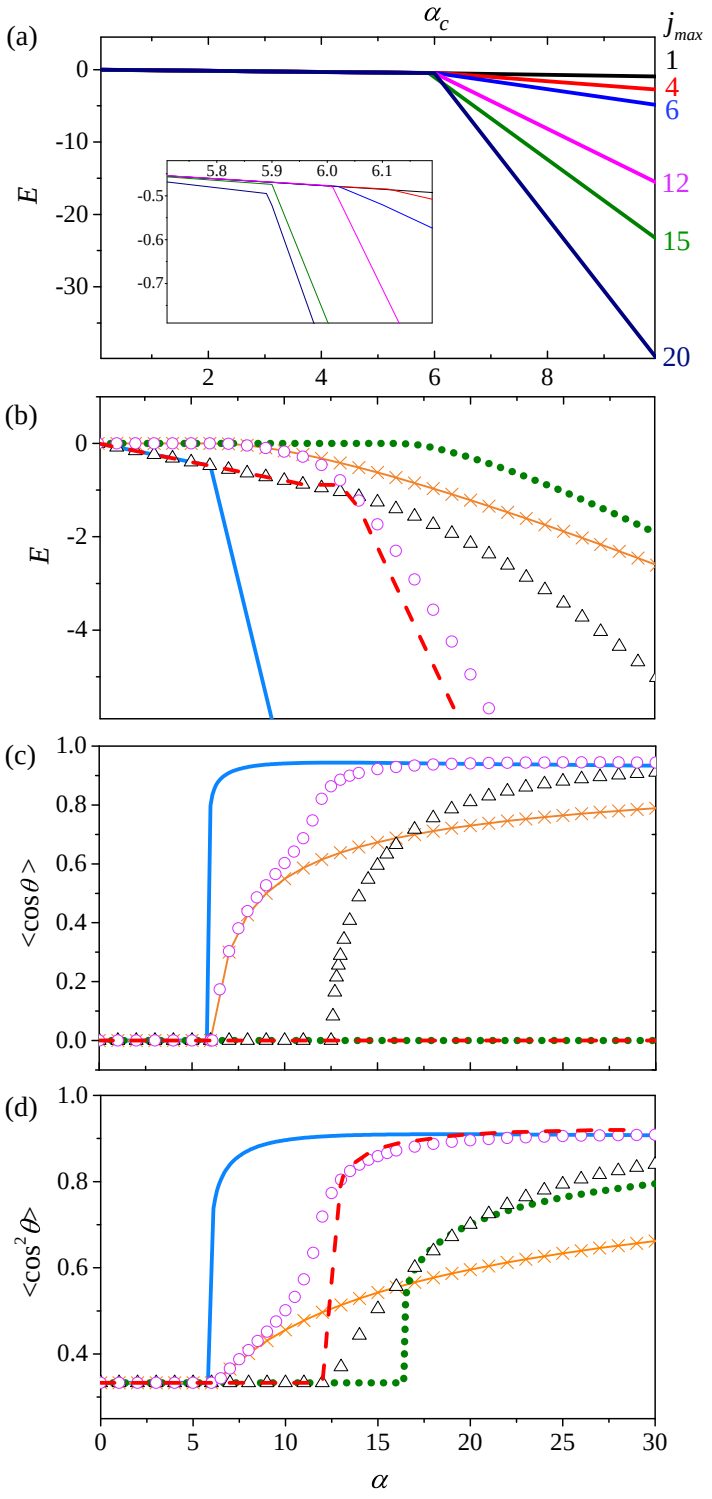

Figure 5.1: (a) Dependence of the impurity ground state energy on the magnitude of the constant impurity-bath coupling strength, $\alpha_{\forall\lambda} = \alpha$, at different values of the cutoff $j_{\max}$. The inset shows the vicinity of the transition point. (b) The case of $j_{\max} = 6$ for various types of the impurity-bath interaction: $\alpha_{\forall\lambda} = \alpha$ (blue solid line); $\alpha_1 = \alpha$, $\alpha_{\neq 1} = 0$ (yellow crosses); $\alpha_2 = \alpha$, $\alpha_{\neq 2} = 0$ (green dotted line); $\alpha_{\text{odd}} = \alpha$, $\alpha_{\text{even}} = 0$; $\alpha_{\text{even}} = \alpha$, $\alpha_{\text{odd}} = 0$; as well as $\alpha_\lambda = \alpha/(1+\lambda)$ (empty triangles). (c) Same as in (b), but for the orientation cosine of the impurity. (c) Same as in (b), but for the alignment cosine of the impurity.

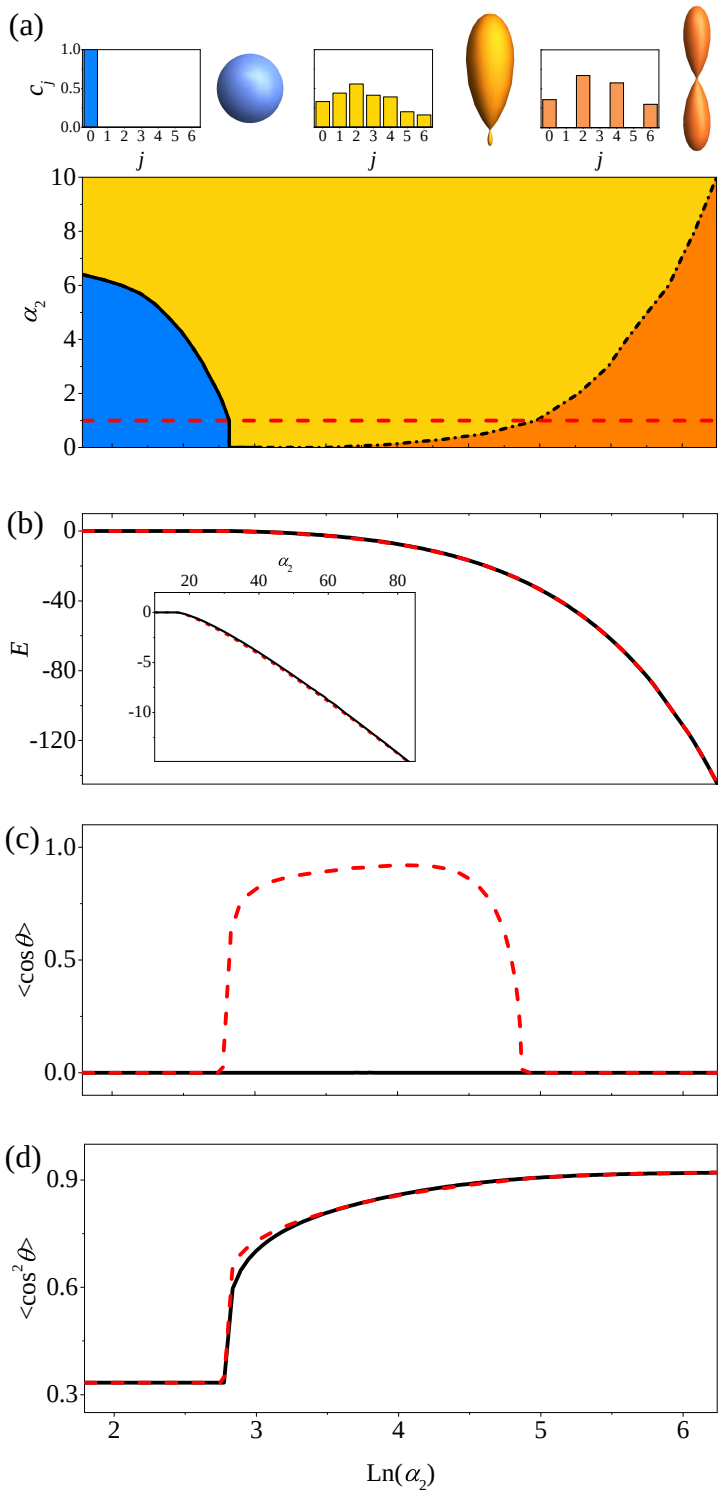

Figure 5.2: (a) 'Localization diagram' of the angulon states, depending on the magnitudes of α_1 and α_2 (all other couplings are set to zero). (b) Dependence of the ground-state energy on α_2 for $\alpha_1 = 1$. (c) Same as in (b), but for the orientation cosine of the impurity. (c) Same as in (b), but for the alignment cosine of the impurity.

6 Intermolecular forces and correlations mediated by a phonon bath

6.1 Introduction

Effective interactions between quantum particles play an important role in several areas in physics. One of the most prominent effective interactions is the Coulomb potential, which emerges in quantum electrodynamics from the exchange of virtual photons in the non-relativistic limit [Feynman, 2018]. Other important examples are provided by bath-mediated interactions as for example the phonon-mediated interaction between two polarons [Devreese, 2015], that is, between two electrons in a crystal that are dressed by a cloud of lattice excitations. This effective attractive interaction can balance the Coulombic repulsion between the electrons and results in the formation of the bipolaron quasiparticle [Devreese and Alexandrov, 2009; Kashirina and Lakhno, 2010] – a bound state that has been proposed as one of the mechanisms behind high-temperature anomalous superconductivity [Alexandrov, 2003]. In case of sufficiently strong electron-phonon interactions, also more complex polaronic structures such as electronic Wigner crystals [Quémerais and Fratini, 1998; Fratini and Quémerais, 2002; Iadonisi *et al.*, 2007], polaron molecules and clusters [Kusmartsev, 2001; Perroni *et al.*, 2004; Bruderer *et al.*, 2007] can form. Moreover, the electron-phonon coupling has been used to explain the thermodynamic and optical properties of quantum dot devices [Fomin *et al.*, 1998; Klimin *et al.*, 2004]. Finally, attractive electron interactions mediated by phonons are found to be able to overcome the direct Coulomb repulsion in deformable molecular quantum dots, paving the way for the realisation of polaronic memory resistors [Alexandrov and Bratkovsky, 2003; Alexandrov and Bratkovsky, 2009].

In the context of ultracold atoms various theoretical methods have been developed to study bath-mediated correlations in Bose-Einstein condensates in the case

of attractive/repulsive couplings [Jørgensen *et al.*, 2016; Hu *et al.*, 2016b] and for weakly [Casteels *et al.*, 2011a]/strongly interacting systems [Roberts and Rica, 2009; Santamore and Timmermans, 2011; Blinova *et al.*, 2013; Casteels *et al.*, 2013]. Effective quasiparticle-quasiparticle interactions have been investigated using variational methods [Devreese and Alexandrov, 2009; Kashirina and Lakhno, 2010], Dyson's equation [Utesov *et al.*, 2018] and a scattering matrix approach [Camacho-Guardian *et al.*, 2018; Bijlsma *et al.*, 2000] to name only a few. Besides electron-phonon coupling, other kinds of indirect interactions play a key role in quantum systems, such as e.g. the Ruderman-Kittel-Kasuya-Yosida interaction [Ruderman and Kittel, 1954; Zhou *et al.*, 2010], giving rise to complex magnetic phases such as spin glasses [Hewson, 1997].

In this chapter we analyse the effective interaction between two diatomic molecules mediated by a bosonic bath. Unlike electrons or ground-state atoms, the low-energy degrees of freedom for molecules involve rotations, leading to an exchange of angular momentum between the molecule and the bath. Recently, it has been shown that individual molecules interacting with a bosonic bath form angulon quasiparticles – rigid rotors dressed by a cloud of excitations carrying angular momentum [Schmidt and Lemeshko, 2015; Schmidt and Lemeshko, 2016; Lemeshko and Schmidt, 2017; Bighin *et al.*, 2018b]. The results of this theory are in good agreement with a wide range of experimental data including static and dynamic molecular properties [Lemeshko, 2017; Shepperson *et al.*, 2017b; Cherepanov and Lemeshko, 2017; Shepperson *et al.*, 2017a; Cherepanov *et al.*, 2019]. In addition to this, it was shown that due to the non-Abelian $SO(3)$ algebra and the discrete energy spectrum inherent to rotations, novel phenomena such as effective magnetic monopoles [Yakaboylu *et al.*, 2017] and anomalous electrostatic screening [Yakaboylu and Lemeshko, 2017] can emerge. During recent years, molecular complexes in He nanodroplets have been created (see e.g. Refs. [Pickering *et al.*, 2018b]), and techniques to control molecular alignment in helium have been developed [Shepperson *et al.*, 2017b; Shepperson *et al.*, 2017a; Cherepanov *et al.*, 2019]. These and other experimental advances pave the way to control and enhance chemical reactivity inside superfluids at the microscopic level.

This motivates us to investigate the effective phonon-mediated interactions between two molecules immersed in a bosonic bath. To investigate the system in various

parameter regimes, we apply different theoretical approaches based on angulon theory and several approximations, such as a product-state ansatz, a one-phonon-excitation variational approach and a diagonalization scheme based on single angulon basis states.

All approaches we use in this chapter suggest the appearance of a correlated state that we call the *biangulon*. It consists of two diatomic molecules that align with respect to each other due to the effective phonon-mediated interaction. We characterize this effective interaction within the Born-Oppenheimer approximation and show that it depends on both the angular momentum quantum number L and the magnetic quantum number M of each of the two molecules and that it favours states whose phonon clouds overlap strongly with the molecules. Within the Pekar approximation [Pekar, 1946b], we show that two diatomic molecules show a strong alignment in the strong-coupling regime. Subsequently, employing a one-phonon ansatz, we find that the biangulon shows two spectral instabilities in the weak-coupling regime as well as a shift of the angulon instabilities. These features are proposed as experimental signature for the formation of a biangulon. Finally, a diagonalization scheme based on single angulon and bare rotor basis functions is used, to investigate a system, where the coupling between the bath and one of the two impurities is weaker than the one of the other. In this situation we study the transition from separated angulons to a biangulon by calculating the wavefunction and the rotational correlations between the two molecules.

6.2 The model

We consider two rigid linear molecules ($i = 1, 2$), whose position is fixed in space at $(0, 0, \pm d/2)$ in the laboratory frame with coordinates $\{X, Y, Z\}$, see Fig. 6.1. The rotational kinetic energy of the i-th molecule is given by [Lemeshko and Schmidt, 2017]

$$\hat{H}_{\mathsf{mol}}^{(i)} = B_i \hat{\mathbf{J}}_i^2, \tag{6.1}$$

where we denote the rotational constant and the angular momentum operator of the i-th molecule by B_i and $\hat{\mathbf{J}}_i$, respectively. Here and in the rest of this chapter, we assume that the two molecules have the same rotational constant $B = B_1 = B_2$.

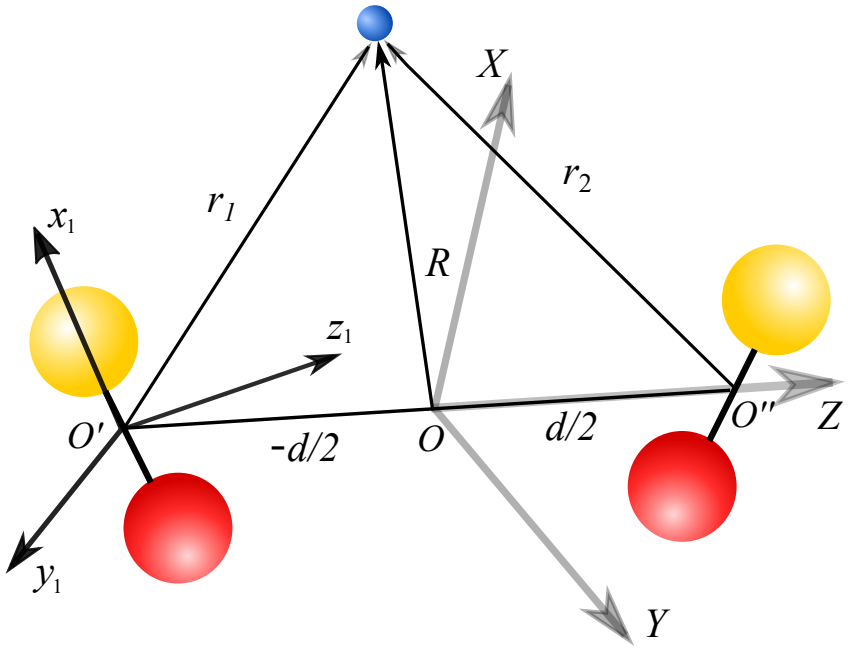

Figure 6.1: Schematic illustration of two rotating molecular impurities interacting with a bosonic atom. The origin of the laboratory frame, $\{X, Y, Z\}$, is chosen in the middle between the two molecules on the Z-axis. Anisotropic molecule-boson interactions are defined in the molecular coordinate frames labeled by $\{x_i, y_i, z_i\}$ $(i = 1, 2)$.

The molecules are immersed in a bath of phonons, whose kinetic energy is given by

$$\hat{H}_{\text{bos}} = \sum_{\mathbf{k}} \omega(k) \hat{b}^{\dagger}_{\mathbf{k}} \hat{b}_{\mathbf{k}}. \tag{6.2}$$

By $\omega(k)$ with $k = |\mathbf{k}|$ we denote the phonon dispersion relation, which will be specified later, and $\hat{b}^{\dagger}_{\mathbf{k}}$, $\hat{b}_{\mathbf{k}}$ with $[\hat{b}_{\mathbf{k}}, \hat{b}^{\dagger}_{\mathbf{q}}] = (2\pi)^3 \delta(\mathbf{k} - \mathbf{q})$ are the usual bosonic creation and annihilation operators of an excitation with momentum $\mathbf{k}$, respectively.

We assume the coupling between the impurities and the phonons to be linear in the phonon field. In the molecular coordinate frame with coordinates $\{x_i, y_i, z_i\}$, see Fig. 6.1, their interaction is therefore given by

$$\hat{H}^{(i)}_{\text{int}} = \sum_{\mathbf{k}} V(\mathbf{k}, \hat{\theta}_i, \hat{\phi}_i) \hat{b}^{\dagger}_{\mathbf{k}} + \text{H.c.}, \tag{6.3}$$

with the effective interaction potential $V(\mathbf{k}, \hat{\theta}_i, \hat{\phi}_i)$. A detailed microscopic derivation of an effective interaction of the form (6.3) for the case of an impurity immersed in a Bose-Einstein condensate is presented in Refs. [Schmidt and Lemeshko, 2015; Lemeshko and Schmidt, 2017]. The interaction (6.3) also serves as a reliable phenomenological

model for molecules immersed in helium nanodroplets [Lemeshko, 2017; Shepperson *et al.*, 2017b; Cherepanov and Lemeshko, 2017; Shepperson *et al.*, 2017a; Cherepanov *et al.*, 2019]. In this chapter we focus on intermolecular forces mediated by phonons, and therefore neglect direct molecule-molecule interactions, such as electrostatic, induction, and dispersion potentials [Stone, 2013a], which can, however, be added to the theory in a straightforward manner. In case of two non-polar diatomic molecules at a moderate distance, the only potentially relevant interaction we neglect is the screened (by the Helium atoms) van-der-Waals interaction between the molecules.

As schematically depicted in Fig. 6.1, the two molecules are placed along the Z axis at the points $(0, 0, \pm d/2)$, so that the Hamiltonian of the full system in the laboratory frame, $\{X, Y, Z\}$, is given by

$$\begin{aligned}\hat{H} &= B\hat{\mathbf{J}}_1^2 + B\hat{\mathbf{J}}_2^2 + \sum_{\mathbf{k}} \omega(k)\hat{b}_{\mathbf{k}}^\dagger \hat{b}_{\mathbf{k}} \\ &+ \sum_{\mathbf{k}} \left[V(\mathbf{k}, \hat{\theta}_1, \hat{\phi}_1) e^{-i\frac{\mathbf{k}\cdot\mathbf{d}}{2}} + V(\mathbf{k}, \hat{\theta}_2, \hat{\phi}_2) e^{i\frac{\mathbf{k}\cdot\mathbf{d}}{2}} \right] \hat{b}_{\mathbf{k}}^\dagger + \text{H.c.}.\end{aligned} \tag{6.4}$$

To obtain this representation, we applied the translation operator $\hat{T}(\mathbf{r}) = \exp\left(-i\mathbf{r} \cdot \sum_{\mathbf{k}} \mathbf{k}\hat{b}_{\mathbf{k}}^\dagger \hat{b}_{\mathbf{k}}\right)$ to the interaction term in Eq. (6.3), see also Ref. [Yakaboylu *et al.*, 2018].

6.3 Angulons and biangulons

If the distance between the two molecules is sufficiently large, each single impurity can be described by a (appropriately translated) Hamiltonian of the form

$$\hat{H}^{(i)} = B\hat{\mathbf{J}}_i^2 + \sum_{\mathbf{k}} \omega(k)\hat{b}_{\mathbf{k}}^\dagger \hat{b}_{\mathbf{k}} + \sum_{\mathbf{k}} V(\mathbf{k}, \hat{\theta}_i, \hat{\phi}_i)\hat{b}_{\mathbf{k}}^\dagger + \text{H.c.} \tag{6.5}$$

describing one rotating impurity immersed in the bosonic bath. It has been shown that the above Hamiltonian allows for a description of the rotating impurity in terms of the angulon quasiparticle in many different experimental settings, ranging from ultracold gases [Midya *et al.*, 2016b] to helium nanodroplets [Lemeshko, 2017]. The concept of the biangulon quasiparticle we propose in this chapter is based on the analysis of the Hamiltonian (6.4). If the two molecules come close enough together they will be subject (as we will see below) to an effective attractive interaction mediated by the bosonic bath. As a consequence, a correlated state, where both rotors are dressed by the bath and

at the same time strongly interact with each other, is formed. This correlated state is characterized by the fact that the two rotating molecules align with respect to each other such that the phonon cloud of each molecule overlaps with the other molecule. This behavior is very different from that of two uncorrelated (or weakly correlated) angulons and can be found in the regimes of moderate and strong coupling.

The system of the two impurities placed at $(0, 0, \pm d/2)$ is rotationally symmetric around the z axis, and hence the biangulon quasiparticle can be characterized by the magnetic quantum number M of the entire system. This should be compared to the angulon, where one has a full rotational symmetry and the total angular momentum L is also a good quantum number.

In the case of two polarons a bipolaron can form if the effective interaction between the two impurities allows for a bound state [Salje *et al.*, 2005]. Since our molecules have a frozen center-of-mass motion, this definition is clearly not appropriate, and we therefore opt for the definition above. In practice we expect the two definitions to coincide if the effective attractive interaction between the molecules allows for a bound state.

In the following Sections we will quantitatively study the above two-impurity system and its properties with various theoretical approaches and in different parameter regimes.

6.4 Product-state ansatz

6.4.1 Phonon-mediated intermolecular forces

When the interaction between impurities and the environment is strong, one can assume that the phonons adjust instantaneously to changes of the molecular orientation in space and a Born-Oppenheimer approximation is valid. This corresponds to a product state ansatz

$$|\psi_{\mathsf{b}}\rangle = |\mathsf{mol}\rangle \hat{U} |0\rangle. \tag{6.6}$$

Analogous to the Pekar ansatz for polarons [Pekar, 1946b; Devreese, 2015] the unitary $\hat{U}$ in the above equation is chosen as

$$\hat{U} = \exp\left[-\sum_{\mathbf{k}} \left(\frac{\langle \hat{f} \rangle}{\omega(k)} \hat{b}^{\dagger}_{\mathbf{k}} - \frac{\langle \hat{f} \rangle^{*}}{\omega(k)} \hat{b}_{\mathbf{k}} \right) \right], \tag{6.7}$$

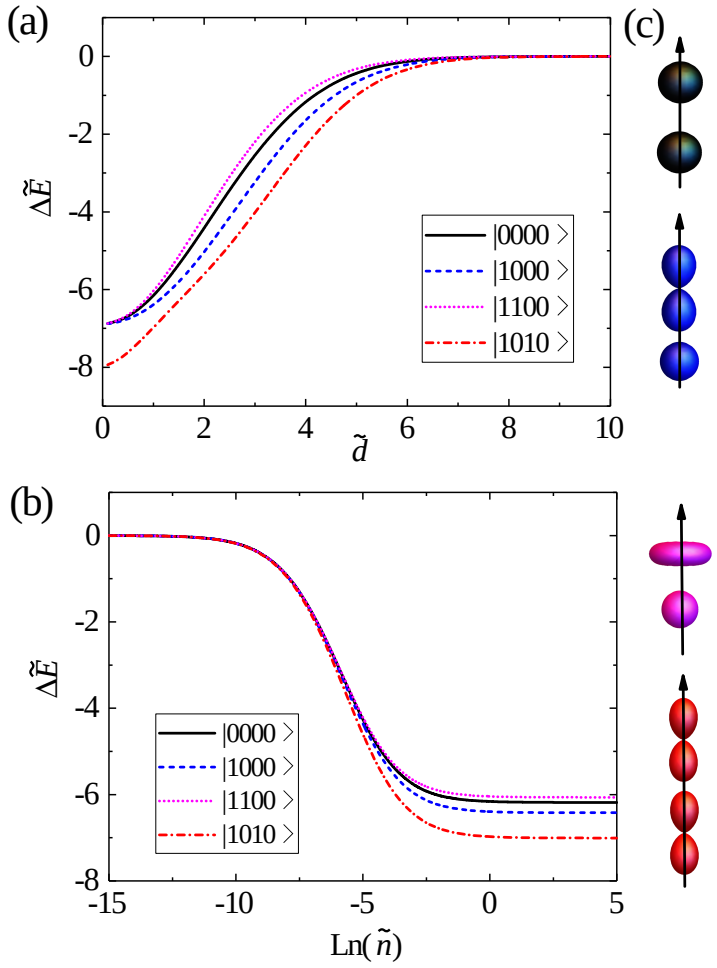

Figure 6.2: Dimensionless angulon-angulon interaction $\Delta\tilde{E} = \Delta E/B$, Eq. (6.12), calculated using the product state ansatz, Eq. (6.6), as a function of (a) the dimensionless molecule-molecule distance $\tilde{d} = d(mB)^{-1/2}$ and (b) the dimensionless bath density $\tilde{n} = n(mB)^{-3/2}$. We have chosen $\tilde{n} = 1$ for the bath density in (a) and $\tilde{d} = 1$ for the distance between the molecules in (b). The black solid line, blue dashed line, magenta dots, and red dashed dots have been computed with the molecular states $|L_1M_1L_2M_2\rangle = |0000\rangle$, $|1000\rangle$, $|1100\rangle$ and $|1010\rangle$, respectively. The squared absolute value of the wave functions related to the different molecular states (with colors as introduced in the legend) are schematically shown in (c). For more information see the text.

where

$$\langle \hat{f} \rangle = \langle \text{mol} | V(\mathbf{k}, \hat{\theta}_1, \hat{\phi}_1) e^{-i\frac{\mathbf{k}\cdot\mathbf{d}}{2}} + V(\mathbf{k}, \hat{\theta}_2, \hat{\phi}_2) e^{i\frac{\mathbf{k}\cdot\mathbf{d}}{2}} | \text{mol} \rangle. \tag{6.8}$$

We stress that the description of the bath in terms of the coherent state $\hat{U}|0\rangle$ in Eq. (6.6) takes an arbitrary number of phonon excitations into account.

Since we are interested in angular momentum exchange between the molecules and the environment, it is convenient to expand the bosonic field operators in the angular momentum basis as

$$\hat{b}^\dagger_{\mathbf{k}} = \frac{(2\pi)^{3/2}}{k} \sum_{\lambda\mu} \hat{b}^\dagger_{k\lambda\mu} i^\lambda Y^*_{\lambda\mu}(\Theta_k, \Phi_k) \tag{6.9}$$

see Ref. [Lemeshko and Schmidt, 2017]. Here $\hat{b}^\dagger_{k\lambda\mu}$ creates a phonon with radial momentum k, angular momentum λ and projection onto the z-axis μ. By $Y_{\lambda\mu}(\Theta_k, \Phi_k)$ we denote the spherical harmonics. Additionally, Θ_k, Φ_k are the angles determined by $\mathbf{k}$ in spherical coordinates and k denotes its absolute value. The inverse relation reads

$$\hat{b}^\dagger_{k\lambda\mu} = \frac{k}{(2\pi)^{3/2}} \int \mathrm{d}\phi_\mathrm{k} \mathrm{d}\theta_\mathrm{k} \sin(\theta_\mathrm{k}) \hat{b}^\dagger_{\mathbf{k}} i^{-\lambda} Y_{\lambda\mu}(\Theta_\mathrm{k}, \Phi_\mathrm{k}). \tag{6.10}$$

We also write the interaction potential as

$$V(\mathbf{k}, \hat{\theta}_i, \hat{\phi}_i) = \sum_{\lambda\mu} (2\pi)^{3/2} i^{-\lambda} \frac{U_\lambda(k)}{k} Y_{\lambda\mu}(\Theta_k, \Phi_k) Y^*_{\lambda\mu}(\hat{\theta}_i, \hat{\phi}_i), \tag{6.11}$$

where the potential has been expanded in partial wave components $U_\lambda(k)$ [Lemeshko and Schmidt, 2017].

For specific molecular rotational states $|\mathrm{mol}\rangle = |L_1 M_1 L_2 M_2\rangle$, where L_i and M_i denote the angular momentum quantum number and the magnetic quantum number of the i-th molecule, the energies $E_{\mathsf{BA}} = \langle \psi_{\mathsf{b}} | \hat{H} | \psi_{\mathsf{b}} \rangle$ of the Hamiltonian (6.4) can be readily calculated. Applying the same approach to a single molecular impurity in a state state $|L_i M_i\rangle$, one obtains the energy $E^{(i)}_{\mathsf{A}}$ of one angulon quasiparticle. In order to measure the strength of the interaction between two angulons we define the *effective angulon-angulon interaction* as

$$\Delta E = E_{\mathsf{BA}} - E^{(1)}_{\mathsf{A}} - E^{(2)}_{\mathsf{A}}. \tag{6.12}$$

A similar definition for two polarons can be found in Refs. [Devreese and Alexandrov, 2009; Kashirina and Lakhno, 2010].

Here and in what follows we choose parameters that are well suited to describe two molecular impurities immersed in a bath of superfluid ^{4}He. More precisely, we choose the phonon dispersion relation as $\omega(k) = \sqrt{\epsilon(k)(\epsilon(k) + 2g_{\mathsf{bb}} n)}$, where $\epsilon(k) = k^2/2m$,

$g_{bb} = 4\pi a/m$ with the scattering length a and the mass m of the Helium atoms. The function $\omega(k)$ is an approximation to the dispersion relation of sound waves in liquid helium that is valid at low momenta. By n we denote the density of the Helium atoms. To describe a typical atom-molecule interaction, we choose

$$U_\lambda(k) = u_\lambda \left(\frac{8nk^2\epsilon(k)}{[\omega(k)(2\lambda+1)]} \right)^{1/2} \int dr r^2 f_\lambda(r) j_\lambda(kr) \tag{6.13}$$

with Gaussian form factors $f_\lambda(r) = (2\pi)^{-3/2} e^{-r^2/(2r_\lambda^2)}$. Here $j_\lambda(kr)$ denotes the spherical Bessel function. The coupling strengths and the potential radii are chosen as $u_0 = u_2 = 218B$, $u_\lambda = 0$ if $\lambda \neq 0, 2$ and $r_0 = r_2 = 1.5(mB)^{-1/2}$, respectively [Stone, 2013b; Schmidt and Lemeshko, 2015]. We also choose $a = 3.3(mB)^{-1/2}$, which reproduces the speed of sound in superfluid Helium for a molecule whose rotational constant is $B = 2\pi \times 1$ GHz [Donnelly and Barenghi, 1998; Schmidt and Lemeshko, 2015]. In Fig. 6.2 we show the dimensionless effective interaction $\Delta\tilde{E} = \Delta E/B$ as a function of (a) the dimensionless molecule-molecule distance $\tilde{d} = d(mB)^{-1/2}$ and (b) the dimensionless bath density $\tilde{n} = n(mB)^{-3/2}$. The squared absolute value of the wave functions related to the different molecular states (with colors as introduced in the legend) are schematically shown in (c). In subgraph (a) the density is $\tilde{n} = 1$ and in (b) the molecule-molecule distance is fixed as $\tilde{d} = 1$. When the two molecules are placed far away from each other or when the surrounding bath is sufficiently dilute, the effective interaction is small and the system resembles two separate angulons.

Outside this parameter regime we observe an attractive interaction between the two rotors ($\Delta\tilde{E} < 0$), which results from the linear coupling in the Hamiltonian (6.4). It is sensitive to the rotational state of the two molecules and takes its largest values when the overlap of the phonon density of each of the two molecules with the other molecule is maximal. Accordingly, it depends also on the magnetic quantum numbers M_1 and M_2. For example, the effective interaction between molecules in the state $|L_1 M_1 L_2 M_2\rangle = |1000\rangle$ (blue dashed line in Fig. 6.2) is stronger than the one between molecules in the state $|1100\rangle$ (magenta dots). The interaction energy of the latter state is even weaker than the one of the state $|0000\rangle$ (black solid line) and the state $|1010\rangle$ shows the largest interaction energy among the ones that have been considered. See also Fig. 6.2(c) for the shapes of the orbitals related to these molecular states. The anisotropy of the molecular wave function of one molecule is responsible for a similar

anisotropy of its phonon cloud. The interaction energy is large if this anisotropy causes a strong overlap of the molecules phonon cloud with the other molecule. In general, the states with $M_1 = M_2 = 0$ show the largest effective interaction. Such an effective interaction clearly favors a biangulon-like behavior if the impurities are sufficiently close.

The saturation of the effective interaction for large densities $\tilde{n}$ in Fig. 6.2 (b) is a consequence of the fact that the phonon dispersion relation $\omega(k)$ and $|\langle\hat{f}\rangle|^2$ are both proportional to $\sqrt{\tilde{n}}$ in this regime, see Eqs. (6.11), (6.13) and Eq. (6.15) in Section 6.4.2 below. The states $|1,1,1,1\rangle$ and $|1,1,1,-1\rangle$ have the same interaction energy. That is, the effective interaction is not sensitive to whether the two molecules rotate in the same or in opposite directions. Since both molecules have the same rotational constant B, one obtains the same result if their quantum numbers are exchanged.

6.4.2 Relative molecular orientation in the ground state

In this Section we study the ground state of two molecules immersed in the bath of phonons within the Pekar approximation. Accordingly, we minimize the expectation of the Hamiltonian (6.4) over the molecular part of the wave function in (6.6), similar to Ref. [Pekar, 1946b]. This approximation is expected to be valid in the strong-coupling regime [Donsker and Varadhan, 1983; Lieb and Thomas, 1997].

More precisely, we expand the molecular wave function in angular momentum eigenfunctions as

$$|\mathrm{mol}\rangle = \sum_{L_1,M_1,L_2,M_2} s_{L_1,M_1,L_2,M_2} |L_1 M_1\rangle |L_2 M_2\rangle. \tag{6.14}$$

In the following, we abbreviate $c = (L_1, M_1, L_2, M_2)$. When we insert (6.14) into (6.6) and compute with this wave function the expectation value of $\hat{H}$, Eq. (6.4), we obtain the Pekar functional

$$\mathcal{E}_{\mathrm{BA}}(s) = \sum_c \left(B[L_1(L_1+1) + L_2(L_2+1)]|s_c|^2 - \sum_{\mathbf{k}} \frac{|\langle\hat{f}\rangle|^2}{\omega(k)} \right), \tag{6.15}$$

as well as the biangulon energy

$$E_{\mathrm{BA}} = \min_{\sum_c |s_c|^2 = 1} \mathcal{E}_{\mathrm{BA}}(s). \tag{6.16}$$

Similarly, we find the energy E_{A} of one impurity within the Pekar approximation and we have

$$\Delta E = E_{\mathrm{BA}} - 2E_{\mathrm{A}}. \tag{6.17}$$

To minimize $\mathcal{E}_{\mathrm{BA}}(s)$ numerically, we introduce the cut-off $L_1, L_2, |M_1|, |M_2| \leq 4$ for the values of the angular momentum quantum number. The minimization is then carried out with a stochastic simulated annealing procedure based on moves that can reach any allowed value of the variational coefficients [Das and Chakrabarti, 2005].

The stochastic simulated annealing method that we applied to minimize ground energy Eq. 6.16, is based on repeated application of the following two moves:

1. Rotation of a variational coefficient in the complex plane, i.e. $s_c \to s_c \exp(\mathrm{i}\phi)$ where the quantum numbers $c = (L_1, M_1, L_2, M_2)$ and the phase ϕ have been chosen from a random distribution.

2. Moving part of the complex modulus of a coefficient to another coefficient, i.e. going from a configuration of two coefficients that we parametrize in the polar representation as $s_c = \rho \exp(\mathrm{i}\phi)$, $s_{c'} = (\rho') \exp(\mathrm{i}\phi')$ to a different configuration $s_c = (\rho - \delta) \exp(\mathrm{i}\phi)$, $s_{c'} = (\rho' + \delta) \exp(\mathrm{i}\phi')$ where again the quantum numbers c and c', as well as δ, are chosen randomly.

It can be easily seen that these two moves span the whole parameter space, while automatically enforcing the normalization condition. In the spirit of simulated annealing methods, each move is accepted or rejected by evaluating the Boltzmann factor of the energy difference, using a monotonously decreasing effective temperature. We have verified that this procedure is solid, yielding a good estimate of the ground state energy at the level of maximum $L_i = 4$ (containing $1,764$ variational coefficients), independently of the starting configuration, in agreement with non-stochastic methods that are usually slower and limited to much smaller cutoffs.

For a better understanding of the resulting state we also consider the alignment cosine

$$\langle \cos^2 \theta_1 \rangle = \sum_{c,c'} \tilde{s}^*_{c'} \tilde{s}_c \langle L'_1 M'_1 | \cos^2 \theta_1 | L_1 M_1 \rangle \delta_{L'_2, L_2} \delta_{M'_2 M_2}, \tag{6.18}$$

where $\tilde{s}$ denotes the minimizer of $\mathcal{E}_{\mathrm{BA}}$. The expectation value on the left-hand side is taken with respect to the state $|\psi_{\mathsf{b}}\rangle$ in Eq. (6.6), where the molecular wave function is replaced by the wave function in Eq. (6.14) with coefficients given by $\tilde{s}$. From our computations we see that the minimizer of $\mathcal{E}_{\mathrm{BA}}$ is a product state that is symmetric in

the two impurities (for the case $B = B_1 = B_2$). This implies $\langle \cos^2 \theta_1 \rangle = \langle \cos^2 \theta_2 \rangle$, and hence we can use Eq. (6.18) to measure the anisotropy of the molecular orientation of both molecules.

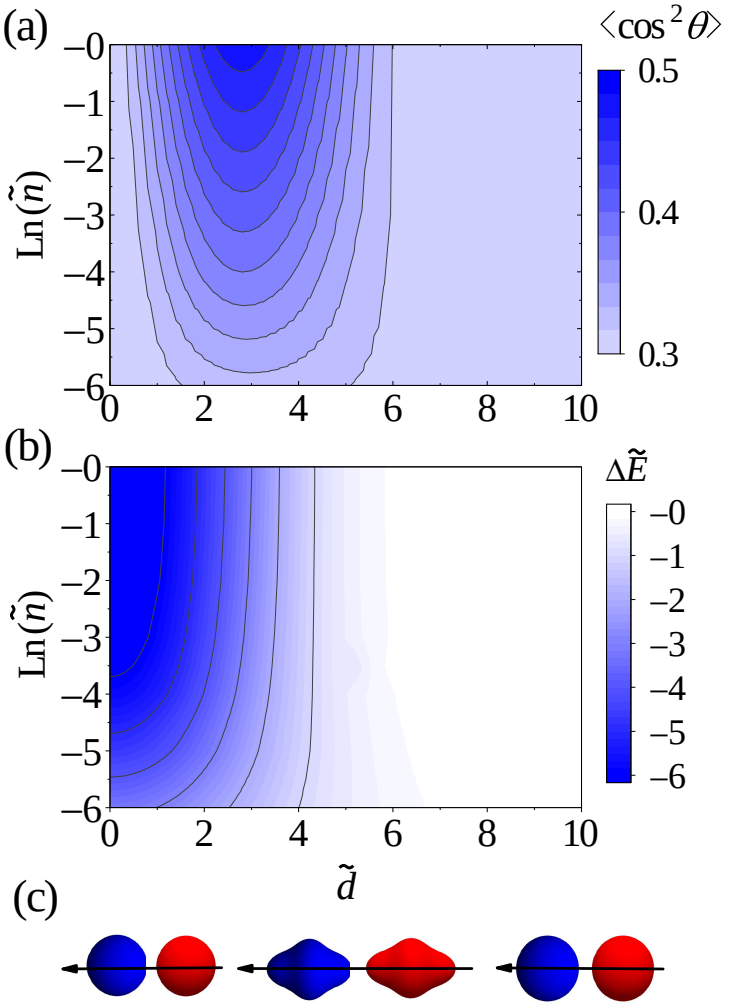

Figure 6.3: Contour plot of (a) the alignment cosine $\langle \cos^2 \theta_1 \rangle$, Eq. (6.18), and (b) the dimensionless effective interaction $\Delta\tilde{E} = \Delta E_{\rm BA}/B$, Eq. (6.17), of one of the molecules computed within the Pekar approximation as a function of the dimensionless molecule-molecule distance $\tilde{d} = d(mB)^{-1/2}$ and dimensionless bath densities $\tilde{n} = n(mB)^{-3/2}$. In (c) we show schematic figures of the wave functions of the two molecules for the parameters $\tilde{n} = 1$ and $\tilde{d} = 0.3$ (left picture), $\tilde{d} = 3$ (picture in the middle) and $\tilde{d} = 8$ (right picture). For more details see the text.

In Fig. 6.3 we show the contour plot of (a) the alignment cosine $\langle \cos^2 \theta_1 \rangle$ and (b) the dimensionless effective interaction $\Delta\tilde{E} = \Delta E/B$ as a function of the dimensionless molecule-molecule distance $\tilde{d} = d(mB)^{-1/2}$ and the dimensionless bath density $\tilde{n} =$

$n(mB)^{-3/2}$. In (c) we show schematic figures of the wave functions of the two molecules for the parameters $\tilde{n} = 1$ and $\tilde{d} = 0.3$ (left picture), $\tilde{d} = 3$ (picture in the middle) and $\tilde{d} = 8$ (right picture). As one would expect, the effective interaction is an increasing function of the bath density and a decreasing function of the distance between the impurities.

For large distances the ground state is given by the impurity wave function $|L_1 M_1 L_2 M_2\rangle = |0000\rangle$ and the two molecules form two isolated angulon quasiparticles with no preferential orientation. In this case the alignment cosine equals $1/3$, see Fig. 6.3(b). If they come closer together, contributions with nonzero angular momentum and $M_i = 0$ for $i = 1, 2$ become relevant, compare with (c). This is in accordance with the analysis in Section 6.4.1, see Fig. 6.2, where we found that such states maximize the overlap of the phonon cloud of each of the two impurities with the other impurity, and therewith also their attractive interaction. This behavior is also captured by the alignment cosine, which takes its largest values around $\tilde{d} = 3$. In this region the two impurities form a biangulon quasiparticle, which is characterized by the fact that their relative orientation is strongly correlated and that their phonon densities are highly anisotropic.

If the distance is further decreased the phonon clouds are already substantially overlapping with the molecules if the molecular wave function is almost rotationally symmetric and an anisotropy of the molecular orientation is no longer beneficial. This is indicated by $\langle \cos^2 \theta_1 \rangle \to 1/3$ for small $\tilde{d}$. In other words, the short distance behavior of the two impurities is a perturbation of the extreme case $\tilde{d} = 0$, where the model has full rotational symmetry. In practice one would need to numerically evaluate the intermolecular interations from the quantum chemistry perspective, taking into account the overlap of the molecular electronic states, in order to describe the relevant physics in the regime of very small $\tilde{d}$ correctly. In addition, attractive and repulsive potentials could lead to chemical reactions. The inclusion of these effects goes, however, beyond the scope of the present chapter.

Finally, let us note that the Gaussian form factors and our choice of the dispersion relation imply that the effective interaction is an exponentially decaying function of the distance $\tilde{d}$. This can be seen as follows: We have already noted that the molecular wave function is given by $s_c = \delta_{L_1,0}\delta_{M_1,0}\delta_{L2,0}\delta_{M_2,0}$ if $\tilde{d}$ is chosen sufficiently large, compare with

Fig. 6.3(b). In this case we can write the effective interaction as

$$\Delta E = \\ -\frac{1}{2\pi}\sum_k \frac{U_0^2(k)}{\omega(k)}\left[\sum_\lambda (2\lambda+1) j_\lambda(kd/2)^2(1+(-1)^\lambda)-1\right]. \tag{6.19}$$

With $\sum_\lambda (2\lambda+1) j_\lambda(x)^2 = 1$ and $\sum_\lambda (-1)^\lambda (2\lambda+1) j_\lambda(x)^2 = \frac{\sin 2x}{2x}$ [Abramowitz and Stegun, 1965], Eq. (6.19) simplifies to

$$\Delta E = -\frac{1}{2\pi}\sum_k \frac{U_0^2(k)}{\omega(k)}\frac{\sin(kd)}{kd}. \tag{6.20}$$

Our choice of the form factor in Sec. 6.4.1 implies

$$U_0(k) = u_0\left(\frac{8nk^2\epsilon(k)}{\omega(k)}\right)^{1/2}\frac{r_0^4 e^{-r_0^2k^2/2}}{2^{5/2}\pi}. \tag{6.21}$$

We insert (6.21) and $\omega(k)$ from Sec. 6.4.1 into (6.20). An application of Ref. [Reed and Simon, 1980], Theorem IX.13 therein, shows the claim.

It should also be noted that for the Fröhlich parameters $\omega(k) = \omega_0$ and $U_0(k) = U_0$ one finds the well-known behavior [Lieb and Thomas, 1997]

$$\Delta E \propto \frac{1}{\tilde{d}}. \tag{6.22}$$

6.5 One-phonon-excitation variational ansatz

The product-state-ansatz of Section 6.4 describes molecular impurities dressed by an arbitrary number of phonons in a coherent state (cf. Eq. (6.7)). Minimization over the impurity wave function yields the Pekar approximation, which is expected to be valid for strong molecule-bath interactions [Donsker and Varadhan, 1983; Lieb and Thomas, 1997]. When the molecule-bath interaction is weak, however, we expect only a small number of phonons to be excited. It is the aim of the present Section to investigate such a situation in detail.

More precisely, we are going to use a one-phonon-excitation variational ansatz, that is, we will allow for at most one phonon in the system. Such an ansatz has been successfully applied in several different contexts, see Refs. [Chevy, 2006b;

Lan and Lobo, 2014; Schmidt and Lemeshko, 2015]. For a system of two rotating molecules immersed in a bosonic bath this variational ansatz reads

$$|\psi_{\text{1-ph}}\rangle = g|L_1M_1\rangle|L_2M_2\rangle|0\rangle + \sum_c \beta_c|j_1m_1\rangle|j_2m_2\rangle\hat{b}^\dagger_{\mathbf{k}}|0\rangle, \tag{6.23}$$

where $c = (j_1, m_1, j_2, m_2, \mathbf{k})$, and the sum over $\mathbf{k}$ is actually an integral. The variational coefficients g and β_c are chosen such that the magnetic quantum number $M = M_1 + M_2$ of the whole system is a good quantum number and such that $|g|^2 + \sum_c |\beta_c|^2 = 1$ holds. The first term in Eq. (6.23) describes two free rotors and a bosonic bath in its vacuum state. In the second term a phonon with momentum $\mathbf{k}$ is excited and introduces correlations between the two molecules and the bath. We expect the ansatz (6.23) to be a good approximation in situations where the helium density $\tilde{n}$ is sufficiently dilute and/or when the distance between the two impurities is such that we still have moderate correlations between them. Accordingly, it describes either a weakly correlated biangulon or two weakly interacting angulons.

When we compute the expectation value of $\hat{H}$ (6.4) in the state $|\psi_{\text{1-ph}}\rangle$ and minimize the functional $F(\psi_{\text{1-ph}}) = \langle\psi_{\text{1-ph}}|\hat{H} - E_{\text{BA}}|\psi_{\text{1-ph}}\rangle$ with respect to the variational coefficients, we obtain the self-consistent equation

$$E_{\text{BA}} = BL_1(L_1+1) + BL_2(L_2+1) - \Sigma^{\text{BA}}_{L_1M_1L_2M_2}(E_{\text{BA}}) \tag{6.24}$$

for the energy E_{BA}. Here the self-energy $\Sigma^{\text{BA}}_{L_1M_1L_2M_2}(E_{\text{BA}})$ is given by

$$\begin{aligned}
&\Sigma^{\text{BA}}_{L_1M_1L_2M_2}(E_{\text{BA}}) = \\
&\sum_{k\lambda j_1} \frac{2\lambda+1}{4\pi} \frac{U^2_\lambda(k)\left[C^{j_10}_{L_10,\lambda0}\right]^2}{Bj_1(j_1+1) + BL_2(L_2+1) + \omega(k) - E_{\text{BA}}} \\
&+ \sum_{k\lambda j_2} \frac{2\lambda+1}{4\pi} \frac{U^2_\lambda(k)\left[C^{j_20}_{L_20,\lambda0}\right]^2}{BL_1(L_1+1) + Bj_2(j_2+1) + \omega(k) - E_{\text{BA}}} \\
&+ \sum_{k\lambda\lambda'\mu} \frac{C^{L_10}_{L_10,\lambda0} C^{L_1M_1}_{L_1M_1,\lambda\mu} C^{L_20}_{L_20,\lambda'0} C^{L_2M_2}_{L_2M_2,\lambda'\mu} \Gamma_{\lambda,\lambda'}(\mathbf{k},d)}{BL_1(L_1+1) + BL_2(L_2+1) + \omega(k) - E_{\text{BA}}}
\end{aligned} \tag{6.25}$$

and

$$\Gamma_{\lambda,\lambda'}(\mathbf{k},d) = \\ i^{\lambda-\lambda'}\sqrt{\frac{(2\lambda+1)(2\lambda'+1)}{(4\pi)^2}}U_\lambda(k)U_{\lambda'}(k)\times \\ \int d\phi_k \int d\theta_k \sin\theta_k \left[e^{i\mathbf{k}\cdot\mathbf{d}}Y_{\lambda,\mu}(\theta_k,\phi_k)Y^*_{\lambda',\mu}(\theta_k,\phi_k) + \text{c.c.}\right]. \tag{6.26}$$

By $C^{l_1 m_1}_{l_2 m_2, l_3 m_3}$ we denote the Clebsch-Gordan coefficients [Varshalovich *et al.*, 1988b].

6.5.1 The spectral function and instabilities

As for a single molecule immersed in a bosonic bath [Lemeshko and Schmidt, 2017], the self-consistent equation (6.24) gives us access to the biangulon spectral function

$$\mathsf{A}_{L_1L_2}(E) = \mathsf{Im}[G^{\mathsf{BA}}_{L_1M_1L_2M_2}(E+i0^+)], \tag{6.27}$$

where

$$G^{\mathsf{BA}}_{L_1M_1L_2M_2}(E) = \\ \frac{1}{BL_1(L_1+1)+BL_1(L_1+1)-E-\Sigma^{\mathsf{BA}}_{L_1M_1L_2M_2}(E)}, \tag{6.28}$$

denotes the retarded Green's function, and therewith to the energy spectrum of the system.

One of the most striking features of the angulon quasiparticle is the onset of an intermediate instability regime, where resonant transfer of angular momentum between the molecule and the bath drastically decreases the quasiparticle weight [Schmidt and Lemeshko, 2015]. This phenomenon has been observed experimentally [Cherepanov and Lemeshko, 2017]. In order to make our results comparable to the case of one molecular impurity, we choose in this Section the same parameters as in Fig. 2 in Ref. [Schmidt and Lemeshko, 2015]. In Fig. 6.4 we study the biangulon spectral function (6.27) as a function of the dimensionless energy $\tilde{E}_{\mathrm{BA}}$ and (a) the dimensionless molecule-molecule distance $\tilde{d}$ as well as (b) the dimensionless bath density $\tilde{n}$. In (a) we have chosen $\ln(\tilde{n}) = -3$, while $\tilde{d} = 0.6$ in (b). States are labeled according to the first term in (6.23). The biangulon instabilities are highlighted by the red dotted circles. The degeneracy of different $M = M_1 + M_2$ states is lifted by the interaction. To keep the

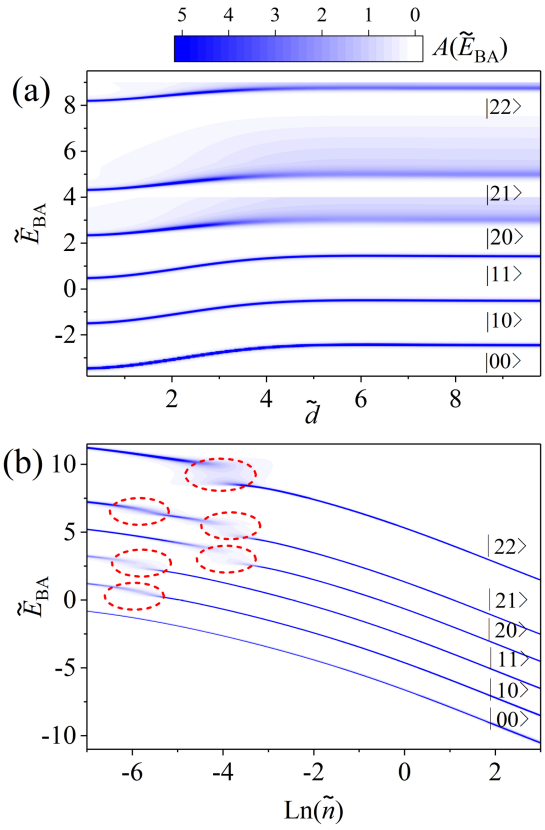

Figure 6.4: Spectral function $\mathrm{A}_{j_1 j_2}(\tilde{E}_{\mathrm{BA}})$, Eq. (6.27), of the biangulon as a function of the dimensionless energy $\tilde{E}_{\mathrm{BA}}$ and (a) the dimensionless molecule-molecule distance $\tilde{d}$ as well as (b) the dimensionless bath density $\tilde{n}$ for different angular momentum states L_1 and L_2 with $M_1 = 0 = M_2$. The states are labeled according to the first term in (6.23) and we use the notation $|L_1 L_2\rangle = |L_1, M_1 = 0, L_2, M_2 = 0\rangle$. In (a) the bath density is chosen as $\ln(\tilde{n}) = -3$ and the distance in (b) is given by $\tilde{d} = 0.6$. Biangulon instabilities are highlighted by red dotted circles. For details see the text.

figures accessible, we, however, only consider state with $M_1 = 0 = M_2$ here. This is on the one hand because the quasiparticle instabilities for states with $M_1, M_2 \neq 0$ are very similar to the ones for states with $M_i = 0$, and on the other hand because their energies are very close.

In Fig. 6.4(a) we see that the biangulon instabilities are only slowly changing with the distance $\tilde{d}$ between the two impurities and appear in a wide region of distances. In this regime a description of the system in terms of the biangulon quasiparticle, or for larger distances in terms of two separate angulons, breaks down. For larger distances this can be explained as follows: The two impurities are weakly interacting and therefore almost

independent. If the parameters are such that one of the two impurities experiences an angulon instability the quasiparticle picture breaks down and a further increase of the molecule-molecule distance does not change this situation.

We note that the instability region, as a function of the adimensional density $\tilde{n}$, has approximately the same size as in the single angulon case, see Fig. 2 in Ref. [Schmidt and Lemeshko, 2015]. We observe, however, that the instability for the biangulon appears at lower densities. For instance, the instability of a single angulon in the molecular state $|LM\rangle = |10\rangle$ is located around $\ln(\tilde{n}) = -5$, see Fig. 2 in Ref. [Schmidt and Lemeshko, 2015], while Fig. 6.4(b) shows that the instability is shifted to the region around $\ln(\tilde{n}) = -6$ when another molecule in the state $|LM\rangle = |00\rangle$ is put at a distance $\tilde{d} = 0.6$ from the first one. Furthermore, two spectral instabilities can be found in the biangulon spectrum where there is only one in the case of the angulon: In Fig. 6.4(b) we see a first instability of the state $|L_1L_2\rangle = |21\rangle$ around $\ln(\tilde{n}) = -6$ and a second around $\ln(\tilde{n}) = -4$. These two instabilities correspond to phonons excited by molecules with different angular momentum quantum number, in this case $L = 1$ and $L = 2$. We can distinguish the two instabilities because, compared to the situation in Fig. 2 in Ref. [Schmidt and Lemeshko, 2015], the relevant angulon instabilties are shifted. Both features, the shift of the spectral instabilities and the appearance of a second instability, can be used in experiments as a measure for correlations between the two impurities, and therewith as a signature for the formation of the biangulon quasiparticle.

We note that the spectral instability of the state $|L_1L_2\rangle = |10\rangle$ appears at $\ln(\tilde{n}) = -5.2$ if $\tilde{d} = 10$ and not at $\ln(\tilde{n}) = -5$, see Fig. 2 in Ref. [Schmidt and Lemeshko, 2015], as one would expect for two (almost) non-interacting impurities. This shift is a consequence of our one-phonon excitation variational ansatz, which forces the impurities to share one phonon also if they are far apart from each other. The result is a slightly different dressing of the two impurities by the phonon compared to the case of a single angulon (described by a one-phonon variational ansatz) and explains the above deviation. A careful discussion of this effect can be found in the following Section.

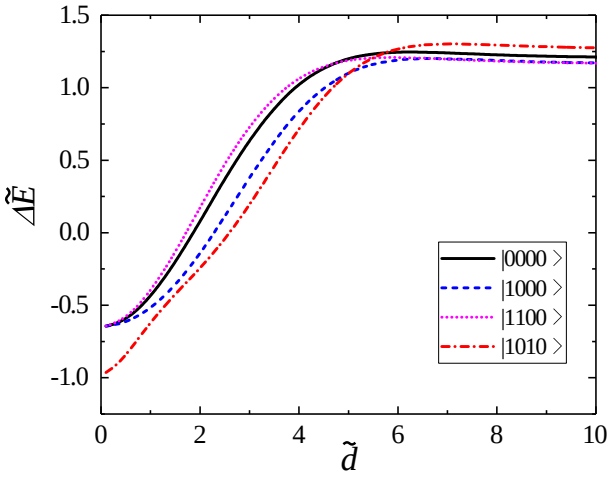

Figure 6.5: Effective interaction $\Delta\tilde{E}$ obtained with the one-phonon-excitation variational ansatz (6.23) for molecular states $|L_1M_1L_2M_2\rangle = |1010\rangle$ (red solid line), $|1110\rangle$ (black dot line), and $|1111\rangle$ (blue dashed line) as a function of the dimensionless molecule-molecule distance $\tilde{d}$. States are labeled according to the first term in Eq. (6.23). The bath density is chosen such that $\ln(\tilde{n}) = 0$. For more details see the text.

6.5.2 Effective interaction

Let us also consider the effective interaction between the impurities

$$\Delta E = E_{\mathrm{BA}} - E_{\mathrm{A}}^{(1)} - E_{\mathrm{A}}^{(2)}, \tag{6.29}$$

where $E_{\mathrm{A}}^{(i)}$ denotes the energy of the i-th impurity computed with a one-phonon-excitation variational ansatz, see Refs. [Schmidt and Lemeshko, 2015; Lemeshko and Schmidt, 2017]. In Fig. 6.5 we show ΔE as a function of the dimensionless distance $\tilde{d}$ for the same quantum numbers as in Fig 6.2, where the Born-Oppenheimer approximation has been considered. As one can expect from our discussion there, ΔE depends on the magnetic quantum numbers of the molecules. The qualitative behavior of the effective interaction is the same as in the case of the Born-Oppenheimer approximation, that is, the state $|1010\rangle$ has the largest effective interaction, followed by $|1000\rangle$ and $|0000\rangle$, and the effective interaction is the smallest in case of $|1100\rangle$. As above, we labeled states according to the first term in Eq. (6.23). In particular, states with $M_1 = 0 = M_2$ have larger effective interaction than states with $M_1, M_2 \neq 0$. The intuition behind this has been explained in detail in Section 6.4.1. In contrast to the strong coupling case,

the effective interaction does not go to zero for large molecule-molecule distances. As we will see below, this is due to the fact that one phonon cannot dress two impurities in the same way as one phonon dresses a single impurity.

To investigate this in some more detail, we have a closer look at the self-energy $\Sigma^{\mathsf{BA}}_{L_1M_1L_2M_2}(E_{\mathsf{BA}})$ in Eq. (6.25) in the limit $d \to \infty$. The first two terms in this equation are the self-energy contributions of the two molecules, while the third term is related to the effective interaction between them. Since this last term vanishes for $d \to \infty$, we only need to consider the first two terms. To keep things simple, we also assume that the two molecules are in the same angular momentum state, i.e., $L_1 = L_2 = l$ and $M_1 = M_2 = m$. The self-consistent equation (6.24) for the energy thus reads

$$\begin{aligned}\widetilde{E}_{\mathsf{BA}}(U_\lambda) &= 2Bl(l+1) \\ &- \sum_{k\lambda l'} \frac{2\lambda+1}{4\pi} \frac{2U_\lambda^2(k)\left[C^{l'0}_{l0,\lambda0}\right]^2}{Bl'(l'+1)+Bl(l+1)+\omega(k)-\widetilde{E}_{BA}(U_\lambda)},\end{aligned} \tag{6.30}$$

where $\widetilde{E}_{\mathsf{BA}}(U_\lambda) = \lim_{d\to\infty} E_{\mathsf{BA}}(U_\lambda)$. We want to compare the solution of this equation to the energy of two separate molecules, that is, to twice the energy of one molecule dressed by one phonon. Such a system has been considered in Ref. [Schmidt and Lemeshko, 2015] and the self-consistent equation for the energy is given by

$$\begin{aligned}E_{\mathsf{A}}(U_\lambda) =& Bl(l+1) \\ &- \sum_{k\lambda l'} \frac{2\lambda+1}{4\pi} \frac{U_\lambda^2(k)[C^{l'0}_{l0,\lambda0}]^2}{Bl'(l'+1)+\omega(k)-E_{\mathsf{A}}(U_\lambda)}\end{aligned} \tag{6.31}$$

in this case. One easily checks that a solution of (6.30) can be written in terms of a solution of (6.31) as

$$\widetilde{E}_{\mathsf{BA}}(U_\lambda) = Bl(l+1) + E_{\mathsf{A}}(\sqrt{2}U_\lambda). \tag{6.32}$$

Here $E_{\mathsf{A}}(\sqrt{2}U_\lambda)$ is the energy of one single molecule but with interaction potential $\sqrt{2}U_\lambda$ instead of U_λ in the relevant Hamiltonian. One also checks that the right-hand side of Eq. (6.32) is strictly larger than $2E_{\mathsf{A}}(U_\lambda)$. These results can be explained with the following simple physical picture: The phonon in the system is located with probability $1/2$ close to one molecule and with probability $1/2$ close to the other molecule. This results in an effective potential, which is, compared to the case of one molecule and one phonon, reduced by a factor of $1/\sqrt{2}$ coming from the phonon wave function. The

fact that we have a linear coupling and that there are two such interaction terms, one for each molecule, explains the factor of $\sqrt{2} = 2/\sqrt{2}$ in front of the interaction potential.

The above physical picture is also present in the wave function of the system. If we substitute the relation between the variational coefficients

$$\begin{aligned} -\beta_{j_1 m_1 j_2 m_2 \mathbf{k}}/g = & \\ & \frac{e^{-i\frac{1}{2}\mathbf{k}\cdot\mathbf{d}}\langle j_1 m_1|\hat{V}|L_1 M_1\rangle \delta_{j_2 L_2}\delta_{m_2 M_2}}{Bj_1(j_1+1)+Bj_2(j_2+1)+\omega(k)-E_{\mathsf{BA}}} \\ & + \frac{e^{i\frac{1}{2}\mathbf{k}\cdot\mathbf{d}}\langle j_2 m_2|\hat{V}|L_2 M_2\rangle \delta_{j_1 L_1}\delta_{m_1 M_1}}{Bj_1(j_1+1)+Bj_2(j_2+1)+\omega(k)-E_{\mathsf{BA}}}, \end{aligned} \tag{6.33}$$

which follows from the first variation of the energy, into the ansatz Eq. (6.23), we find

$$\begin{aligned} |\psi_{\mathsf{c}}\rangle = \frac{1}{\sqrt{2}}\Big[& |L_1 M_1\rangle \otimes |\psi^{\mathsf{A}}_{L_2 M_2}(-d)\rangle \\ & + |\psi^{\mathsf{A}}_{L_1 M_1}(d)\rangle \otimes |L_2 M_2\rangle\Big]. \end{aligned} \tag{6.34}$$

Here $|\psi^{\mathsf{A}}_{LM}\rangle$ denotes the wave function of one single angulon and reads

$$|\psi^{\mathsf{A}}_{LM}(d)\rangle = \frac{g}{\sqrt{2}}|LM\rangle|0\rangle + \frac{g}{\sqrt{2}}\sum_{j_1\mathbf{k}} f_{L_1,j_1,L_2}(\mathbf{k},d)|j_1 m_1\rangle\hat{b}^\dagger_{\mathbf{k}}|0\rangle, \tag{6.35}$$

with

$$f_{l_1,l_2,l_3}(\mathbf{k},d) = \frac{2e^{i\frac{1}{2}\mathbf{k}\cdot\mathbf{d}}\langle l_2|\hat{V}|l_1\rangle}{Bl_3(l_3+1)+Bl_2(l_2+1)+\omega(k)-E_{\mathsf{BA}}}. \tag{6.36}$$

The wave function of the two impurities in Eq. (6.34) is given by an equal weight superposition of a tensor product of one dressed and one bare molecule, that is, the phonon is with probability $1/2$ located close to the first molecule and with probability $1/2$ close to the second.

From this simple example we learn that one phonon cannot dress each of the two molecules in the same way as one phonon would dress one single molecule. Accordingly, the effective interaction ΔE (6.29) does not go to zero as $d \to \infty$, see Fig. 6.5. We checked that this is still true if we consider a trial state with two phonons of the form

$$\begin{aligned} |\psi\rangle = & g|L_1 M_1\rangle|L_2 M_2\rangle|0\rangle + \sum \beta|j_1 m_1\rangle|j_2 m_2\rangle\hat{b}^\dagger_{\mathbf{k}}|0\rangle \\ & + \sum \gamma|j_1' m_1'\rangle|j_2' m_2'\rangle\hat{b}^\dagger_{\mathbf{k}_1}\hat{b}^\dagger_{\mathbf{k}_2}|0\rangle, \end{aligned} \tag{6.37}$$

with variational coefficients g, β and γ, to compute E_{BA} (and a trial state with one phonon (or with two phonons) to compute $E_{\mathsf{A},1}$ and $E_{\mathsf{A},2}$). That is, as the above physical picture

suggests, two phonons do not dress each of the two molecules (for $d \to \infty$) as one phonon dresses (or two phonons dress) a single impurity. In order to obtain an effective potential with the property $\lim_{d\to\infty} \Delta E = 0$ one would need to consider a sufficiently large number of phonons to compute E_{BA}. In case of a one-phonon or a two-phonon variational state

$$\Delta E = E_{\mathrm{BA}} - \lim_{d\to\infty} E_{\mathrm{BA}} \tag{6.38}$$

is therefore clearly a better definition for the effective interaction between the two impurities than Eq. (6.29). Based on the above analysis, we expect that a trial state with one or two phonons yields a good approximation if the distance d between the two impurities is not too large.

6.6 The angulon diagonalization technique

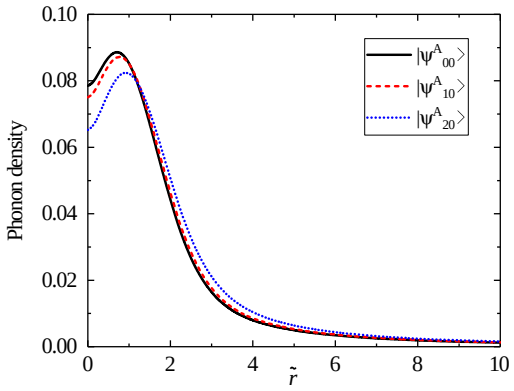

Figure 6.6: Angle-averaged phonon density $\rho_{LM}(r)$ (6.41) around one single molecule sitting at $\mathbf{r} = 0$ as a function of the dimensionless distance $\tilde{r} = r(mB)^{-1/2}$ to the origin. We have chosen $u_0 = u_1 = u_2 = 218B$, $u_\lambda = 0$ for $\lambda \geq 3$ and $\tilde{r}_0 = \tilde{r}_1 = \tilde{r}_2 = 1.5(mB)^{-1/2}$, $\tilde{r}_\lambda = 0$ if $\lambda \geq 3$ as well as $\tilde{n} = 1$. The quantum numbers of the angulon are $L = 0, M = 0$ (solid black line), $L = 1, M = 0$ (red dashed line), $L = 2, M = 0$ (blue dotted line). For more information see the text.

In the one-phonon variational ansatz in Eq. (6.23), we fix the angular momentum quantum numbers L_1, M_1, L_2, M_2 in the first term on the right-hand side. It is important to note, however, that the magnetic quantum number M of the whole system is its

only good quantum number. In this section we ask the question whether the ansatz in Eq. (6.23) is a good approximation also for small molecule-molecule distances, and therefore choose a class of trial states, which allows for a substantial mixing of the different basis states $|L_1, M_1, L_2, M_2\rangle$ with fixed $M_1 + M_2 = M$ in the term proportional to the quasiparticle weight. To simplify the calculations, we assume that the interaction of one of the impurities with the bath is weaker than that of the other impurity. This could correspond e.g. to the case of one heavier and one lighter molecule. The system is described by the wave function

$$|\psi_d\rangle = \sum_{L,M,j,m} \alpha_{j,m}^{L,M} |\psi_{L,M}^{\mathsf{A}}\rangle |jm\rangle. \tag{6.39}$$

Here $\alpha_{j,m}^{L,M}$ are variational coefficients that obey the usual normalization condition and assure that $M + m = \widetilde{M}$ holds with some fixed $\widetilde{M}$. Additionally,

$$\begin{aligned} |\psi_{LM}^{\mathsf{A}}\rangle =& \sqrt{Z_L} |LM\rangle |0\rangle \\ &+ \sum_{k\lambda j_1} \beta_{k\lambda j_1} C_{j_1 m_1, \lambda\mu}^{LM} |j_1 m_1\rangle \hat{b}_{k\lambda\mu}^{\dagger} |0\rangle \end{aligned} \tag{6.40}$$

denotes the wave function of one single angulon with angular momentum quantum numbers L, M. We obtain the coefficients in Eq. (6.40) by considering the relevant one-impurity system, see Ref. [Schmidt and Lemeshko, 2015]. The impurity described by the first tensor factor in Eq. (6.39) is the one with stronger molecule-bath interaction, and therefore it is assumed to be already dressed by the phonon in the system. The second impurity is described by a free rotor. Due to the generality of the variational coefficients, the above ansatz allows for a substantial mixing of different free rotor states in the part of the wave function with no phonons. Using it, we can therefore describe the transition from two weakly coupled angulons, where the wave function is approximately given by $|\psi_{L,M}^{\mathsf{A}}\rangle |jm\rangle$ for some quantum numbers L, M, j, m, to a strongly correlated biangulon quasiparticle, where more than one of the coefficients $\alpha_{j,m}^{L,M}$ are unequal to zero. The above ansatz efficiently describes phonon-induced interactions between the two molecules as long as the weakly interacting impurity has a substantial overlap with the phonon density located around the first molecule.

In Fig. 6.6 we show an example of such a phonon density. More precisely, we show

the angle-averaged phonon density

$$\begin{aligned}\rho_{LM}(r) &= \int \mathrm{d}\phi_{\mathbf{r}}\mathrm{d}\theta_{\mathbf{r}}\langle\psi^{\mathsf{A}}_{L,M}|\hat{b}^{\dagger}_{\mathbf{r}}\hat{b}_{\mathbf{r}}|\psi^{\mathsf{A}}_{L,M}\rangle \\ &= \sum_{\lambda\mu}\langle\psi^{\mathsf{A}}_{L,M}|\hat{b}^{\dagger}_{r\lambda\mu}\hat{b}_{r\lambda\mu}|\psi^{\mathsf{A}}_{L,M}\rangle \end{aligned} \tag{6.41}$$

of one single impurity described by the angulon wave function (6.40). Here $\hat{b}^{\dagger}_{\mathbf{r}}$ creates one phonon at position $\mathbf{r}$ and we used

$$\hat{b}^{\dagger}_{\mathbf{r}} = \frac{1}{r}\sum_{\lambda\mu}\hat{b}^{\dagger}_{r\lambda\mu}Y^{*}_{\lambda\mu}(\theta_{\mathrm{r}},\phi_{\mathrm{r}}), \tag{6.42}$$

see [Lemeshko and Schmidt, 2017]. The operator $\hat{b}^{\dagger}_{r\lambda\mu}$ creates one phonon at distance r from the origin with angular momentum quantum numbers λ,μ. It can be written in terms of the operators $\hat{b}^{\dagger}_{k\lambda\mu}$ as

$$\hat{b}^{\dagger}_{r\lambda\mu} = \sqrt{\frac{2}{\pi}}r\int k\mathrm{d}k j_{\lambda}(kr)\hat{b}^{\dagger}_{k\lambda\mu}, \tag{6.43}$$

where $j_{\lambda}(kr)$ denotes the spherical Bessel function [Abramowitz and Stegun, 1965]. The parameters are chosen to be $u_0 = u_1 = u_2 = 218B$, $u_{\lambda} = 0$ for $\lambda \geq 3$ and $\tilde{r}_0 = \tilde{r}_1 = \tilde{r}_2 = 1.5(mB)^{-1/2}$, $\tilde{r}_{\lambda} = 0$ if $\lambda \geq 3$. The density is given by $\tilde{n} = 1$ and the quantum numbers of the angulon are chosen as $L = 0, M = 0$ (solid black line), $L = 1, M = 0$ (red dashed line), $L = 2, M = 0$ (blue dotted line). As long as the distance between the two impurities is below $\tilde{d} \approx 6$ for this choice of the parameters, the ansatz (6.39) allows us to capture the interactions between the two impurities.

For mathematical convenience we assume from now on that the stronger interacting impurity is sitting at the origin of the laboratory frame and that the weaker interacting impurity is located at $(0,0,d)$. To diagonalize the biangulon Hamiltonian (6.4) with the basis set (6.39), we write it as $\hat{H} = \hat{H}_{\mathsf{A}} + \hat{H}_{\mathsf{I}}$, where

$$\begin{aligned}\hat{H}_{\mathsf{A}} =& B_1\hat{\mathbf{J}}_1^2 + B_2\hat{\mathbf{J}}_2^2 + \sum_{\mathbf{k}}\omega(k)\hat{b}^{\dagger}_{\mathbf{k}}\hat{b}_{\mathbf{k}} \\ &+ \sum_{k\lambda\mu}\Big[V(\mathbf{k},\hat{\theta}_1,\hat{\phi}_1)\hat{b}^{\dagger}_{\mathbf{k}} + \mathsf{H.c.}\Big]\end{aligned} \tag{6.44}$$

and

$$\hat{H}_{\mathsf{I}} = \sum_{\mathbf{k}}\Big[V(\mathbf{k},\hat{\theta}_2,\hat{\phi}_2)e^{i\mathbf{k}\cdot\mathbf{d}}\hat{b}^{\dagger}_{\mathbf{k}} + \mathsf{H.c.}\Big]\ . \tag{6.45}$$

The Hamiltonian $\hat{H}_{\mathsf{A}}$ describes a single angulon [Schmidt and Lemeshko, 2015; Lemeshko, 2017] and a bare rotating molecule, and can therefore be considered as diagonal within our approximation scheme. This allows us to write the matrix elements of the biangulon Hamiltonian $\hat{H}$ with respect to the basis states in Eq. (6.39) as

$$\begin{aligned} H_{LMjm}^{L'M'j'm'} &= \left[E_{\mathsf{A}}^{L,M} + Bj(j+1)\right]\delta_{L',L}\delta_{M',M}\delta_{j',j}\delta_{m',m} \\ &\quad + \langle\psi_{L',M'}^{\mathsf{A}}|\langle j'm'|\hat{H}_{\mathsf{I}}|jm\rangle|\psi_{L,M}^{\mathsf{A}}\rangle. \end{aligned} \tag{6.46}$$

In order to obtain the energies and eigenfunctions, we diagonalize the Hamiltonian matrix (6.46) numerically with the angular momentum cut-off $L, L', j, j', |M|, |M'|, |m|, |m'| \leq 2$.

As parameters we choose $u_{\lambda,1} = 2u_{\lambda,2}$, where the second index refers to the first and the second impurity, $u_{0,1} = u_{1,1} = u_{2,1} = 218B$ and $\tilde{n} = 1$. We label eigenstates by their dominant basis vector contribution at $\tilde{d} = 10$, that is, at that distance the eigenfunction $|\psi_{L,M}^{\mathsf{A}}; j, m\rangle$ approximately equals $|\psi_{L,M}^{\mathsf{A}}\rangle|j, m\rangle$. The results of the diagonalization are presented in Fig. 6.7. In Fig. 6.7(a) we show the energy of the ground state $|\psi_{0,0}^{\mathsf{A}}; 0, 0\rangle$ and of six excited states. States which differ only by the magnetic quantum number of the two molecules are degenerate if the distance between them is sufficiently large because $E_{\mathsf{A}}^{L,M} = E_{\mathsf{A}}^{L,-M}$. This degeneracy is lifted when the particles start to substantially interact around $\tilde{d} \approx 6$. In this regime the eigenvalues related to $|\psi_{1,0}^{\mathsf{A}}; 0, 0\rangle$ (red solid line) and $|\psi_{2,0}^{\mathsf{A}}; 0, 0\rangle$ (solid black line) start to split from those related to $|\psi_{1,\pm1}^{\mathsf{A}}; 0, 0\rangle$ (red dashed line) and $|\psi_{2,\pm1}^{\mathsf{A}}; 0, 0\rangle$ (black dashed line), $|\psi_{2,\pm2}^{\mathsf{A}}; 0, 0\rangle$ (black dotted line), respectively. The states $|\psi_{1,\pm1}^{\mathsf{A}}; 1, \mp1\rangle$ remain degenerate.

In Fig. 6.7 In (b)–(e) we show the squared overlap of the eigenstate $|\psi_{2,0}^{\mathsf{A}}; 0, 0\rangle$ (b), $|\psi_{1,\pm1}^{\mathsf{A}}; 1, \mp1\rangle$ (c), $|\psi_{1,0}^{\mathsf{A}}; 1, 0\rangle$ (d) and $|\psi_{0,0}^{\mathsf{A}}; 0, 0\rangle$ (e) with the different basis states. We note that all these states have $M + m = 0$. The grey lines show the occupation of all other basis vectors. As can be seen from these figures, different eigenstates of the Hamiltonian matrix (6.46) show different behavior during the transition from two separate angulons to a biangulon if the distance between them is decreased. The states $|\psi_{1,\pm1}^{\mathsf{A}}; 1, \mp1\rangle$ and $|\psi_{1,0}^{\mathsf{A}}; 0, 0\rangle$ for example show a sharp transition, while this transition is less pronounced for the state $|\psi_{2,0}^{\mathsf{A}}; 0, 0\rangle$ and it is almost not present in case of the ground state $|\psi_{0,0}^{\mathsf{A}}; 0, 0\rangle$. This behavior is a result of the SO(3) algebra of angular momentum ruling the interaction between the two impurities. More precisely, the contribution of each different angular momentum basis state to a matrix element

of the form $\langle V(\mathbf{k},\hat{\theta}_2,\hat{\phi}_2)e^{i\mathbf{k}\cdot\mathbf{d}}\rangle$ shows a different dependence on the molecule-molecule distance d. How these contributions are mixed is determined by the Clebsch-Gordan coefficients, and therefore by the SO(3) algebra. In general, we can say that the states with $M=0=m$ and $L\neq j$ show the most pronounced angulon to biangulon transitions. In case of $M=0=m$ the wave function is with good approximation a superposition of two basis states. As an example we consider states of the form

$$|\psi^{\mathsf{A}}_{L,0};j,0\rangle \approx c_1(d)|\psi^{\mathsf{A}}_{L,0}\rangle|j,0\rangle + c_2(d)|\psi^{\mathsf{A}}_{j,0}\rangle|L,0\rangle, \tag{6.47}$$

compare with Fig. 6.7(b) and (d). This representation implies that angular momentum is transferred from one impurity to the other during the transition from two separated angulons to a biangulon quasiparticle. The fact that exactly these two basis states appear in Eq. (6.47) is again a result of the SO(3) algebra of angular momentum. For several other basis states we find a similar but less pronounced angulon-biangulon transition. The weakest transition can be seen in states of the form $|\psi^{\mathsf{A}}_{L,0};L,0\rangle$.

In order to investigate the transition from two angulons to a biangulon for states that show a pronounced transition in more detail, we consider correlation functions of the form

$$F_{\hat{O}} = \frac{\langle\hat{O}_1\hat{O}_2\rangle - \langle\hat{O}_1\rangle\langle\hat{O}_2\rangle}{\langle\hat{O}_1\hat{O}_2\rangle_{\max} - \langle\hat{O}_1\rangle_{\max}\langle\hat{O}_2\rangle_{\max}}, \tag{6.48}$$

where $\langle\cdot\rangle$ denotes the expectation w.r.t. one of the eigenfunctions of the two impurity problem and $\hat{O}_i$, $i=1,2$, is an operator acting on the i-th impurity. As an example, we consider eigenstates that can with a good approximation be written as a distance-dependent superposition of two basis states $|v\rangle$ and $|w\rangle$, that is, states of the form

$$|\psi_d\rangle \approx c_1(d)|v\rangle + c_2(d)|w\rangle, \tag{6.49}$$

compare with Eq. (6.47). The normalization in (6.48) is chosen such that $|F_{\hat{O}}|$ takes values between zero and one. More precisely, we assume that the expectation $\langle\cdot\rangle_{\max}$ is taken with respect to the state

$$|\psi_{\max}\rangle = \frac{1}{\sqrt{2}}\left(|v\rangle + |w\rangle\right). \tag{6.50}$$

In the cases we consider, the state $|\psi_{\mathsf{max}}\rangle$ maximizes the correlation function among normalized states of the form given by Eq. (6.49). Since the different eigenfunctions of the Hamiltonian matrix (6.46) we consider here have different dominant basis vectors in their expansion we also have to use different operators $\hat{O}$ to measure their correlations.

The correlation functions related to four eigenstates of the Hamiltonian matrix can be found in Fig. 6.8. We have chosen $\hat{O} = \cos(\theta)$, $|\psi^{\mathsf{A}}_{1,0}; 0, 0\rangle$ (red solid line), $\hat{O} = \cos^2(\theta)$, $|\psi^{\mathsf{A}}_{2,0}; 0, 0\rangle$ (solid black line), $\hat{O} = \sin(\theta)e^{\pm i\varphi}$, $|\psi^{\mathsf{A}}_{1,1}; 0, 0\rangle$ (red dashed line) and $\hat{O} = \sin^2(\theta)e^{\pm i2\varphi}$, $|\psi^{\mathsf{A}}_{2,2}; 0, 0\rangle$ (black dotted line). The interaction between the impurities is attractive, and hence all correlation functions are positive. The particular patterns that these functions show are related to the shape of our interaction potential. All correlation functions indicate that after the onset of interactions between the two impurities around $\tilde{d} \sim 6$, the eigenstates of the Hamiltonian matrix (6.46) we considered in Fig. 6.8 quickly start to be substantially entangled and correlated when the distance between them is further reduced – a clear signature that a biangulon quasiparticle forms.

A similar but less pronounced behavior can be found for several other eigenstates. The states $|\psi^{\mathsf{A}}_{L,0}; L, 0\rangle$ show, however, almost no correlations and have $|\psi^{\mathsf{A}}_{L,0}\rangle|L, 0\rangle$ as a dominant basis vector for all distances. The weakest correlation can be found in the ground state. The fact that its wave function is with good approximation given by $|\psi^{\mathsf{A}}_{0,0}\rangle|0, 0\rangle$ is in accordance with the analysis in the strong-coupling regime in Sec. 6.4.2, where we found that the ground state is a product of two (the same) impurity wave function. Here the system looked like a biangulon quasiparticle because of the substantial anisotropy of the molecular orientations and because the phonon cloud related to one molecules had a substantial overlap with the other molecule (and the other way round). Due to the simplicity of our approach, this is clearly not captured by the analysis in this Section. To take such effects into account, which would allow us to investigate the transition from two separate angulons to a biangulon also for the states $|\psi^{\mathsf{A}}_{L,0}; L, 0\rangle$ in more detail, we would need to allow for more basis states in the expansion of the molecular states. Additionally, we would need to treat also the phonon wave function variationally. This, however, is beyond the scope of the present chapter.

In summary, by applying translation operators to the previously introduced angulon Hamiltonian, we obtained the Hamiltonian describing two rotating molecules immersed in a bosonic bath. This model was studied in different parameter regimes and using several theoretical approaches. In all the parameter regimes we found that the molecules align with respect to each other as a result of the phonon mediated effective attractive interaction (6.12) between them. To describe the resulting correlated state, we introduced the *biangulon* quasiparticle. In analogy to the bipolaron quasiparticle, it

describes two rotating molecules dressed by bosonic excitations.

In the regime where the molecular rotation is much slower than the characteristic timescale of the phonons. The phonon cloud adjusts itself instantaneously to changes of the molecular orientation and a Born-Oppenheimer approximation is valid. Within this approach we showed that the effective intermolecular force mediated by the phonons is sensitive to the rotational state of both molecules and takes its largest values when the overlap of the phonon density with each of the two molecules is maximal. Accordingly, the states with magnetic quantum numbers $M_1 = 0 = M_2$, which preserve the symmetries of the Hamiltonian, show the largest effective interaction. Accordingly, we expect the alignment of diatomic molecules in helium droplets to be observable in experiments similar to the single-molecule case [Shepperson *et al.*, 2017b; Shepperson *et al.*, 2017a; Cherepanov *et al.*, 2019; Pickering *et al.*, 2018a].

In the opposite regime, where the impurity-bath coupling is relatively weak, we investigated the system with the help of a one-phonon excitation variational ansatz, which allowed us to access the excitation spectrum of the biangulon. In comparison to the angulon spectrum, we observed an additional spectral instability, as well as a shift of the angulon spectral instabilities due to the presence of the second molecule. If one varies the density of the doped molecular impurities in the solvent from a dilute to a moderately dense regime, we therefore expect to observe the shifts of their spectral instabilities in their spectra as a signature for the formation of the biangulon quasiparticle. Additionally, we pointed out that in our model one or two phonons cannot dress two molecules that are far apart from each other as one phonon dresses one single molecule, which leads to a subtlety in the definition of the effective phonon-mediated interaction for large distances.

Finally, by using products of angulon and bare rotor states as basis states, We show that, in the parameter regime where a biangulon has formed, the wavefunction is a superposition of at least two of the above basis states. Accordingly, angular momentum is transferred between the two molecules and the state is strongly correlated. This has to be contrasted with the appearance of two uncorrelated or weakly correlated angulons at larger molecule-molecule distance.

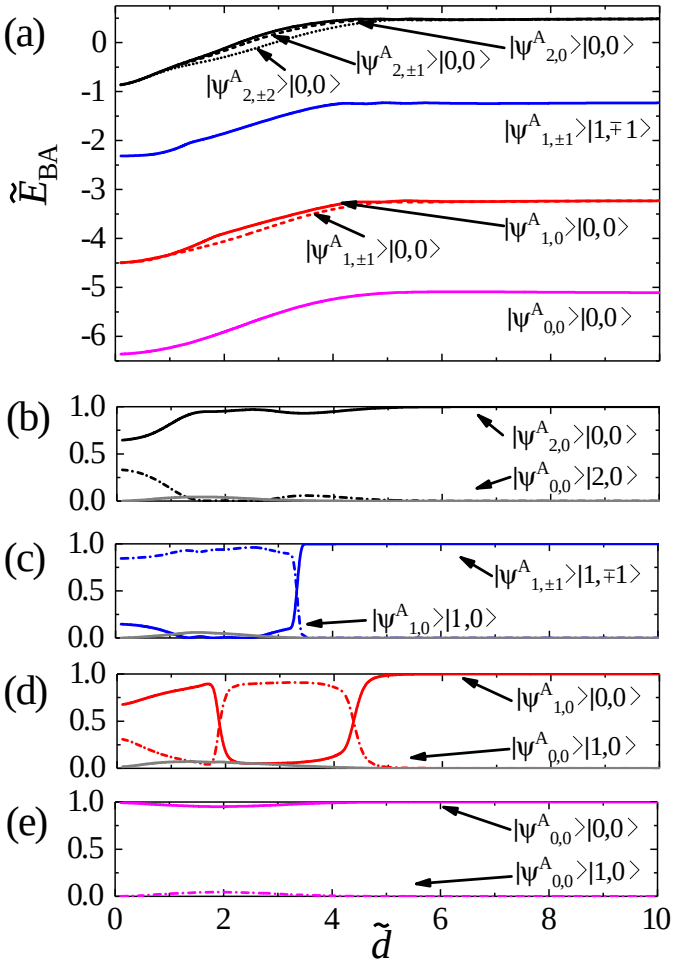

Figure 6.7: (a) The dimensionless biangulon energy of the ground state and of six excited states obtained by diagonalizing the biangulon Hamiltonian (6.4) with the base vectors used in (6.39). In (b)–(e) we show the squared overlap of the eigenstate $|\psi^{\mathsf{A}}_{2,0};0,0\rangle$ (b), $|\psi^{\mathsf{A}}_{1,\pm1};1,\mp1\rangle$ (c), $|\psi^{\mathsf{A}}_{1,0};1,0\rangle$ (d) and $|\psi^{\mathsf{A}}_{0,0};0,0\rangle$ (e) with the different basis states. The bath density has been chosen as $\tilde{n}=1$. The grey lines show the occupation all other basis vectors. For more information see the text.

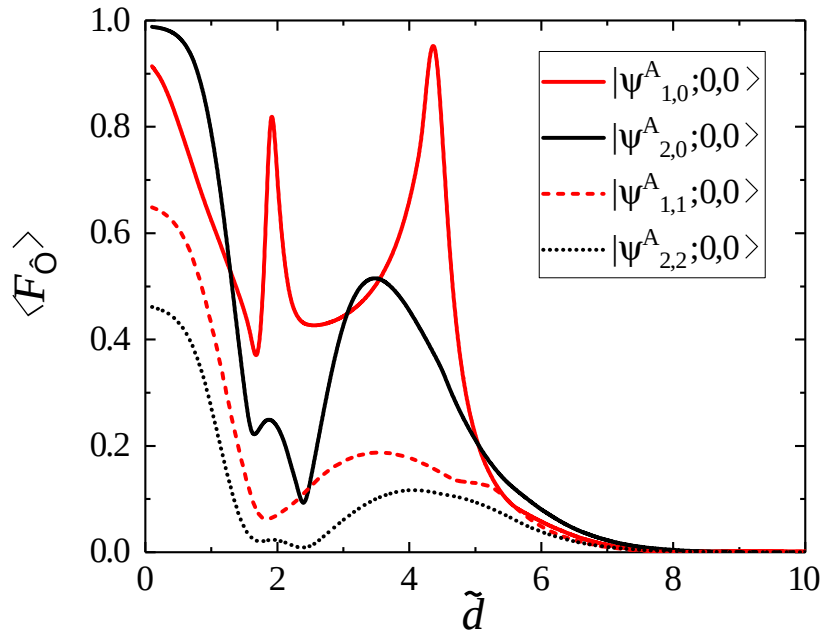

Figure 6.8: Correlation function $F_{\hat{O}}$, Eq. (6.48), as a function of the dimensionless molecule-molecule distance $\tilde{d}$. The parameters are the same as in Fig. 6.7. The colors of the graphs refer to the same states as in Fig. 6.7(a). For the operator $\hat{O}$ and for the state $\langle\cdot\rangle$ we made the following choice: $\hat{O} = \cos(\theta)$, $|\psi^{\mathsf{A}}_{1,0};0,0\rangle$ (red solid line), $\hat{O} = \cos^2(\theta)$, $|\psi^{\mathsf{A}}_{2,0};0,0\rangle$ (solid black line), $\hat{O} = \sin(\theta)e^{\pm i\varphi}$, $|\psi^{\mathsf{A}}_{1,1};0,0\rangle$ (red dashed line) and $\hat{O} = \sin^2(\theta)e^{\pm i2\varphi}$, $|\psi^{\mathsf{A}}_{2,2};0,0\rangle$ (black dotted line). For more information see the text.

7 Conclusions

This thesis introduces a toolbox of theoretical models, describing rotating molecules immersed in a bosonic bath. The models we introduced are based on the mean-field approximation (chapter 2), variational approaches (chapter 3), and diagonalization approach (chapter 4).

We have applied the theory to study the angular self-localization of single molecules immersed in the superfluid (chapter 5) as well as to two molecules, where we derived effective phonon-mediated interactions between them (chapter 6). he content and details of chapters 4, 5, and 6 can also be found in [Li *et al.*, 2019; Li *et al.*, 2017; Li *et al.*, 2020], respectively.

As a concept of quasiparticle, one objective of angulon theory is to develop the theoretical machinery describing the rotating impurity properties within a broad range of parameters. The exploratory results discussed in Chapter 4 are devised based on the variational and analytical approaches. They provides a reasonable estimate of the ground- and excited-state energies both for weak and strong interactions and therefore can be applied in our further studies.

The similarities between the effective Hamiltonian of angulon and Fröhlich Hamiltonian suggest a possibility of observing angular localization. In the other hand, the intrinsic property of quantum angular momentum, separated eigenvalues, distinguishes itself from the polaron systems with only translational momentum. Unlike in the polaron problem, the transition from a spherically symmetric to a localized ground state occurs already at the mean-field level. Furthermore, depending on the symmetry of the interactions, the state can be oriented (broken parity) or aligned (definite parity), making it possible to observe a crossover between the two symmetries in the localized phase.

Among the experimental systems to address the localization transition, the most

promising one is given by cold molecules trapped in superfluid helium nanodroplets [Toennies and Vilesov, 2004b; Lemeshko, 2017]. There, it is possible to trap slowly rotating molecules featuring highly anisotropic interactions with helium. Moreover, angulon self-localization can potentially be studied in experiments on Rydberg excitations in BECs [Balewski *et al.*, 2013], where orbital-angular-momentum-changing collisions between the Rydberg electron and ultracold atoms have already been observed [Schlagmüller *et al.*, 2016]. Finally, studies of coupling between rotations and vibrations have a long history in the context of finite systems, such as nonspherical atomic nuclei [Rowe and Wood, 2010], flexible polyatomic molecules [Schmiedt *et al.*, 2016], and electron bubbles in superfluid helium [Tempere *et al.*, 2003; Vadakkumbatt *et al.*, 2014]. Recasting these problems in terms of the angulon quasiparticle might give further insights into the angular localization transition discussed here.

It is worth noting that here we undertook only the first step in the studies of self-localization of quantum rotors. For Fröhlich polarons it has been demonstrated that a sharp self-trapping transition arises as an artifact of the mean-field approximation, since mean field favors symmetry breaking even if it is prevented by quantum fluctuations [Fisher and Zwerger, 1986; Peeters and Devreese, 1982b; Gerlach and Löwen, 1991a; Mishchenko *et al.*, 2000b; Feranchuk and Komarov, 2005].

Thus, it still remains to investigate whether such a transition actually takes place for rotating impurities. Therefore, in order to get a deeper understanding of angular self-localization, approaches beyond mean field need to be developed for the angulon problem. We hope that the results presented here will stimulate future studies of angular self localization, both in the context of the angulon Hamiltonian, and for extended angulon models including nonlinear coupling terms. Finally, studying an ensemble of interacting quantum rotors in a superfluid might pave the way to studying new phenomena related to quantum glassiness [Ye *et al.*, 1993] and many-body localization [Nandkishore and Huse, 2015].

As another main interest of this thesis (chapter 6), we focus on the effective interaction and the resulting correlations between two diatomic molecules immersed in a bath of bosons. Unlike electrons or ground-state atoms, the low-energy degrees of freedom for molecules involve rotations, leading to an exchange of angular momentum between the molecule and the bath.

We introduce the biangulon quasiparticle describing two rotating molecules that align with respect to each other due to the effective attractive interaction mediated by the excitations of the bath. We show that, the molecules tend to have a strong alignment in the ground state in the strong-coupling regime. In the weak-coupling regime, we access the energy spectrum, and the biangulon shows shifted angulon instabilities and an additional spectral instability. Furthermore, we show the correlations of two molecules and the transition from two separated angulons to a biangulon as a function of the distance between the two molecules.

The phenomenon of effective interactions between quantum particles can emerge due to a surrounding bath has received a lot of attention since 1940s. Aside the fully discussed bipolaron quasiparticle [Devreese, 2016], more complex polaronic structures can form, such as electronic Wigner crystals [Quémerais and Fratini, 1998; Fratini and Quémerais, 2002; Iadonisi *et al.*, 2007], polaron molecules and clusters [Kusmartsev, 2001; Perroni *et al.*, 2004; Bruderer *et al.*, 2007]. In quantum dot devices, the effects of electron-phonon coupling on the thermodynamic and optical properties are applied to explain the optical absorption spectra of high-critical-temperature cuprates and their electronic transitions (see Ref. [Fomin *et al.*, 1998; Klimin *et al.*, 2004] and references therein). The attractive electron correlations mediated by phonons are found to be able to overcome the direct Coulomb repulsion in deformable molecular quantum dots, which are suggested as a basis for polaronic memory resistors [Alexandrov and Bratkovsky, 2003; Alexandrov and Bratkovsky, 2009]. Beyond electron-phonon coupling, other indirect interactions play a key role in quantum systems, for instance the Ruderman-Kittel-Kasuya-Yosida interaction [Ruderman and Kittel, 1954; Zhou *et al.*, 2010] gives rise to complex magnetic phases such as spin glasses [Hewson, 1997].

In chapter 6 , we have shown that two molecular impurities without direct interaction can exchange their angular momentum by coupling with surrounding boson bath. The effective force between two impurities changes as a function of distance between impurities. This promising result imply that we can further study the correlation between multiple molecular impurities. As we discussed in chapter 6, the single phonon dresses the impurities in a superposition state. Whether a supperradiance of phonons could happen in the molecular impurities immersing in many-body environment becomes an interesting question to be asked.

In addition, our results also show that the effective force aligns two molecular impurities to maximize the wavefunction overlap, then the situation becomes more complex when three or more impurities are considered. The phonon-mediated coupling could therefore play a role in cluster formation. The above topics can be applied to molecules immersed in superfluid helium droplets [Toennies and Vilesov, 2004c] or in atomic Bose-Einstein condensates [Lemeshko and Schmidt, 2017], and can be extended to systems where the impurity particles are Rydberg atoms [Schmidt *et al.*, 2016; Camargo *et al.*, 2018] or defects in solids [Pushkarov, 1991].

As compared to atoms, molecules possess a richer internal structure that overs many opportunities for technological and scientic advancement. The work shown here pushes the theory of controllable molecules further by extending it to the collective behavior in the presence of a many-body environment, where molecules turn into the angulon quasiparticles. The theory of biangulon, which is a bound state of two angulons, will be developed aiming at describing the interaction between two rotating impurities in a bosonic bath, as well as the redistribution of orbital angular momentum in the context of quantum many-particle systems. In a broader perspective, the biangulon theory will serve as a basic understanding for treating few-, and many-particle processes involving angular momentum exchange with an environment, such as reactivity, molecular collisions, and formation of molecular clusters. Finally, the biangulon study will develop and advance the study of the ‘newborn’ angulon quasiparticle, holding a potential for exciting and unexpected applications in the years to come.

Bibliography

[Abramowitz and Stegun, 1965] Milton Abramowitz and Irene A Stegun, *Handbook of mathematical functions: with formulas, graphs, and mathematical tables*, volume 55, Courier Corporation, 1965.

[Akram and Pelster, 2016] Javed Akram and Axel Pelster, "Numerical study of localized impurity in a Bose-Einstein condensate," *Physical Review A*, 93(3):033610, 2016.

[Alexandrov, 2003] Alexandre S Alexandrov, *Theory of superconductivity: from weak to strong coupling*, CRC Press, 2003.

[Alexandrov and Bratkovsky, 2003] AS Alexandrov and AM Bratkovsky, "Memory effect in a molecular quantum dot with strong electron-vibron interaction," *Physical Review B*, 67(23):235312, 2003.

[Alexandrov and Bratkovsky, 2009] AS Alexandrov and AM Bratkovsky, "Polaronic memory resistors strongly coupled to electrodes," *Physical Review B*, 80(11):115321, 2009.

[Anderson, 1967] Philip W Anderson, "Infrared catastrophe in Fermi gases with local scattering potentials," *Physical Review Letters*, 18(24):1049, 1967.

[Appel, 1968] J Appel, "Solid state physics," *New York, Academic Press*, 21:193, 1968.

[Ardila and Giorgini, 2015] LA Pena Ardila and S Giorgini, "Impurity in a Bose-Einstein condensate: study of the attractive and repulsive branch using quantum Monte Carlo methods," *Physical Review A*, 92(3):033612, 2015.

[Balewski *et al.*, 2013] Jonathan B Balewski, Alexander T Krupp, Anita Gaj, David Peter, Hans Peter Büchler, Robert Löw, Sebastian Hofferberth, and Tilman Pfau, "Coupling a single electron to a Bose-Einstein condensate," *Nature*, 502(7473):664–667, 2013.

[Becker *et al.*, 1983] W Becker, B Gerlach, and H Schliffke, "Monte Carlo calculation of the ground-state energy of an optical polaron," *Physical Review B*, 28(10):5735, 1983.

[Bernath, 2005] P F Bernath, *Spectra of atoms and molecules*, Oxford University Press, 2 edition, 2005.

[Bighin and Lemeshko, 2017] G. Bighin and M. Lemeshko, "Diagrammatic approach to orbital quantum impurities interacting with a many-particle environment," *Phys. Rev. B*, 96:085410, Aug 2017.

[Bighin *et al.*, 2018a] G Bighin, T V Tscherbul, and M Lemeshko, "Diagrammatic Monte Carlo Approach to Angular Momentum in Quantum Many-Particle Systems," *Phys. Rev. Lett.*, 121:165301, 2018.

[Bighin *et al.*, 2018b] Giacomo Bighin, Timur Tscherbul, and Mikhail Lemeshko, "Diagrammatic Monte Carlo approach to rotating molecular impurities," *Physical Review Letters*, 121(16), 2018.

[Bijlsma *et al.*, 2000] MJ Bijlsma, BA Heringa, and HTC Stoof, "Phonon exchange in dilute Fermi-Bose mixtures: Tailoring the Fermi-Fermi interaction," *Physical Review A*, 61(5):053601, 2000.

[Blinova *et al.*, 2013] AA Blinova, MG Boshier, and Eddy Timmermans, "Two polaron flavors of the bose-einstein condensate impurity," *Physical Review A*, 88(5):053610, 2013.

[Bloch *et al.*, 2008] Immanuel Bloch, Jean Dalibard, and Wilhelm Zwerger, "Many-body physics with ultracold gases," *Reviews of modern physics*, 80(3):885, 2008.

[Boudjemâa, 2014] Abdelâali Boudjemâa, "Self-localized state and solitons in a Bose-Einstein-condensate–impurity mixture at finite temperature," *Physical Review A*, 90(1):013628, 2014.

[Bruderer *et al.*, 2008] M Bruderer, W Bao, and D Jaksch, "Self-trapping of impurities in Bose-Einstein condensates: Strong attractive and repulsive coupling," *EPL (Europhysics Letters)*, 82(3):30004, 2008.

[Bruderer *et al.*, 2007] Martin Bruderer, Alexander Klein, Stephen R Clark, and Dieter Jaksch, "Polaron physics in optical lattices," *Physical Review A*, 76(1):011605, 2007.

[Callegari *et al.*, 1999] C Callegari, A Conjusteau, I Reinhard, KK Lehmann, G Scoles, and F Dalfovo, "Superfluid Hydrodynamic Model for the Enhanced Moments of Inertia of Molecules in Liquid 4 He," *Physical Review Letters*, 83(24):5058, 1999.

[Camacho-Guardian *et al.*, 2018] Arturo Camacho-Guardian, Luis Aldemar Peña Ardila, Thomas Pohl, and Georg M Bruun, "Bipolarons in a Bose-Einstein condensate," *arXiv preprint arXiv:1804.00402*, 2018.

[Camargo *et al.*, 2018] F Camargo, Richard Schmidt, JD Whalen, R Ding, G Woehl Jr, S Yoshida, J Burgdörfer, FB Dunning, HR Sadeghpour, E Demler, *et al.*, "Creation of Rydberg polarons in a Bose Gas," *Physical review letters*, 120(8):083401, 2018.

[Cao *et al.*, 2017] L Cao, V Bolsinger, SI Mistakidis, GM Koutentakis, S Krönke, JM Schurer, and P Schmelcher, "A unified ab initio approach to the correlated quantum dynamics of ultracold fermionic and bosonic mixtures," *J. Chem. Phys.*, 147(4):044106, 2017.

[Carr *et al.*, 2009] Lincoln D Carr, David DeMille, Roman V Krems, and Jun Ye, "Cold and ultracold molecules: science, technology and applications," *New Journal of Physics*, 11(5):055049, 2009.

[Casteels *et al.*, 2011a] W Casteels, J Tempere, and JT Devreese, "Many-polaron description of impurities in a Bose-Einstein condensate in the weak-coupling regime," *Physical Review A*, 84(6):063612, 2011.

[Casteels *et al.*, 2012] W Casteels, J Tempere, and JT Devreese, "Polaronic properties of an impurity in a Bose-Einstein condensate in reduced dimensions," *Physical Review A*, 86(4):043614, 2012.

[Casteels *et al.*, 2013] W Casteels, J Tempere, and JT Devreese, "Bipolarons and multipolarons consisting of impurity atoms in a Bose-Einstein condensate," *Physical Review A*, 88(1):013613, 2013.

[Casteels *et al.*, 2011b] W Casteels, T Van Cauteren, J Tempere, and JT Devreese, "Strong coupling treatment of the polaronic system consisting of an impurity in a condensate," *Laser Phys.*, 21(8):1480, 2011.

[Cetina *et al.*, 2016] M Cetina, M Jag, RS Lous, I Fritsche, JTM Walraven, R Grimm, J Levinsen, MM Parish, R Schmidt, M Knap, *et al.*, "Ultrafast many-body interferometry of impurities coupled to a Fermi sea," *arXiv:1604.07423*, 2016.

[Cetina *et al.*, 2015] Marko Cetina, Michael Jag, Rianne S. Lous, Jook T. M. Walraven, Rudolf Grimm, Rasmus S. Christensen, and Georg M. Bruun, "Decoherence of Impurities in a Fermi Sea of Ultracold Atoms," *Phys. Rev. Lett.*, 115:135302, 2015.

[Cherepanov *et al.*, 2019] Igor N Cherepanov, Giacomo Bighin, Lars Christiansen, Anders Vestergaard Jørgensen, Richard Schmidt, Henrik Stapelfeldt, and Mikhail Lemeshko, "Far-from-equilibrium dynamics of angular momentum in a quantum many-particle system," *arXiv preprint arXiv:1906.12238*, 2019.

[Cherepanov and Lemeshko, 2017] Igor N. Cherepanov and Mikhail Lemeshko, "Fingerprints of angulon instabilities in the spectra of matrix-isolated molecules," *Phys. Rev. Materials*, 1:035602, Aug 2017.

[Chevy, 2006a] F. Chevy, "Universal phase diagram of a strongly interacting Fermi gas with unbalanced spin populations," *Phys. Rev. A*, 74:063628, Dec 2006.

[Chevy, 2006b] Frédéric Chevy, "Universal phase diagram of a strongly interacting Fermi gas with unbalanced spin populations," *Physical Review A*, 74(6):063628, 2006.

[Chikkatur *et al.*, 2000] A. P. Chikkatur, A. Görlitz, D. M. Stamper-Kurn, S. Inouye, S. Gupta, and W. Ketterle, "Suppression and Enhancement of Impurity Scattering in a Bose-Einstein Condensate," *Phys. Rev. Lett.*, 85:483, 2000.

[Chin *et al.*, 2010] Cheng Chin, Rudolf Grimm, Paul Julienne, and Eite Tiesinga, "Feshbach resonances in ultracold gases," *Reviews of Modern Physics*, 82(2):1225, 2010.

[Cooper and Shlyapnikov, 2009] NR Cooper and Georgi V Shlyapnikov, "Stable topological superfluid phase of ultracold polar fermionic molecules," *Physical review letters*, 103(15):155302, 2009.

[Crawford and Slifkin, 2013] James H Crawford and Lawrence M Slifkin, *Point Defects in Solids: General and ionic crystals*, Springer Science & Business Media, 2013.

[Cubizolles *et al.*, 2003] J Cubizolles, T Bourdel, SJJMF Kokkelmans, GV Shlyapnikov, and C Salomon, "Production of Long-Lived Ultracold L i 2 Molecules from a Fermi Gas," *Physical review letters*, 91(24):240401, 2003.

[Cucchietti and Timmermans, 2006a] Fernando M Cucchietti and Eddy Timmermans, "Strong-coupling polarons in dilute gas Bose-Einstein condensates," *Physical review letters*, 96(21):210401, 2006.

[Cucchietti and Timmermans, 2006b] Fernando M Cucchietti and Eddy Timmermans, "Strong-coupling polarons in dilute gas Bose-Einstein condensates," *Physical review letters*, 96(21):210401, 2006.

[Dagotto, 1994] Elbio Dagotto, "Correlated electrons in high-temperature superconductors," *Reviews of Modern Physics*, 66(3):763, 1994.

[Das and Chakrabarti, 2005] Arnab Das and Bikas K Chakrabarti, *Quantum annealing and related optimization methods*, volume 679, Springer Science & Business Media, 2005.

[De Lange *et al.*, 2012] Gijs De Lange, Toeno Van Der Sar, Machiel Blok, Zhi-Hui Wang, Viatcheslav Dobrovitski, and Ronald Hanson, "Controlling the quantum dynamics of a mesoscopic spin bath in diamond," *Scientific reports*, 2:382, 2012.

[Devreese, 2015] J. T. Devreese, "Lectures on Fröhlich Polarons from $3D$ to $0D$ — including detailed theoretical derivations," *arXiv:1012.4576*, 2015.

[Devreese and Alexandrov, 2009] Jozef T Devreese and Alexandre S Alexandrov, "Fröhlich polaron and bipolaron: recent developments," *Reports on Progress in Physics*, 72(6):066501, 2009.

[Devreese, 2007] JT Devreese, "Fröhlich polarons from 0D to 3D: concepts and recent developments," *Journal of Physics: Condensed Matter*, 19(25):255201, 2007.

[Devreese, 2016] JT Devreese, "Fr\" ohlich Polarons. Lecture course including detailed theoretical derivations," *arXiv preprint arXiv:1611.06122*, 2016.

[Donnelly and Barenghi, 1998] Russell J Donnelly and Carlo F Barenghi, "The observed properties of liquid helium at the saturated vapor pressure," *Journal of physical and chemical reference data*, 27(6):1217–1274, 1998.

[Donsker and Varadhan, 1983] M. Donsker and S.R.S. Varadhan, "Asymptotics for the polaron," *Comm. Pure Appl. Math.*, 36:505–528, 1983.

[Dudin and Kuzmich, 2012] YO Dudin and A Kuzmich, "Strongly interacting Rydberg excitations of a cold atomic gas," *Science*, 336(6083):887–889, 2012.

[Dürr *et al.*, 2004] Stephan Dürr, Thomas Volz, Andreas Marte, and Gerhard Rempe, "Observation of molecules produced from a Bose-Einstein condensate," *Physical review letters*, 92(2):020406, 2004.

[Emin, 2013] D Emin, *Polarons*, Cambridge University Press, 2013.

[Fantoni, 2012] Riccardo Fantoni, "Localization of acoustic polarons at low temperatures: A path-integral Monte Carlo approach," *Physical Review B*, 86(14):144304, 2012.

[Feranchuk and Komarov, 2005] ID Feranchuk and LI Komarov, "New solution for the polaron problem," *arXiv preprint cond-mat/0510510*, 2005.

[Feynman, 1955a] R P Feynman, "Slow Electrons in a Polar Crystal," *Physical Review*, 97(3):660–665, 1955.

[Feynman, 2018] Richard P Feynman, *Quantum electrodynamics*, CRC Press, 2018.

[Feynman, 1955b] Richard Phillips Feynman, "Slow electrons in a polar crystal," *Physical Review*, 97(3):660, 1955.

[Fisher and Zwerger, 1986] Matthew PA Fisher and Wilhelm Zwerger, "Ground-state symmetry of a generalized polaron," *Physical Review B*, 34(8):5912, 1986.

[Fomin *et al.*, 1998] VM Fomin, VN Gladilin, JT Devreese, EP Pokatilov, SN Balaban, and SN Klimin, "Photoluminescence of spherical quantum dots," *Physical Review B*, 57(4):2415, 1998.

[Fratini and Quémerais, 2002] S Fratini and P Quémerais, "Polarization catastrophe in the polaronic Wigner crystal," *The European Physical Journal B-Condensed Matter and Complex Systems*, 29(1):41–49, 2002.

[Fröhlich, 1954] Herbert Fröhlich, "Electrons in lattice fields," *Advances in Physics*, 3(11):325–361, 1954.

[Fukuhara *et al.*, 2013a] Takeshi Fukuhara, Adrian Kantian, Manuel Endres, Marc Cheneau, Peter Schauß, Sebastian Hild, David Bellem, Ulrich Schollwöck, Thierry Giamarchi, Christian Gross, Immanuel Bloch, and Stefan Kuhr, "Quantum dynamics of a mobile spin impurity," *Nat. Phys.*, 9:235, 2013.

[Fukuhara *et al.*, 2013b] Takeshi Fukuhara, Peter Schauß, Manuel Endres, Sebastian Hild, Marc Cheneau, Immanuel Bloch, and Christian Gross, "Microscopic observation of magnon bound states and their dynamics," *Nature*, 502(7469):76–79, 2013.

[Geim *et al.*, 1994] AK Geim, PC Main, N La Scala Jr, L Eaves, TJ Foster, PH Beton, JW Sakai, FW Sheard, M Henini, G Hill, *et al.*, "Fermi-edge singularity in resonant tunneling," *Physical review letters*, 72(13):2061, 1994.

[Gerlach and Löwen, 1991a] B Gerlach and H Löwen, "Analytical properties of polaron systems or: do polaronic phase transitions exist or not?," *Reviews of Modern Physics*, 63(1):63, 1991.

[Gerlach and Löwen, 1991b] B Gerlach and H Löwen, "Analytical properties of polaron systems or: do polaronic phase transitions exist or not?," *Reviews of Modern Physics*, 63(1):63, 1991.

[Gorshkov *et al.*, 2011] Alexey V Gorshkov, Salvatore R Manmana, Gang Chen, Jun Ye, Eugene Demler, Mikhail D Lukin, and Ana Maria Rey, "Tunable superfluidity and quantum magnetism with ultracold polar molecules," *Physical review letters*, 107(11):115301, 2011.

[Grebenev *et al.*, 2000] Slava Grebenev, Matthias Hartmann, Martina Havenith, Boris Sartakov, J Peter Toennies, and Andrei F Vilesov, "The rotational spectrum of single OCS molecules in liquid 4 He droplets," *The Journal of Chemical Physics*, 112(10):4485–4495, 2000.

[Gross, 1959a] Eugene P Gross, "Analytical methods in the theory of electron lattice interactions Part I," *Annals of Physics*, 8(1):78–99, 1959.

[Gross, 1959b] Eugene P Gross, "Analytical methods in the theory of electron lattice interactions Part I," *Annals of Physics*, 8(1):78–99, 1959.

[Grusdt and Demler, 2016] F Grusdt and E Demler, "New theoretical approaches to bose polarons," *Quantum Matter at Ultralow Temperatures*, 191:325, 2016.

[Grusdt *et al.*, 2015] F Grusdt, YE Shchadilova, AN Rubtsov, and E Demler, "Renormalization group approach to the Fröhlich polaron model: application to impurity-BEC problem," *Scientific reports*, 5, 2015.

[Grusdt, 2016] Fabian Grusdt, "All-coupling theory for the Fröhlich polaron," *Physical Review B*, 93(14):144302, 2016.

[Grusdt and Demler, 2015a] Fabian Grusdt and Eugene Demler, "New theoretical approaches to bose polarons," *Quantum Matter at Ultralow Temperatures*, 2015.

[Grusdt and Demler, 2015b] Fabian Grusdt and Eugene Demler, "New theoretical approaches to bose polarons," *arXiv preprint arXiv:1510.04934*, 2015.

[Grusdt and Fleischhauer, 2016] Fabian Grusdt and Michael Fleischhauer, "Tunable Polarons of Slow-Light Polaritons in a Two-Dimensional Bose-Einstein Condensate," *Physical review letters*, 116(5):053602, 2016.

[Guinea *et al.*, 1985] F Guinea, V Hakim, and A Muramatsu, "Diffusion and localization of a particle in a periodic potential coupled to a dissipative environment," *Physical review letters*, 54(4):263, 1985.

[Hagen *et al.*, 1970] DE Hagen, LL Van Zandt, and EW Prohofsky, "Excited States in a Model Polaron Hamiltonian," *Physical Review B*, 2(2):553, 1970.

[Hazzard *et al.*, 2014] Kaden RA Hazzard, Bryce Gadway, Michael Foss-Feig, Bo Yan, Steven A Moses, Jacob P Covey, Norman Y Yao, Mikhail D Lukin, Jun Ye, Deborah S Jin, *et al.*, "Many-body dynamics of dipolar molecules in an optical lattice," *Physical review letters*, 113(19):195302, 2014.

[Hewson, 1997] Alexander Cyril Hewson, *The Kondo problem to heavy fermions*, volume 2, Cambridge university press, 1997.

[Holstein, 1959a] Th Holstein, "Studies of polaron motion: Part I. The molecular-crystal model," *Annals of physics*, 8(3):325–342, 1959.

[Holstein, 1959b] Th Holstein, "Studies of polaron motion: Part II. The "mall" polaron," *Annals of Physics*, 8(3):343–389, 1959.

[Hu *et al.*, 2016a] Ming-Guang Hu, Michael J. Van de Graaff, Dhruv Kedar, John P. Corson, Eric A. Cornell, and Deborah S. Jin, "Bose polarons in the strongly interacting regime," *arXiv:1605.00729*, 2016.

[Hu *et al.*, 2016b] Ming-Guang Hu, Michael J Van de Graaff, Dhruv Kedar, John P Corson, Eric A Cornell, and Deborah S Jin, "Bose polarons in the strongly interacting regime," *Physical review letters*, 117(5):055301, 2016.

[Hubač and Wilson, 2010] Ivan Hubač and Stephen Wilson, *Brillouin-Wigner methods for many-body systems*, Springer, Dordrecht, Netherlands, 2010.

[Iadonisi *et al.*, 2007] Giuseppe Iadonisi, Vladimir Mukhomorov, Giovanni Cantele, and Domenico Ninno, "Formation of a large polaron crystal from a homogeneous, dilute polaron gas," *Physical Review B*, 76(14):144303, 2007.

[Jackson and Platzman, 1981] SA Jackson and PM Platzman, "Polaronic aspects of two-dimensional electrons on films of liquid He," *Physical Review B*, 24(1):499, 1981.

[Jin and Ye, 2012] D S Jin and J Ye, "Introduction to Ultracold Molecules: New Frontiers in Quantum and Chemical Physics," *Chem. Rev.*, 112:4801, 2012.

[Jørgensen *et al.*, 2016] N. B. Jørgensen, L. Wacker, K. T. Skalmstang, M. M. Parish, J. Levinsen, R. S. Christensen, G. M. Bruun, and J. J. Arlt, "Observation of Attractive and Repulsive Polarons in a Bose-Einstein Condensate," *arXiv:1604.07883*, 2016.

[Jørgensen *et al.*, 2016] Nils B Jørgensen, Lars Wacker, Kristoffer T Skalmstang, Meera M Parish, Jesper Levinsen, Rasmus S Christensen, Georg M Bruun, and Jan J Arlt, "Observation of attractive and repulsive polarons in a Bose-Einstein condensate," *Physical review letters*, 117(5):055302, 2016.

[Kalas and Blume, 2006] Ryan M Kalas and D Blume, "Interaction-induced localization of an impurity in a trapped Bose-Einstein condensate," *Physical Review A*, 73(4):043608, 2006.

[Kaminski and Sarma, 2002] A Kaminski and S Das Sarma, "Polaron percolation in diluted magnetic semiconductors," *Physical Review Letters*, 88(24):247202, 2002.

[Kashirina and Lakhno, 2010] Nataliya Ivanovna Kashirina and Viktor D Lakhno, "Large-radius bipolaron and the polaron–polaron interaction," *Physics-Uspekhi*, 53(5):431, 2010.

[Kazimierczuk *et al.*, 2014] Tomasz Kazimierczuk, Dietmar Fröhlich, Stefan Scheel, Heinrich Stolz, and Manfred Bayer, "Giant Rydberg excitons in the copper oxide Cu 2 O," *Nature*, 514(7522):343–347, 2014.

[Klimin *et al.*, 2004] SN Klimin, VM Fomin, F Brosens, and JT Devreese, "Ground state and optical conductivity of interacting polarons in a quantum dot," *Physical Review B*, 69(23):235324, 2004.

[Koch *et al.*, 2018] Christiane P Koch, Mikhail Lemeshko, and Dominique Sugny, "Quantum control of molecular rotation," *arXiv preprint arXiv:1810.11338*, 2018.

[Kohstall *et al.*, 2012] C. Kohstall, M. Zaccanti, M. Jag, A. Trenkwalder, P. Massignan, G. M. Bruun, F. Schreck, and R. Grimm, "Metastability and coherence of repulsive polarons in a strongly interacting Fermi mixture," *Nature*, 485:615, 2012.

[Kondo, 1964] Jun Kondo, "Resistance minimum in dilute magnetic alloys," *Progress of theoretical physics*, 32(1):37–49, 1964.

[Kornilovitch, 2007] PE Kornilovitch, "Path-integral approach to lattice polarons," *Journal of Physics: Condensed Matter*, 19(25):255213, 2007.

[Koschorreck *et al.*, 2012] Marco Koschorreck, Daniel Pertot, Enrico Vogt, Bernd Frohlich, Michael Feld, and Michael Kohl, "Attractive and repulsive Fermi polarons in two dimensions," *Nature*, 485(7400):619–624, 2012.

[Krems *et al.*, 2009] Roman Krems, Bretislav Friedrich, and William C Stwalley, *Cold molecules: theory, experiment, applications*, CRC press, 2009.

[Kuper and Whitfield, 1962] C.G. Kuper and G. D. Whitfield, editors, *Polarons and Excitons*, Plenum Press, NY, 1962.

[Kusmartsev, 2001] FV Kusmartsev, "Electronic molecules in solids," *EPL (Europhysics Letters)*, 54(6):786, 2001.

[Lan and Lobo, 2014] Zhihao Lan and Carlos Lobo, "A single impurity in an ideal atomic Fermi gas: current understanding and some open problems," *arXiv preprint arXiv:1404.3220*, 2014.

[Landau, 1933a] L. D. Landau, "Über die Bewegung der Elektronen in Kristalgitter," *Phys. Z. Sowjetunion*, 3:155, 1933.

[Landau, 1933b] LD Landau, "On the motion of electrons in a crystal lattice," *Phys. Z. Sowjetunion*, 3:664–665, 1933.

[Landau and Pekar, 1948] LD Landau and SI Pekar, "* EFFEKTIVNAYA MASSA POLYARONA," *ZHURNAL EKSPERIMENTALNOI I TEORETICHESKOI FIZIKI*, 18(5):419–423, 1948.

[Lee *et al.*, 1953] TD Lee, FE Low, and Do Pines, "The motion of slow electrons in a polar crystal," *Physical Review*, 90(2):297, 1953.

[Lefebvre-Brion and Field, 2004] Helene Lefebvre-Brion and Robert W Field, *The Spectra and Dynamics of Diatomic Molecules: Revised and Enlarged Edition*, Academic Press, 2004.

[Leggett *et al.*, 1987] Anthony J Leggett, SDAFMGA Chakravarty, AT Dorsey, Matthew PA Fisher, Anupam Garg, and W Zwerger, "Dynamics of the dissipative two-state system," *Reviews of Modern Physics*, 59(1):1, 1987.

[Lemeshko and Schmidt, 2017] M. Lemeshko and R. Schmidt, "Molecular impurities interacting with a many-particle environment: from ultracold gases to helium nanodroplets," In O Dulieu and A Osterwalder, editors, *Cold Chemistry: Molecular Scattering and Reactivity Near Absolute Zero*, chapter 9. Royal Society of Chemistry, Cambridge, 2017.

[Lemeshko, 2017] Mikhail Lemeshko, "Quasiparticle approach to molecules interacting with quantum solvents," *Physical Review Letters*, 118(9):095301, 2017.

[Lemeshko *et al.*, 2013] Mikhail Lemeshko, Roman V Krems, John M Doyle, and Sabre Kais, "Manipulation of molecules with electromagnetic fields," *Molecular Physics*, 111(12-13):1648–1682, 2013.

[Lépine and Matz, 1979] Y Lépine and D Matz, "Mean field theory of a single fröhlich polaron possible existence of phase transitions," *physica status solidi (b)*, 96(2):797–806, 1979.

[Lépine *et al.*, 1979] Y Lépine *et al.*, "Mean field theory of a single fröhlich polaron possible existence of phase transitions," *physica status solidi (b)*, 96(2):797–806, 1979.

[Li and Sarma, 2014] Weiran Li and S Das Sarma, "Variational study of polarons in Bose-Einstein condensates," *Physical Review A*, 90(1):013618, 2014.

[Li *et al.*, 2019] Xiang Li, Giacomo Bighin, Enderalp Yakaboylu, and Mikhail Lemeshko, "Variational approaches to quantum impurities: from the Fröhlich polaron to the angulon," *Molecular Physics*, pages 1–8, 2019.

[Li *et al.*, 2017] Xiang Li, Robert Seiringer, and Mikhail Lemeshko, "Angular self-localization of impurities rotating in a bosonic bath," *Physical Review A*, 95(3):033608, 2017.

[Li *et al.*, 2020] Xiang Li, Enderalp Yakaboylu, Giacomo Bighin, Richard Schmidt, Mikhail Lemeshko, and Andreas Deuchert, "Intermolecular forces and correlations mediated by a phonon bath," *The Journal of Chemical Physics*, 152(16):164302, 2020.

[Lieb and Thomas, 1997] E.H. Lieb and L. E. Thomas, "Exact ground state energy of the strong-coupling polaron," *Commun. Math. Phys.*, 183:511–519, 1997.

[Lieb, 1977] Elliott H Lieb, "Existence and uniqueness of the minimizing solution of Choquard's nonlinear equation," *Studies in Applied Mathematics*, 57(2):93–105, 1977.

[Löwen, 1988a] H Löwen, "Analytical behavior of the ground-state energy and pinning transitions for a bound polaron," *Journal of mathematical physics*, 29(6):1505–1513, 1988.

[Löwen, 1988b] H Löwen, "The pinning transition of a bound large polaron," *Zeitschrift für Physik B Condensed Matter*, 72(1):59–64, 1988.

[Lühmann *et al.*, 2008] Dirk-Sören Lühmann, Kai Bongs, Klaus Sengstock, and Daniela Pfannkuche, "Self-trapping of bosons and fermions in optical lattices," *Physical review letters*, 101(5):050402, 2008.

[Luttinger and Lu, 1980a] J. M. Luttinger and Chih-Yuan Lu, "Generalized path-integral formalism of the polaron problem and its second-order semi-invariant correction to the ground-state energy," *Phys. Rev. B*, 21:4251–4263, May 1980.

[Luttinger and Lu, 1980b] JM Luttinger and Chih-Yuan Lu, "Generalized path-integral formalism of the polaron problem and its second-order semi-invariant correction to the ground-state energy," *Physical Review B*, 21(10):4251, 1980.

[Mahan, 1990] G D Mahan, *Many-particle physics*, Physics of solids and liquids. Plenum, New York, NY, 1990.

[Mańka, 1978] R Mańka, "The first-order phase transition in the large polaron ground state," *Physics Letters A*, 67(4):311–312, 1978.

[Manka, 1978] R Manka, "The first-order phase transition in the large polaron ground state," *Physics Letters A*, 67:311–312, 1978.

[Massignan *et al.*, 2014] Pietro Massignan, Matteo Zaccanti, and Georg M Bruun, "Polarons, dressed molecules and itinerant ferromagnetism in ultracold Fermi gases," *Rep. Prog. Phys.*, 77:034401, 2014.

[Matz and Burkey, 1971a] D. Matz and B. C. Burkey, "Dynamical Theory of the Large Polaron: Fock Approximation," *Phys. Rev. B*, 3:3487–3497, May 1971.

[Matz and Burkey, 1971b] D Matz and BC Burkey, "Dynamical theory of the large polaron: Fock approximation," *Physical Review B*, 3(10):3487, 1971.

[Micheli *et al.*, 2006] Andrea Micheli, GK Brennen, and Peter Zoller, "A toolbox for lattice-spin models with polar molecules," *Nature Physics*, 2(5):341–347, 2006.

[Midya *et al.*, 2016a] Bikashkali Midya, Michał Tomza, Richard Schmidt, and Mikhail Lemeshko, "Rotation of cold molecular ions inside a Bose-Einstein condensate," *Physical Review A*, 94(4):041601, 2016.

[Midya *et al.*, 2016b] Bikashkali Midya, Michal Tomza, Richard Schmidt, and Mikhail Lemeshko, "Rotation of cold molecular ions inside a Bose-Einstein condensate," *Physical Review A*, 94:041601, 2016.

[Mishchenko *et al.*, 2000a] A. S. Mishchenko, N. V. Prokof'ev, A. Sakamoto, and B. V. Svistunov, "Diagrammatic quantum Monte Carlo study of the Fröhlich polaron," *Physical Review B*, 62(10):6317, 2000.

[Mishchenko *et al.*, 2000b] AS Mishchenko, NV Prokof'ev, A Sakamoto, and BV Svistunov, "Diagrammatic quantum Monte Carlo study of the Fröhlich polaron," *Physical Review B*, 62(10):6317, 2000.

[Mistakidis *et al.*, 2018] SI Mistakidis, GC Katsimiga, GM Koutentakis, and P Schmelcher, "Repulsive Fermi Polarons and Their Induced Interactions in Binary Mixtures of Ultracold Atoms," *arXiv preprint arXiv:1808.00040*, 2018.

[Moses *et al.*, 2017] Steven A Moses, Jacob P Covey, Matthew T Miecnikowski, Deborah S Jin, and Jun Ye, "New frontiers for quantum gases of polar molecules," *Nature Physics*, 13(1):13–20, 2017.

[Mukhomorov, 2001] VK Mukhomorov, "Ground state of an optical bipolaron with an intermediate strength of coupling," *Journal of Physics: Condensed Matter*, 13(15):3633, 2001.

[Nakano and Yabu, 2016] Eiji Nakano and Hiroyuki Yabu, "BEC-polaron gas in a boson-fermion mixture: A many-body extension of Lee-Low-Pines theory," *Physical Review B*, 93(20):205144, 2016.

[Nandkishore and Huse, 2015] Rahul Nandkishore and David A Huse, "Many-body localization and thermalization in quantum statistical mechanics," *Annu. Rev. Condens. Matter Phys.*, 6(1):15–38, 2015.

[Ngampruetikorn *et al.*, 2012] Vudtiwat Ngampruetikorn, Jesper Levinsen, and Meera M Parish, "Repulsive polarons in two-dimensional Fermi gases," *EPL (Europhysics Letters)*, 98(3):30005, 2012.

[Ni *et al.*, 2008] K-K Ni, S Ospelkaus, MHG De Miranda, A Pe'er, B Neyenhuis, JJ Zirbel, S Kotochigova, PS Julienne, DS Jin, and J Ye, "A high phase-space-density gas of polar molecules," *science*, 322(5899):231–235, 2008.

[Palzer *et al.*, 2009] Stefan Palzer, Christoph Zipkes, Carlo Sias, and Michael Köhl, "Quantum Transport through a Tonks-Girardeau Gas," *Phys. Rev. Lett.*, 103:150601, 2009.

[Peeters and Devreese, 1982a] FM Peeters and JT Devreese, "On the existence of a phase transition for the Fröhlich polaron," *physica status solidi (b)*, 112(1):219–229, 1982.

[Peeters and Devreese, 1982b] FM Peeters and JT Devreese, "On the existence of a phase transition for the Fröhlich polaron," *physica status solidi (b)*, 112(1):219–229, 1982.

[Peeters and Devreese, 1982c] FM Peeters and JT Devreese, "Phase Transition of Fröhlich Polarons, in the Feynman Approximation, Subjected to a Magnetic Field," *physica status solidi (b)*, 110(2):631–635, 1982.

[Peeters and Devreese, 1982d] FM Peeters and JT Devreese, "Phase Transition of Fröhlich Polarons, in the Feynman Approximation, Subjected to a Magnetic Field," *physica status solidi (b)*, 110(2):631–635, 1982.

[Peeters and Devreese, 1985] FM Peeters and JT Devreese, "Acoustical polaron in three dimensions: The ground-state energy and the self-trapping transition," *Physical Review B*, 32(6):3515, 1985.

[Pekar, 1946a] S Pekar, "Autolocalization of the electron in a dielectric inertially polarizing medium," *Zhurnal Eksperimentalnoi i Teoreticheskoi Fiziki*, 16(4):335–340, 1946.

[Pekar, 1946b] S Pekar, "Local quantum states of electrons in an ideal ion crystal," *Zhurnal Eksperimentalnoi I Teoreticheskoi Fiziki*, 16(4):341–348, 1946.

[Perroni *et al.*, 2004] CA Perroni, G Iadonisi, and VK Mukhomorov, "Formation of polaron clusters," *The European Physical Journal B-Condensed Matter and Complex Systems*, 41(2):163–170, 2004.

[Pickering *et al.*, 2018a] James D. Pickering, Benjamin Shepperson, Bjarke A. K. Hübschmann, Frederik Thorning, and Henrik Stapelfeldt, "Alignment and Imaging of the CS_2 Dimer Inside Helium Nanodroplets," *Phys. Rev. Lett.*, 120:113202, Mar 2018.

[Pickering *et al.*, 2018b] James D Pickering, Benjamin Shepperson, Bjarke AK Hübschmann, Frederik Thorning, and Henrik Stapelfeldt, "Alignment and imaging of the CS 2 dimer inside helium nanodroplets," *Physical review letters*, 120(11):113202, 2018.

[Pitaevskii and Stringari, 2016] Lev Pitaevskii and Sandro Stringari, *Bose-Einstein condensation and superfluidity*, volume 164, Oxford University Press, 2016.

[Pupillo *et al.*, 2008] G Pupillo, A Griessner, A Micheli, M Ortner, D-W Wang, and P Zoller, "Cold atoms and molecules in self-assembled dipolar lattices," *Physical review letters*, 100(5):050402, 2008.

[Pushkarov, 1991] Dimitur Ivanov Pushkarov, *Quasiparticle theory of defects in solids*, World scientific, 1991.

[Quémerais and Fratini, 1998] P Quémerais and S Fratini, "Polaron Crystallization and the Metal–Insulator Transition," *International Journal of Modern Physics B*, 12(29n31):3131–3136, 1998.

[Rath and Schmidt, 2013] Steffen Patrick Rath and Richard Schmidt, "Field-theoretical study of the bose polaron," *Physical Review A*, 88(5):053632, 2013.

[Redchenko and Lemeshko, 2016a] E S Redchenko and M Lemeshko, "Libration of strongly-oriented polar molecules inside a superfluid," *Chem. Phys. Chem.*, 17:3649, 2016.

[Redchenko and Lemeshko, 2016b] ES Redchenko and Mikhail Lemeshko, "Libration of Strongly-Oriented Polar Molecules inside a Superfluid," *ChemPhysChem*, 17(22):3649–3654, 2016.

[Reed and Simon, 1980] Michael Reed and Barry Simon, *Methods of modern mathematical physics I, Functional Analysis*, Academic Press, 1980.

[Regal *et al.*, 2003] Cindy A Regal, Christopher Ticknor, John L Bohn, and Deborah S Jin, "Creation of ultracold molecules from a Fermi gas of atoms," *Nature*, 424(6944):47–50, 2003.

[Rica and Roberts, 2009] Sergio Rica and David C Roberts, "Induced interaction and crystallization of self-localized impurity fields in a Bose-Einstein condensate," *Physical Review A*, 80(1):013609, 2009.

[Roberts and Rica, 2009] David C Roberts and Sergio Rica, "Impurity crystal in a Bose-Einstein condensate," *Physical review letters*, 102(2):025301, 2009.

[Rowe and Wood, 2010] David J Rowe and John L Wood, *Fundamentals of nuclear models: foundational models*, World Scientific, 2010.

[Ruderman and Kittel, 1954] Melvin A Ruderman and Charles Kittel, "Indirect exchange coupling of nuclear magnetic moments by conduction electrons," *Physical Review*, 96(1):99, 1954.

[Rudzikas, 1997] Z Rudzikas, *Theoretical Atomic Spectroscopy*, Cambridge University Press, 1997.

[Rzadkowski and Lemeshko, 2018] Wojciech Rzadkowski and Mikhail Lemeshko, "Effect of a magnetic field on molecule–solvent angular momentum transfer," *The Journal of Chemical Physics*, 148(10):104307, 2018.

[Sacha and Timmermans, 2006a] Krzysztof Sacha and Eddy Timmermans, "Self-localized impurities embedded in a one-dimensional Bose-Einstein condensate and their quantum fluctuations," *Physical Review A*, 73(6):063604, 2006.

[Sacha and Timmermans, 2006b] Krzysztof Sacha and Eddy Timmermans, "Self-localized impurities embedded in a one-dimensional Bose-Einstein condensate and their quantum fluctuations," *Physical Review A*, 73(6):063604, 2006.

[Salje *et al.*, 2005] Ekhard KH Salje, AS Alexandrov, and WY Liang, *Polarons and bipolarons in high-Tc superconductors and related materials*, Cambridge University Press, 2005.

[Santamore and Timmermans, 2011] DH Santamore and Eddy Timmermans, "Multi-impurity polarons in a dilute Bose–Einstein condensate," *New Journal of Physics*, 13(10):103029, 2011.

[Scelle *et al.*, 2013] R. Scelle, T. Rentrop, A. Trautmann, T. Schuster, and M. K. Oberthaler, "Motional Coherence of Fermions Immersed in a Bose Gas," *Phys. Rev. Lett.*, 111:070401, 2013.

[Schirotzek *et al.*, 2009] André Schirotzek, Cheng-Hsun Wu, Ariel Sommer, and Martin W. Zwierlein, "Observation of Fermi Polarons in a Tunable Fermi Liquid of Ultracold Atoms," *Phys. Rev. Lett.*, 102:230402, 2009.

[Schlagmüller *et al.*, 2016] Michael Schlagmüller, Tara Cubel Liebisch, Felix Engel, Kathrin S Kleinbach, Fabian Böttcher, Udo Hermann, Karl M Westphal, Anita Gaj, Robert Löw, Sebastian Hofferberth, *et al.*, "Ultracold chemical reactions of a single Rydberg atom in a dense gas," *Physical Review X*, 6(3):031020, 2016.

[Schmidt and Lemeshko, 2015] Richard Schmidt and Mikhail Lemeshko, "Rotation of quantum impurities in the presence of a many-body environment," *Physical review letters*, 114(20):203001, 2015.

[Schmidt and Lemeshko, 2016] Richard Schmidt and Mikhail Lemeshko, "Deformation of a quantum many-particle system by a rotating impurity," *Physical Review X*, 6(1):011012, 2016.

[Schmidt *et al.*, 2016] Richard Schmidt, HR Sadeghpour, and E Demler, "Mesoscopic Rydberg Impurity in an Atomic Quantum Gas," *Physical review letters*, 116(10):105302, 2016.

[Schmiedt *et al.*, 2016] Hanno Schmiedt, Per Jensen, and Stephan Schlemmer, "Collective molecular superrotation: a model for extremely flexible molecules applied to protonated methane," *Physical Review Letters*, 117(22):223002, 2016.

[Sengupta *et al.*, 2005] Pinaki Sengupta, Leonid P Pryadko, Fabien Alet, Matthias Troyer, and Guido Schmid, "Supersolids versus phase separation in two-dimensional lattice bosons," *Physical review letters*, 94(20):207202, 2005.

[Shadkhoo and Bruinsma, 2015] Shahriar Shadkhoo and Robijn Bruinsma, "Impurities in Bose-Einstein Condensates: From Polaron to Soliton," *Physical review letters*, 115(13):135305, 2015.

[Shchadilova *et al.*, 2016a] Yulia E Shchadilova, Fabian Grusdt, Alexey N Rubtsov, and Eugene Demler, "Polaronic mass renormalization of impurities in Bose-Einstein condensates: Correlated Gaussian-wave-function approach," *Physical Review A*, 93(4):043606, 2016.

[Shchadilova *et al.*, 2016b] Yulia E Shchadilova, Richard Schmidt, Fabian Grusdt, and Eugene Demler, "Quantum dynamics of ultracold bose polarons," *Physical review letters*, 117(11):113002, 2016.

[Shepperson *et al.*, 2017a] Benjamin Shepperson, Adam S Chatterley, Anders A Søndergaard, Lars Christiansen, Mikhail Lemeshko, and Henrik Stapelfeldt, "Strongly aligned molecules inside helium droplets in the near-adiabatic regime," *The Journal of Chemical Physics*, 147(1):013946, 2017.

[Shepperson *et al.*, 2017b] Benjamin Shepperson, Anders A Søndergaard, Lars Christiansen, Jan Kaczmarczyk, Robert E Zillich, Mikhail Lemeshko, and Henrik Stapelfeldt, "Laser-Induced Rotation of Iodine Molecules in Helium Nanodroplets: Revivals and Breaking Free," *Physical Review Letters*, 118(20):203203, 2017.

[Spethmann *et al.*, 2012] Nicolas Spethmann, Farina Kindermann, Shincy John, Claudia Weber, Dieter Meschede, and Artur Widera, "Dynamics of single neutral impurity atoms immersed in an ultracold gas," *Physical review letters*, 109(23):235301, 2012.

[Spohn, 1986] Herbert Spohn, "Roughening and pinning transitions for the polaron," *Journal of Physics A: Mathematical and General*, 19(4):533, 1986.

[Stamm *et al.*, 2007] C Stamm, T Kachel, N Pontius, R Mitzner, T Quast, K Holldack, S Khan, C Lupulescu, EF Aziz, M Wietstruk, *et al.*, "Femtosecond modification of electron localization and transfer of angular momentum in nickel," *Nature materials*, 6(10):740–743, 2007.

[Stienkemeier and Lehmann, 2006] Frank Stienkemeier and Kevin K Lehmann, "Spectroscopy and dynamics in helium nanodroplets," *Journal of Physics B: Atomic, Molecular and Optical Physics*, 39(8):R127, 2006.

[Stone, 2013a] A Stone, *The Theory of Intermolecular Forces*, Oxford University Press, 2013.

[Stone, 2013b] Anthony Stone, *The theory of intermolecular forces*, oUP oxford, 2013.

[Sumi, 1977] Atsuko Sumi, "Phase diagram of an exciton in the phonon field," *Journal of the Physical Society of Japan*, 43(4):1286–1294, 1977.

[Sumi and Toyozawa, 1973] Atsuko Sumi and Yutaka Toyozawa, "Discontinuity in the polaron ground state," *Journal of the Physical Society of Japan*, 35(1):137–145, 1973.

[Syzranov *et al.*, 2014] Sergey V Syzranov, Michael L Wall, Victor Gurarie, and Ana Maria Rey, "Spin–orbital dynamics in a system of polar molecules," *Nature communications*, 5(1):1–7, 2014.

[Szalewicz, 2008] Krzysztof Szalewicz, "Interplay between theory and experiment in investigations of molecules embedded in superfluid helium nanodroplets," *International Reviews in Physical Chemistry*, 27(2):273–316, 2008.

[Tempere *et al.*, 2009a] J Tempere, W Casteels, MK Oberthaler, S Knoop, E Timmermans, and JT Devreese, "Feynman path-integral treatment of the BEC-impurity polaron," *Physical Review B*, 80(18):184504, 2009.

[Tempere *et al.*, 2009b] J Tempere, W Casteels, MK Oberthaler, S Knoop, E Timmermans, and JT Devreese, "Feynman path-integral treatment of the BEC-impurity polaron," *Physical Review B*, 80(18):184504, 2009.

[Tempere *et al.*, 2003] J Tempere, SN Klimin, IF Silvera, and JT Devreese, "Wigner lattice of ripplopolarons in a multielectron bubble in helium," *The European Physical Journal B-Condensed Matter and Complex Systems*, 32(3):329–338, 2003.

[Tempere and Devreese, 2001] Jacques Tempere and JT Devreese, "Optical absorption of an interacting many-polaron gas," *Physical Review B*, 64(10):104504, 2001.

[Toennies and Vilesov, 2004a] J Peter Toennies and Andrey F Vilesov, "Superfluid helium droplets: a uniquely cold nanomatrix for molecules and molecular complexes," *Angewandte Chemie International Edition*, 43(20):2622–2648, 2004.

[Toennies and Vilesov, 2004b] J Peter Toennies and Andrey F Vilesov, "Superfluid helium droplets: a uniquely cold nanomatrix for molecules and molecular complexes," *Angewandte Chemie International Edition*, 43(20):2622–2648, 2004.

[Toennies and Vilesov, 2004c] J. Peter Toennies and F. Andrey Vilesov, "Superfluid Helium Droplets: A Uniquely Cold Nanomatrix for Molecules and Molecular Complexes," *Angewandte Chemie*, 43:2622, 2004.

[Tokuda *et al.*, 1981] Naoki Tokuda, Hisashi Shoji, and Kazuyuki Yoneya, "The optical polaron bound in a Coulomb potential and its phase diagram," *Journal of Physics C: Solid State Physics*, 14(29):4281, 1981.

[Toyozawa, 1961] Yutaka Toyozawa, "Self-trapping of an electron by the acoustical mode of lattice vibration. I," *Progress of Theoretical Physics*, 26(1):29–44, 1961.

[Utesov *et al.*, 2018] OI Utesov, MI Baglay, and SV Andreev, "Effective interactions in a quantum Bose-Bose mixture," *Physical Review A*, 97(5):053617, 2018.

[Vadakkumbatt *et al.*, 2014] Vaisakh Vadakkumbatt, Emil Joseph, Anustuv Pal, and Ambarish Ghosh, "Studying electrons on curved surfaces by trapping and manipulating multielectron bubbles in liquid helium," *Nature communications*, 5(1):1–6, 2014.

[Varshalovich *et al.*, 1988a] Dmitriĭ Aleksandrovich Varshalovich, AN Moskalev, and VK Khersonskii, *Quantum theory of angular momentum*, World Scientific, Singapore, 1988.

[Varshalovich *et al.*, 1988b] Dmitriĭ Aleksandrovich Varshalovich, Anatolï Nikolaevitch Moskalev, and Valerii Kel'manovich Khersonskii, *Quantum theory of angular momentum*, World Scientific, 1988.

[Vlietinck *et al.*, 2015] Jonas Vlietinck, Wim Casteels, Kris Van Houcke, Jacques Tempere, Jan Ryckebusch, and Jozef T Devreese, "Diagrammatic Monte Carlo study of the acoustic and the Bose–Einstein condensate polaron," *New Journal of Physics*, 17(3):033023, 2015.

[Wang, 1998] Xiaoqun Wang, "Ground State Properties of Three-Dimensional Acoustic Polarons," *Modern physics letters B*, 12(19):775–783, 1998.

[Weinstein, 1983] M I Weinstein, "Nonlinear Schrtidinger Equations and Sharp Interpolation Estimates," *Commun. Math. Phys.*, 87:567, 1983.

[Weiss, 2012] U. Weiss, *Quantum Dissipative Systems*, World Scientific, 4 edition, 2012.

[Yakaboylu *et al.*, 2017] Enderalp Yakaboylu, Andreas Deuchert, and Mikhail Lemeshko, "Emergence of non-abelian magnetic monopoles in a quantum impurity problem," *arXiv preprint arXiv:1705.05162*, 2017.

[Yakaboylu and Lemeshko, 2017] Enderalp Yakaboylu and Mikhail Lemeshko, "Anomalous screening of quantum impurities by a neutral environment," *Physical review letters*, 118(8):085302, 2017.

[Yakaboylu *et al.*, 2018] Enderalp Yakaboylu, Bikashkali Midya, Andreas Deuchert, Nikolai Leopold, and Mikhail Lemeshko, "Theory of the rotating polaron: Spectrum and self-localization," *Phys. Rev. B*, 98(22):224506, 2018.

[Yan *et al.*, 2013] Bo Yan, Steven A Moses, Bryce Gadway, Jacob P Covey, Kaden RA Hazzard, Ana Maria Rey, Deborah S Jin, and Jun Ye, "Observation of dipolar spin-exchange interactions with lattice-confined polar molecules," *Nature*, 501(7468):521–525, 2013.

[Ye *et al.*, 1993] Jinwu Ye, Subir Sachdev, and N Read, "Solvable spin glass of quantum rotors," *Physical review letters*, 70(25):4011, 1993.

[Yin *et al.*, 2015] Tao Yin, Daniel Cocks, and Walter Hofstetter, "Polaronic effects in one-and two-band quantum systems," *Physical Review A*, 92(6):063635, 2015.

[Zhou *et al.*, 2010] Lihui Zhou, Jens Wiebe, Samir Lounis, Elena Vedmedenko, Focko Meier, Stefan Blügel, Peter H Dederichs, and Roland Wiesendanger, "Strength and directionality of surface Ruderman–Kittel–Kasuya–Yosida interaction mapped on the atomic scale," *Nature Physics*, 6(3):187, 2010.